



POLITECNICO DI TORINO

Master degree course in Automotive engineering

Master Degree Thesis

**Design of an epicycloidal  
geartrain for a four-wheel drive  
Formula Student electric  
vehicle**

**Supervisors**

prof. Andrea Tonoli

**Candidates**

Marco COVA

S 253438

ACADEMIC YEAR 2019-2020

This work is subject to the Creative Commons Licence

## **Abstract**

Formula Student or Formula SAE is a competition between student teams in charge of designing, building and testing a new formula-style race car per each season. Those vehicles are divided into three classes: Combustion, Electric and Driverless. The competition consists in both a static part where the design, the cost-performance relationship and the marketing aspects of the project are evaluated by the judges and a dynamic part where the vehicle must race in four different type of events. Each dynamic event highlights different aspects of the car performance, from standstill acceleration to lateral grip, reliability and energy efficiency.

In 2005 Politecnico di Torino's Formula Student team called Squadra Corse PoliTo was founded and since then fifteen cars have been built. Seven of them are powered by an Internal Combustion Engine, one is a Hybrid Electric Vehicle, while the last six cars built are Battery Electric Vehicles.

SC18integrale is the vehicle presented by Squadra Corse PoliTo for the 2018/2019 racing season. It is a four-wheel drive Battery Electric Vehicle with four independent in-wheel motors. The motors need a devoted gearbox in order to match the vehicle's traction requirement. Due to the in-wheel position both the weight and the volume of the gearbox are critical parameters. The weight impacts on the unsprung masses, while a small volume is beneficial for suspension hardpoints package.

In this thesis the project of the SC18integrale epicycloidal transmission is presented in all its aspects, from the concept design until the track validation. The first phase of the design after the target has been set is the development

of the transmission model and of the gear life calculation, carried by KISSsoft and KISSsys software tools, then the integration of the gearbox with the wheel assembly is studied. Finally the mechanical design of each component and of the assembly is detailed.

Catia V5 is the software used for the development of CAD models while Altair Hyperworks the software used to carry the structural FEA. The experimental validation is done on track during the pre-season tests, the racing events and the post-season test phase.

# Acknowledgements

Alla fine di questo percorso che, malgrado la grande soddisfazione, per qualche motivo mi è sembrato più lungo di quanto effettivamente sia stato, ci tengo a scrivere qualche parola di ringraziamento rivolta a quelle persone che hanno reso il raggiungimento di questo traguardo possibile e più semplice.

Prima di tutto e di tutti vorrei ringraziare i miei genitori, Paolo e Mariangela, che da sempre mi supportano in ogni modo possibile, senza il loro costante aiuto ed i loro sacrifici tutto ciò sarebbe stato certamente irrealizzabile. Un ringraziamento particolare va a mia sorella, Francesca, una delle persone più importanti della mia vita, nonché una delle prime che mi abbia sopportato e che mi sia stata vicina; malgrado l'attualmente maggiore distanza geografica continua a fare entrambe le cose.

Vorrei anche ringraziare le mie nonne, Angela e Lena, sempre presenti nella mia vita e probabilmente il massimo esempio di gentilezza e disponibilità che una persona possa pensare di raggiungere. Sono sicuro che questo traguardo le renda felici e fiere di me.

Desidero ringraziare i miei zii, Stefano e Antonella, e con loro i miei cugini, Pietro, Marta e Giacomo. Mai distanti, ho sempre potuto contare su di loro in questi anni e sono certo di poter continuare a farlo.

Doveroso ringraziare il Team Squadra Corse, palestra di vita e di Motorsport, per me grande fattore di crescita personale e professionale. In particolare il Professor Andrea Tonoli che da oramai quindici anni crede in noi e fa sì che sempre più studenti conoscano questa realtà, Stefano e Marco con i quali ho condiviso moltissimo tempo, prima in Squadra e poi come colleghi, Edoardo che ha lavorato con me su questo progetto, diventandone parte integrante e contribuendo in modo sostanziale alla sua riuscita, e Giovanni che un po' di anni fa mi mise una "pulce nell'orecchio". Grazie anche a tutte le altre persone che con me non si sono mai risparmiate e hanno investito tutte le loro energie nel progetto, colleghi, ma soprattutto amici.

Lascio per ultimo un ringraziamento per me molto importante, a Giulia, che da più di due anni mi sostiene, mi sopporta, mi incoraggia e rende migliore ogni istante trascorso. Insieme siamo cresciuti in molti aspetti delle nostre vite e continueremo a farlo, non potrei immaginare una persona migliore al mio fianco.

# Contents

<b>List of Figures</b>	10
<b>List of Tables</b>	17
<b>I First part</b>	<b>19</b>
<b>1 Introduction</b>	<b>21</b>
1.1 Formula Student . . . . .	21
1.2 Squadra Corse PoliTo . . . . .	23
1.3 SC18integrale project . . . . .	23
<b>2 Gear trains for Formula Student Electric cars</b>	<b>25</b>
2.1 Solutions designed by Squadra Corse . . . . .	25
2.1.1 Before planetary gear trains . . . . .	25
2.1.2 SCXV and SCXV Evo . . . . .	26
2.1.3 SCdiciassette . . . . .	27
2.2 Benchmark . . . . .	28
2.2.1 University Racing Eindhoven . . . . .	28
2.2.2 AMZ Racing Team . . . . .	29
2.2.3 DHBW Engineering Stuttgart e.V. . . . .	30
2.2.4 KA-RaceIng . . . . .	31

<b>3</b>	<b>Project Set-Up</b>	<b>33</b>
3.1	SC18integrale wheel assembly . . . . .	33
3.2	Target setting . . . . .	34
3.3	Gear train integration with the vehicle . . . . .	35
3.3.1	Motors . . . . .	35
3.3.2	Wheel integration . . . . .	36
3.4	Transmission ratio choice . . . . .	37
3.5	Layout choice . . . . .	38
3.6	Meshing rule . . . . .	40
3.7	Load spectrum and required service life . . . . .	41
3.8	Design flow . . . . .	44
<b>4</b>	<b>Transmission model</b>	<b>47</b>
4.1	Introduction to KISSsys . . . . .	47
4.2	SC18integrale transmission model . . . . .	48
4.2.1	Elements involved . . . . .	48
4.2.2	Model build . . . . .	49
4.3	Calculation modules . . . . .	54
4.3.1	Coaxial shafts calculation . . . . .	54
4.3.2	Gear pair calculation module . . . . .	56
<b>5</b>	<b>Gear life calculation</b>	<b>57</b>
5.1	Introduction to KISSsoft . . . . .	57
5.1.1	Basic data . . . . .	58
5.1.2	Reference profile . . . . .	58
5.1.3	Tolerances . . . . .	59
5.1.4	Rating . . . . .	59
5.1.5	Factors . . . . .	59
5.1.6	Output plots . . . . .	60
5.2	ISO 6336:2006 Standard . . . . .	60

5.2.1	Pitting load capacity . . . . .	62
5.2.2	Fracture load capacity . . . . .	63
5.3	Material choice . . . . .	63
5.4	Calculation set-up . . . . .	69
5.5	Results . . . . .	74
5.5.1	Final geometry definition . . . . .	74
5.5.2	Life calculation results . . . . .	78
<b>6</b>	<b>Wheel bearings</b>	<b>83</b>
6.1	Layout and bearing choice . . . . .	83
6.2	Bearings life calculation . . . . .	86
6.2.1	Load spectrum . . . . .	86
6.2.2	Life calculation results . . . . .	88
6.3	Axial preload . . . . .	90
<b>7</b>	<b>Mechanical design of gear train components</b>	<b>95</b>
7.1	Sun gear . . . . .	95
7.1.1	Component engineering . . . . .	95
7.1.2	Geometric oscillations of the motor output shaft . . . . .	99
7.1.3	Analysis of the motor output shaft under load . . . . .	101
7.1.4	Manufacturing . . . . .	103
7.2	Ring gear . . . . .	105
7.2.1	Component engineering . . . . .	105
7.2.2	Structural analysis . . . . .	108
7.2.3	Manufacturing . . . . .	109
7.3	Planetary gears assembly . . . . .	110
7.3.1	Components engineering . . . . .	110
7.3.2	Torque transmission . . . . .	114
7.3.3	Pin shaft structural analysis . . . . .	116
7.3.4	Planet gear structural analysis . . . . .	117

7.3.5	Assembly tolerances . . . . .	120
7.3.6	Manufacturing . . . . .	123
<b>8</b>	<b>Planetary carrier mechanical design</b>	<b>125</b>
8.1	Layout . . . . .	125
8.2	Wheel locknut . . . . .	126
8.3	Materials choice . . . . .	127
8.4	FEM analysis and optimization . . . . .	129
8.4.1	Loads . . . . .	129
8.4.2	Optimization . . . . .	131
8.4.3	Final FEM model . . . . .	135
8.5	Manufacturing and tolerances . . . . .	145
<b>9</b>	<b>Lubrication</b>	<b>147</b>
9.1	Lubricant choice . . . . .	147
9.2	Seals . . . . .	149
9.2.1	Radial shaft seal . . . . .	150
9.2.2	O-Ring . . . . .	152
9.3	Lubricant level . . . . .	153
<b>10</b>	<b>Efficiency analysis</b>	<b>155</b>
10.1	Power losses . . . . .	155
10.2	Gearbox efficiency model . . . . .	157
10.3	Results . . . . .	159
<b>11</b>	<b>Assembly</b>	<b>163</b>
11.1	Upright group assembly . . . . .	163
11.2	Motor group assembly . . . . .	169
<b>12</b>	<b>Final transmission assembly</b>	<b>171</b>
12.1	Transmission assembly . . . . .	171

12.2 Transmission integration . . . . .	173
<b>II Second part</b>	<b>175</b>
<b>13 Results obtained</b>	<b>177</b>
13.1 Weight reduction . . . . .	177
13.2 Volume reduction . . . . .	179
13.3 Assembly process . . . . .	180
13.4 Formula Student Spain failure . . . . .	183
13.5 Gearbox life . . . . .	184
13.6 Motor working points . . . . .	185
<b>14 Conclusions and future perspectives</b>	<b>189</b>
14.1 Conclusions . . . . .	189
14.2 Future perspectives . . . . .	190
<b>APPENDICES</b>	<b>190</b>
<b>A AMK motor datasheet</b>	<b>191</b>
<b>B Double stage epicycloidal gearboxes layouts</b>	<b>195</b>
<b>C Wheel locknut tightening torque computation</b>	<b>197</b>
<b>D Gear train technical drawings</b>	<b>201</b>
<b>E Planetary carrier assembly technical drawings</b>	<b>211</b>
<b>F Lubricant datasheet</b>	<b>217</b>
<b>Bibliography</b>	<b>219</b>

# List of Figures

1.1	SC18integrale . . . . .	24
2.1	SC12e with its gear train [19] . . . . .	26
2.2	SCR with its geartrain [19] . . . . .	26
2.3	SCXV with its gear train [19] . . . . .	27
2.4	SCdiciassette with its gear train . . . . .	28
2.5	University Racing Eindhoven transmission . . . . .	29
2.6	University Racing Eindhoven transmission . . . . .	29
2.7	AMZ Racing Team transmission . . . . .	30
2.8	DHBW Engineering Stuttgart e.V. . . . .	30
2.9	KA-RaceIng wheel assembly . . . . .	31
3.1	SC18integrale view . . . . .	34
3.2	Characteristic curves of the AMK DD5-14-10-POW motor . . . . .	36
3.3	Section view of the wheel assembly . . . . .	37
3.4	Dual stage planetary gearbox . . . . .	39
3.5	Schematic of the SC18integrale transmission . . . . .	39
3.6	Example of load spectrum, showing both the front and the rear requested motor torque . . . . .	41
3.7	Front transmission load spectrum . . . . .	43
3.8	Rear transmission load spectrum . . . . .	43
3.9	Design flow . . . . .	45
4.1	KISSsys model 3D view . . . . .	48

4.2	KISSsys model tree . . . . .	50
4.3	Diagram of the transmission model . . . . .	54
4.4	Main line calculation module . . . . .	55
5.1	Reference profile . . . . .	59
5.2	Length of path of contact for a cylindrical gear . . . . .	60
5.3	Solutions for aluminum gears scattered as a function of the normal module . . . . .	65
5.4	Solutions for aluminum gears scattered as a function of the centre distance . . . . .	65
5.5	Properties comparison of case-hardening steels commonly used for gears manufacturing . . . . .	66
5.6	Nominal time and temperature requirements for different case depths . . . . .	67
5.7	Type of pinion shaft according to ISO 6336 Picture 13e . . . . .	72
5.8	Tooth trace modification . . . . .	72
5.9	Alternate load factor determination . . . . .	73
5.10	Tip and root relief . . . . .	75
5.11	First stage without (left) and with (right) tip relief modification	75
5.12	First stage meshing gears . . . . .	76
5.13	Second stage without (left) and with (right) end relief modifi- cation . . . . .	77
5.14	Second stage meshing gears . . . . .	77
5.15	First stage specific sliding . . . . .	78
5.16	Root stresses for the sun gear (left) and for the first planet gear (right) under maximum torque . . . . .	79
5.17	First stage hardness curve recommendation . . . . .	79
5.18	Second stage specific sliding . . . . .	80
5.19	Root stresses for the second planet gear (left) and for the ring gear (right) under maximum torque . . . . .	81

5.20	Second stage hardness curve recommendation . . . . .	81
6.1	SC18integrale wheel bearings layout . . . . .	84
6.2	Main dimensions for bearings of the type ACD,CD . . . . .	84
6.3	Fx load spectrum where $F_x \geq 20$ N . . . . .	87
6.4	Fx load spectrum where $F_y \geq 20$ N . . . . .	87
6.5	Fz load spectrum . . . . .	88
6.6	Wheel bearings life as a function of axial preload . . . . .	89
6.7	Front peak contact loads on the external bearing (left) and on the internal bearing (right) [14] . . . . .	90
6.8	Rear peak contact loads on the external bearing (left) and on the internal bearing (right) [14] . . . . .	90
6.9	SC17 wheel assembly section . . . . .	91
6.10	SC18 wheel bearings preload . . . . .	92
7.1	SC17 sun shaft . . . . .	95
7.2	Comparison between the sun gear assembly of the SCdcias- sette (left) and the sun gear assembly of the SC18integrale (right) . . . . .	96
7.3	Motor mounting flange detail . . . . .	97
7.4	Motor output spline . . . . .	98
7.5	Motor output spline section view . . . . .	98
7.6	Sun gear . . . . .	99
7.7	Measurement set-up . . . . .	100
7.8	Oscillation of the motor output spline top and root diameters from their nominal value . . . . .	100
7.9	Maximum oscillation of the motor output shaft non-splined section . . . . .	101
7.10	Radial forces due to meshing gear pairs acting on the sun gear	102
7.11	Model of the motor output shaft in KISSsoft . . . . .	103
7.12	Motor shaft deflection . . . . .	103

7.13	Carburized case pattern . . . . .	104
7.14	SCdiciassette ring gear retention system . . . . .	105
7.15	Curved flank teeth solution . . . . .	106
7.16	SC18 integrale ring gear retention system . . . . .	107
7.17	Ring gear . . . . .	107
7.18	Ring gear FEM model . . . . .	108
7.19	Ring gear stress contour plot . . . . .	109
7.20	Nominal times required for different nitride case depths . . . . .	110
7.21	Planetary gears assembly . . . . .	111
7.22	Anti-rotation pin in the carrier (left) and spacer (right) . . . . .	113
7.23	Planet pin shaft . . . . .	113
7.24	Planet pin shaft rotational constrain . . . . .	114
7.25	Left display: tolerance field only takes allowances into account, centre display: tolerance field takes into account temperature and centrifugal force (without pressure), right display: tol- erance field takes into account temperature, centrifugal force and pressure . . . . .	115
7.26	Plot of the stresses of the press fit in the shaft and in the hub	115
7.27	Planetary gear assembly model in KISSsoft . . . . .	116
7.28	Planet pin shaft displacement (left) and stresses (right) . . . . .	117
7.29	Planetary gear FEM model . . . . .	118
7.30	Planetary gear displacement . . . . .	119
7.31	Planetary gear stress on a mid-plane section . . . . .	119
7.32	First stage meshing profiles with 33.6 centre distance . . . . .	120
8.1	Planetary carrier . . . . .	126
8.2	Maximum stress vs fatigue life for 7068-T6511 aluminum alloy	128
8.3	Autocross g-g diagram . . . . .	130
8.4	Hub-carrier assembly before optimization . . . . .	131
8.5	Optimization design and non-design spaces . . . . .	132

8.6	Element density contour, rear view . . . . .	133
8.7	Element density contour, isometric view . . . . .	133
8.8	Element density contour, section view . . . . .	133
8.9	Hub before (left) and after optimization (right) . . . . .	134
8.10	Planetary carrier before (left) and after optimization (right) . . . . .	134
8.11	Components meshed in the model . . . . .	135
8.12	Particular showing the mesh size variation in the hub . . . . .	136
8.13	View of the contact interfaces between the hub-carrier and the bearings inner rings . . . . .	137
8.14	Pin shaft constraints . . . . .	137
8.15	Wheel bearings constraints . . . . .	138
8.16	Loads application . . . . .	139
8.17	Von Mises average stress contour plot - Hub . . . . .	140
8.18	Von Mises average stress contour plot - Hub . . . . .	140
8.19	Signed Von Mises average stress contour plot - Hub . . . . .	140
8.20	Signed Von Mises average stress contour plot - Hub . . . . .	141
8.21	Von Mises alternate stress contour plot - Hub . . . . .	141
8.22	Signed Von Mises alternate stress contour plot - Hub . . . . .	142
8.23	Haigh diagram example . . . . .	142
8.24	Haigh diagram of the most stressed section of the wheel hub . . . . .	143
8.25	Von Mises stress contour plot - Planetary carrier . . . . .	144
8.26	Von Mises stress contour plot - Planetary carrier . . . . .	144
8.27	Displacement contour plot . . . . .	145
8.28	View of the technical drawing about the machining process with mating hub and planetary carrier . . . . .	146
9.1	Section view of the transmission inside the upright . . . . .	149
9.2	CRW1 type seal (left and HMS5 type seal (right) [13] . . . . .	150
9.3	Permissible speeds for spring-loaded sealing lips when no pres- sure differential exists across the seal in operation . . . . .	151

9.4	O-Ring groove . . . . .	152
9.5	CAD determined oil level . . . . .	153
9.6	Tested oil level . . . . .	154
10.1	Gearbox efficiency example . . . . .	156
10.2	Transmission case model for efficiency analysis . . . . .	158
10.3	Side view of the transmission model in its case . . . . .	159
10.4	SC18integrale direct efficiency (traction conditions) . . . . .	159
10.5	SC18integrale inverse efficiency (regenerative braking conditions) . . . . .	160
10.6	SCdiciassette direct efficiency (traction conditions) . . . . .	160
10.7	SCdiciassette inverse efficiency (regenerative braking conditions)	161
11.1	Transmission assembly . . . . .	164
11.2	Fit of the bearing and of the seal onto the hub . . . . .	166
11.3	Ring gear installation . . . . .	167
11.4	Fit of the hub into the upright . . . . .	167
11.5	Satellites phase . . . . .	168
11.6	Needle roller bearings assembly . . . . .	168
11.7	Planet pin shaft correct position . . . . .	169
12.1	Final gears assembly . . . . .	171
12.2	Final gearbox assembly . . . . .	172
12.3	Final gearbox assembly . . . . .	172
12.4	Final gearbox assembly . . . . .	173
12.5	SC18integrale transmission assembled . . . . .	173
13.1	Comparison between the SCdiciassette ring gear (left) and the SC18integrale one (right) . . . . .	178
13.2	Comparison between the SCdiciassette planet gears assembly (left) and the SC18integrale one (right) . . . . .	179
13.3	Transmission parts before assembly . . . . .	180
13.4	Hardness check on the ring gear . . . . .	181

13.5	Ring gear mounted into the upright . . . . .	182
13.6	SC18itegrale transmission assembled . . . . .	183
13.7	Formula Student Spain Failure . . . . .	184
13.8	SC18itegrale gears inspection after 25 h . . . . .	185
13.9	Rear motor working points . . . . .	186
13.10	Rear motor working points in regenerative braking . . . . .	186
13.11	Front motor working points in traction . . . . .	187
13.12	Front motor working points in regenerative braking . . . . .	187
A.1	AMK motor datasheet [20] . . . . .	192
A.2	AMK motor datasheet [20] . . . . .	193
B.1	ANSI/AGMA 6123-B06 [1] . . . . .	196
C.1	Section view of the clamped parts between the hub and the wheel locknut . . . . .	198
C.2	Measures on the wheel hub . . . . .	199
D.1	Sun gear drawing [28] . . . . .	202
D.2	First stage planet gear drawing [28] . . . . .	203
D.3	Second stage planet gear drawing [28] . . . . .	204
D.4	Planet gears assembly drawing [28] . . . . .	205
D.5	Planet pin shaft drawing [28] . . . . .	206
D.6	Planet gears spacer drawing . . . . .	207
D.7	Ring gear drawing . . . . .	208
D.8	Ring gear drawing . . . . .	209
D.9	Ring gear screws drawing . . . . .	210
E.1	Hub drawing . . . . .	212
E.2	Planetary carrier drawing . . . . .	213
E.3	Planetary carrier assembly drawing . . . . .	214
E.4	H-shaped bushing drawing . . . . .	215
E.5	Wheel locknut drawing . . . . .	216
F.1	Motul Gear 300 75w90 dataheet [27] . . . . .	218

# List of Tables

5.1	EN AW AlSi1MgMnT4 properties [2]	64
5.2	17NiCrMo6-4 properties [2]	67
5.3	Nominal temperatures used in nitriding and hardness obtained [3]	68
5.4	34CrAlNi7-10 properties [2]	69
5.5	42CrMo4 properties [2]	69
5.6	First stage data	74
5.7	Second stage data	76
5.8	First stage safety factors	78
5.9	Second stage safety factors	80
8.1	Titanium Ti-6Al-4V (Grade 5), Annealed properties [24]	128
8.2	Aluminum 7075-T6 properties [26]	129
9.1	ISO grade per ambient temperature, mineral oil [4]	148
10.1	SC18integrale recorded running time and distances	161
13.1	Weight comparison	177
13.2	Main dimensions comparison	179
13.3	SC18integrale recorded running time and distances	184



# Part I

## First part



# Chapter 1

## Introduction

### 1.1 Formula Student

Formula Student or Formula SAE (FASE), depending on the event organizer, is a competition between student teams in charge of designing, building and testing a new formula-style race car per each season. In Formula SAE two classes exist, Class 1 is for cars both racing and judged in static events and Class 2 is for cars that are only judged during static events.

Formula Student vehicles are divided into three categories: "Combustion" for vehicles powered by an Internal Combustion Engine, "Electric" for Battery Electric vehicles independently by their powertrain layout and since 2017/2018 season also "Driverless" where self-driving control strategies substitute totally the driver. For few years in the past also a category for Hybrid Electric Vehicle was racing, but today it is abandoned.

A Formula Student event has both a static and a dynamic part. The events composing the static part are: "Cost event" where the cost-performance trade-off is judged, "Design Presentation" where the engineering and design

aspects of the car are evaluated and the "Business Case Presentation" where the Team is in charge to develop a marketing analysis on their vehicle planning to sell small batch production of race cars and the business case developed is evaluated. Instead, the events composing the dynamic part are: "Acceleration" where the winner is the faster to complete a 75 m straight track starting from standstill, "Skidpad" where a circular track has to be completed in the shortest time, the "Autocross" or "AutoX" that is a quick lap where the winner is the faster to complete it, the "Endurance" where the car is requested to complete around 20-22 laps (25-30 km) with a driver change and without reporting any failures, finally the "Efficiency" where the energy consumption compared to the event race time is evaluated on the Endurance track. The dynamic events are the most valuable from a scoring point of view, in particular the efficiency.

Formula Student has a devoted rulebook, aimed mainly to give limitations to the power achievable and to impose safety rules. The compliance to this rulebook is checked before any race and it may be checked in every moment of the race.

Formula Student cars have no minimum weight and they have quite impressive performances, like more than 1 g of longitudinal acceleration during traction and more than 1.5 g during braking, also more than 2 g of lateral acceleration are recorded often. The vehicles changes every year with a lot of engineering and testing effort by all the teams, creating a very competitive environment.

## 1.2 Squadra Corse PoliTo

Politecnico di Torino has its own Team since 2005, called Squadra Corse PoliTo. Since its foundation, Squadra Corse designed and built almost one vehicle every year, seven of them are powered by an Internal Combustion Engine, one is a Hybrid Electric Vehicle, while the last six cars built are Battery Electric Vehicles. At the time of writing the Team is also designing a Driverless vehicle.

Amongst all those year plenty of different solution have been engineered by the students, bringing to a lot of success and victories.

## 1.3 SC18integrale project

SC18integrale is the vehicle presented by Squadra Corse PoliTo for the 2018/2019 racing season. It is a four-wheel drive Battery Electric Vehicle with four independent in-wheel motors.

The previous season was the first successful season for an electric vehicle designed and manufactured by Squadra Corse PoliTo, the car raced in three events all around the Europe, finishing all the Endurance events in every race and it also achieved the third place during the first race of the year, Formula SAE Italy held in Varano de' Melegari (PR).

The task of the 2018/2019 season was to further improve the results already obtained, trying to bring on track an even more performant car without losing the reliability achieved during the previous season.

SC18integrale is a four wheel drive Battery Electric Vehicle featuring a

carbon fiber monocoque, a high downforce aerodynamic package, a 600 V 7.8 kWh team developed battery pack capable of large discharge and charge currents. The motor are installed in-wheel and they are controlled by a team developed software. The peak power of the vehicle is 80 kW and it is limited by the rules.



Figure 1.1. SC18integrale

## Chapter 2

# Gear trains for Formula Student Electric cars

### 2.1 Solutions designed by Squadra Corse

#### 2.1.1 Before planetary gear trains

The SC12e is the first electric car designed by Squadra Corse. It is a 2 rear wheels drive with two Magneti Marelli TMG Small Size electric motors, the transmission is a twin chain drive with adjustable gear ratio from 4:1 to 6:1 [19].

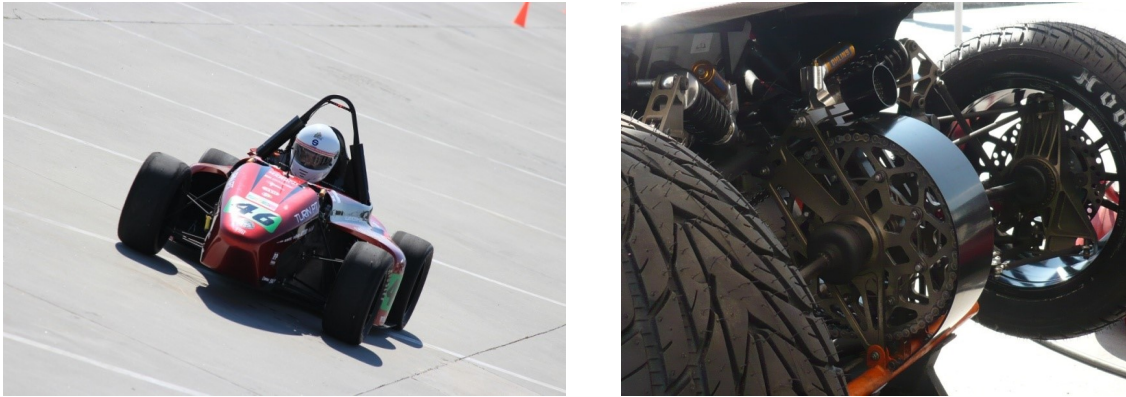


Figure 2.1. SC12e with its gear train [19]

The SCR (as the following SCRevo) is again a two rear wheels drive again powered by with two Magneti Marelli TMG Small Size electric motors installed transversally. This car had two twin gearboxes with double stage gears, the first of which is a bevel stage and 9:1 gear ratio [19].



Figure 2.2. SCR with its geartrain [19]

### 2.1.2 SCXV and SCXV Evo

The SCXV Evo is the upgraded version of the SCXV, those cars share indeed the same powertain layout and the same transmission.

The SCXV is the first four-wheel drive electric power vehicle designed by

Squadra Corse. The electric motor are installed in-wheel and the transmission is a dual-stage planetary one, with the input on the sun shaft, the ring gear fixed to the case and the output on the planetary carrier. The gear ratio is 16:1 [19].

This layout with the new concept of powertrain architecture was successful and a bit step forward for the team but it was quite heavy with respect to the other competitors, as the overall vehicle was.



Figure 2.3. SCXV with its gear train [19]

Regarding the gears data, this car featured gears with 1.25 mm normal module and  $25^\circ$  of pressure angle [19].

### 2.1.3 SCdiciassette

SCdiciassette is the vehicle that followed SCXV EVO. Giving the success of the powertrain architecture, it was not changed.

The basic concept of the transmission remained also the same: the transmission ratio was not changed and so the gear geometry. That year job was instead focused in solving some issues that the SCXV transmission had, achieving a good reliability, without any needs of service along the whole

season and it reducing the overall weight of the gearbox by working on FEA optimization of metallic components.



Figure 2.4. SCdiciassette with its gear train

## 2.2 Benchmark

Amongst the top teams the most widespread layout is the one with in-wheel motors with the gearbox in series to the motor and so adopting an epicycloidal layout. Only one team amongst them uses in-board motors.

In what follows a quick description of some of the world's top teams (before 2017/2018 season) powertrain and gearbox layouts is presented.

### 2.2.1 University Racing Eindhoven

URE is a Dutch team that has showed important innovations in the gearbox field for years. Their work was really inspiring for this project.

The interesting aspects of this transmission are numerous: the extremely thin normal module (0.7 mm), the weight reduction of the planet gears that evolves every year, the coupling between the two planet gears that is done through an involute profile and the asymmetrical wheel bearings.

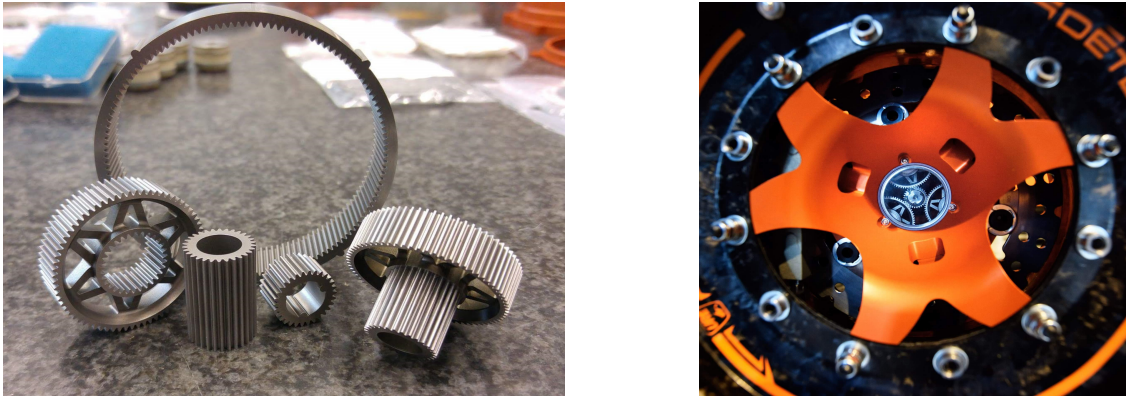


Figure 2.5. University Racing Eindhoven transmission

Source: University Racing Eindhoven’s Facebook page

The gears are manufactured through EDM so the gear profiles can be designed with large freedom and low manufacturing constraints.

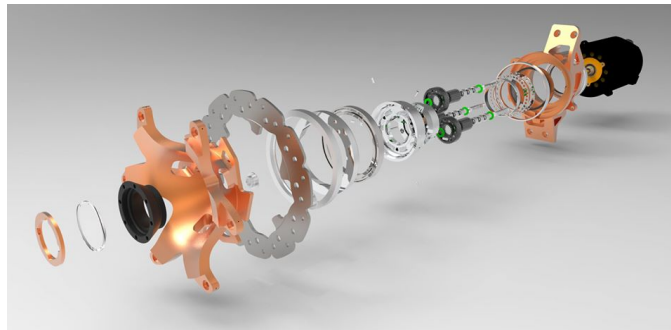


Figure 2.6. University Racing Eindhoven transmission

Source: University Racing Eindhoven’s Facebook page

### 2.2.2 AMZ Racing Team

AMZ Racing Team is a Swiss team and in 2017/2018 racing season led the World Ranking. The planetary carrier layout is very similar to the already described SCXV one, it is anyway lighter and more optimized.

It is worth noticing the team features custom design electric motors so from a gearbox point of view there is more freedom for the sun shaft design.

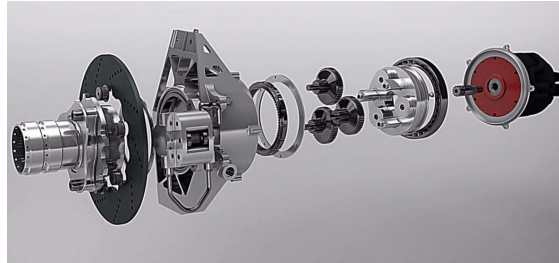


Figure 2.7. AMZ Racing Team transmission

Source: AMZ Racing Team’s Facebook page

### 2.2.3 DHBW Engineering Stuttgart e.V.

DHBW Engineering Stuttgart e.V. is another German team the features the epicycloidal gear train layout that is similar to SCXV one and very common among Formula Student Electric teams.

The optimization of the planet gears and the integration with the upright are interesting aspects.



Figure 2.8. DHBW Engineering Stuttgart e.V. transmission

Source: DHBW Engineering Stuttgart e.V.’s Facebook page

### 2.2.4 KA-RaceIng

KA-RaceIng is German team worthy to be mentioned because it lead the World Ranking for a lot of years until 2016/2017 racing season. This is the only car amongst top teams with on-board motors, the latter being an advantage for wheel package and unsprung mass reduction but being a serious issue of monocoque package and for suspension design due to the presence of drive shafts both at the front and at the rear axis.



Figure 2.9. KA-RaceIng wheel assembly

Source: KA-RaceIng's Facebook page



# Chapter 3

## Project Set-Up

### 3.1 SC18integrale wheel assembly

SC18integrale is the electric car built by Squadra Corse for the 2017/2018 racing season and the fourth four-wheel drive with in-wheel motors. This layout has been maintained since 2015 because it offers different advantages. The four-wheel drive allows to exploit at best the available traction force and it offers the best potential for the implementation of the torque vectoring control system.

The in-wheel motors offer a compact solution and avoid the motors volume to be subtracted to the internal volume of the monocoque and avoids a complex system as the drive shaft or a differential to be implemented. Those advantages come at the expense of a more complex wheel package and the necessity to route the motor cooling hoses and the motor power cables towards the wheel, mostly critical for the front steering wheels.

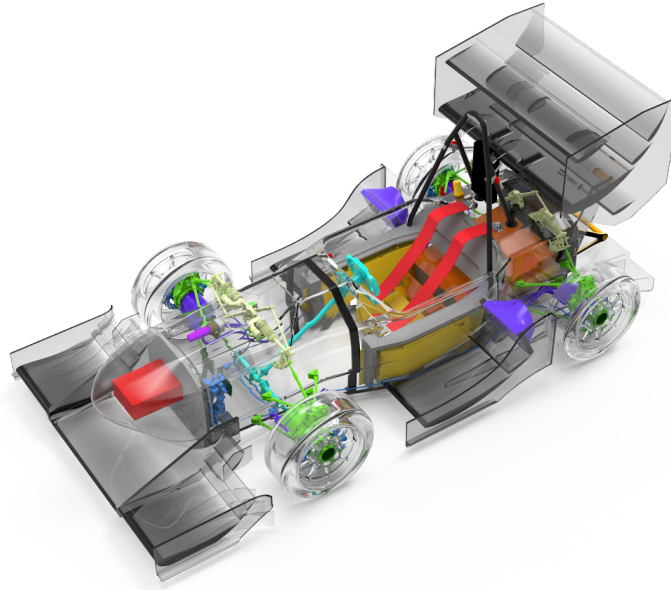


Figure 3.1. SC18integrale view

## 3.2 Target setting

The competitor teams of 2017/2018 had far lighter cars, the weight reduction of the vehicle is indeed one of the main targets of the SC18integrale project. The previous season gear train is an outdated project slightly modified and updated from its first release of 2015/2016 racing season; the competitors' transmissions were significantly lighter the Squadra Corse one. Moreover, since the vehicle features in-wheel motors with the transmission in series to the motor, a weight loss on the gear train means a weight loss in the unsprung masses that is further valuable. A weight reduction target of 30 % was set.

Along with the weight loss comes the reduction of the total volume of the

gear train in order to improve the integration with the vehicle. As already experienced with previous year's vehicles, in wheel motors represent a challenge in terms of packaging of the wheel assembly. A small package means more freedom for the suspension design (i.e. more room for the position of suspension hard points) and for the package of the caliper. A reduction target of 15 % was set for both the outer diameter of the transmission and its axial length.

The assembly of the SCdiciassette transmission was very demanding in terms of time. The procedure was also complicated so the risk of committing assembly mistakes were high. The serviceability role is even more relevant during testing and racing periods where the risk of having failures is high and the timeline is tight.

## 3.3 Gear train integration with the vehicle

### 3.3.1 Motors

The motors chosen are DD5-14-10-POW, supplied by AMK inside a kit developed for Formula Student applications that includes also the inverters. Those motors are synchronous three-phased machines, providing an extremely high power density. The peak power is 20 kW, the peak torque 21 Nm and the motor can reach the maximum rotational velocity of 20 000 rpm. The component weight is only 3.55 kg [20].

Below the characteristic curves of the motors are shown.

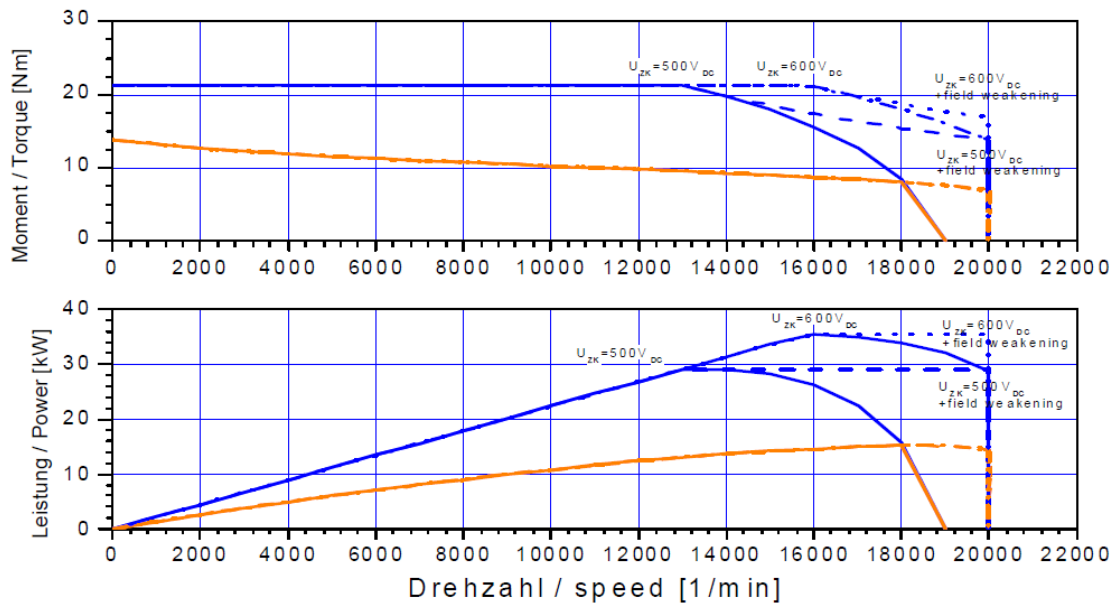


Figure 3.2. Characteristic curves of the AMK DD5-14-10-POW motor [20]

### 3.3.2 Wheel integration

As already mentioned, the motors are mounted in-wheel in the vehicle, with the output shaft coaxial with the gear train input one and of course of the wheel one. In order to achieve those results, the gear train must be integrated in the upright. The motor also is mounted on the upright by mean of a flange.

Anticipating some topics that will be dealt in more detail in the following sections, the planetary carrier is the output shaft of the gearbox, for this reason the planetary carrier is also the wheel hub. The wheel must be retained to the wheel hub and this is achieved by mean of a single locknut.

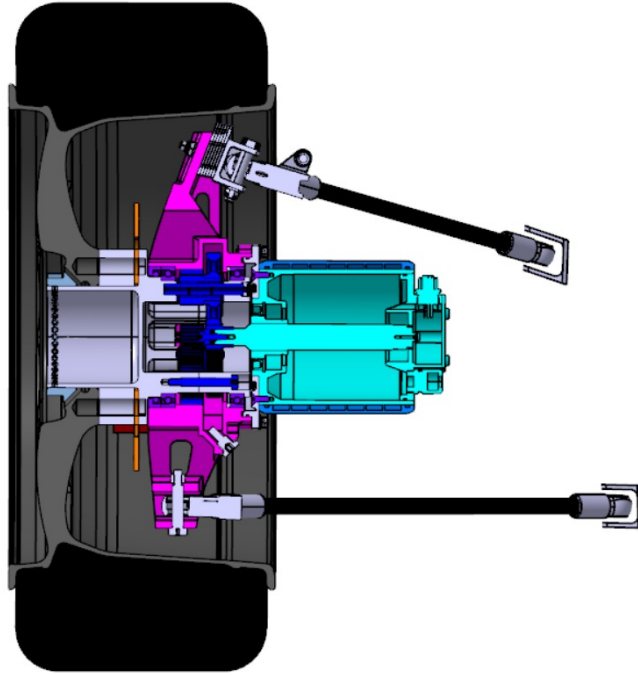


Figure 3.3. Section view of the wheel assembly

A more extensive description of how the transmission is integrated in the upright and how the latter component is designed can be found in [23].

### 3.4 Transmission ratio choice

Between SCdiciassette and SC18integrale the wheel radius is reduced from 265 mm to 245 mm due to tire model change. For this reason the optimal transmission ratio for the gearbox has to be re-evaluated.

The choice of the optimal transmission ratio is done using a lap time simulator and using a script that simulates the Acceleration test. The lap time simulator can evaluate both the performance and the energy consumption of the car.

The optimal transmission ratio resulted to be 15:1, which is lower with respect to SCdiciassette one that was 16:1. The simulated vehicle featuring 16:1 transmission ratio resulted to be slower on the lap time, while the vehicle equipped with 14:1 transmission ratio resulted slightly faster on the lap time but the acceleration performance was excessively impaired. 15:1 revealed to be the best trade off.

### 3.5 Layout choice

Aiming to reduce as much as possible the volume hence the weight of the gearbox it is apparent the advantage of the choice of a planetary gearbox. Anyway, by using a single stage planetary gearbox the volume of the transmission remains unacceptable for this project's purpose.

In order to minimize the volume of the gearbox it was chosen to use a dual stage planetary layout, with the input on the sun shaft, the output on the planetary carrier and the ring gear fixed to the case. Basically the sun gear transmits the motion to the first stage planet gears that are on the same shaft of the second stage planet gears, the latter meshing with the ring gear that is fixed to the case. The output of the gearbox is the planetary carrier.

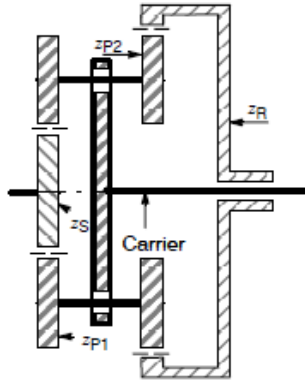


Figure 3.4. Dual stage planetary gearbox [1]

With reference to Figure the transmission ratio is equal to:

$$i = \frac{z_{P2}z_s + z_{P1}z_R}{z_{P2}z_s} \quad (3.1)$$

Below the schematic of the SC18integrale gearbox is shown.

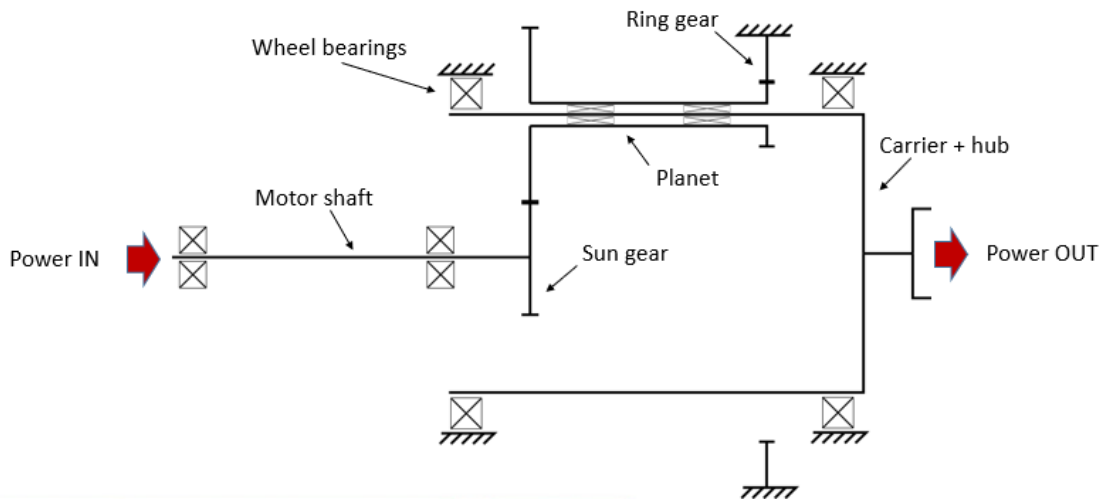


Figure 3.5. Schematic of the SC18integrale transmission

## 3.6 Meshing rule

When evaluating the various gears combination that satisfy the transmission ratio it must be taken into account that not every combination of gears can be assembled, especially for what concerns a double stage layout.

In order to guarantee the proper assembly, the number of teeth of all the four gears must respect the following rule:

$$\frac{z_S z_{P2} - z_R z_{P1}}{P\eta} = k \quad (3.2)$$

Where:

- $z$  the number of teeth are already defined in Section 3.5;
- $P$  is the maximum common divisor between  $z_{p1}$  and  $z_{p2}$ ;
- $\eta = 3$  is the number of planet gears;
- $k$  is an integer number.

It must be noticed that it can physically impossible to assemble the gearset even though the meshing rule is not respected, in particular if the teeth have large backlash. This is anyway not desirable because it brings to a wrong meshing condition, strongly impairing the load sharing between the gears, thus causing high reaction forces.

Finally, in order to guarantee the proper meshing, the three planetary gears couples must be phased equally.

### 3.7 Load spectrum and required service life

The power and torque demand of a Formula Student vehicle is very irregular during its duty life, for this reason sizing the mechanical components and in particular the gear wheels on the maximum load condition can bring to an unnecessary weight on the parts. Also, the torque can be either positive and negative due to the regenerative braking implementation.

For the abovementioned reasons is important to implement the calculations based on a reference load spectrum, that is iterated through the service life. The load spectrum used to develop the calculations regarding the gear life is extracted from an Autocross event, that is the most demanding working condition for the vehicle.

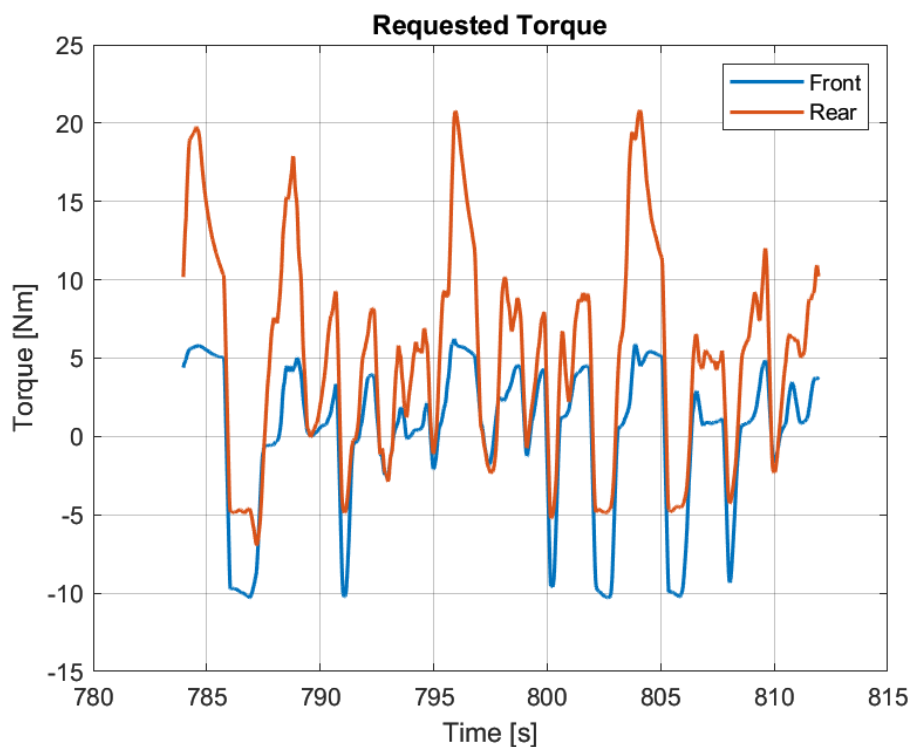


Figure 3.6. Example of load spectrum, showing both the front and the rear requested motor torque

From the graph shown is clear that the most stressed axle is the rear one (statistically the stress between the wheels of the same axle is equally distributed). This difference is mainly due to the fact that the vertical load on the front wheels is never enough to allow them to transfer the whole torque available to the ground. The scenario just described is clearly more apparent in traction conditions, where the overall weight balance that is slightly towards the rear axle and the load transfer brings to a large difference in the vertical load during acceleration.

During braking condition the weight transfer is towards the front axle and especially during hard braking, it allows the wheels to transfer a significant torque to the ground, however this condition doesn't make the front axle the most critical for gears sizing because the hydraulic brake torque is the main contributor to the overall brake torque (not the regenerative one), also in order not to impair too much the driver pedal feedback, the setting of the regenerative braking most of the times doesn't exploit the full capabilities of the electric motor.

Even though it could be possible to adopt two different transmission sizing between the front and the rear axis by downsizing the front ones, it was decided to realize only one type of gearbox for all the wheels in order to reduce the complexity of the project, given also the tight timeline of a project like that. Also the spare parts management is far easier by having only one type of gearbox.

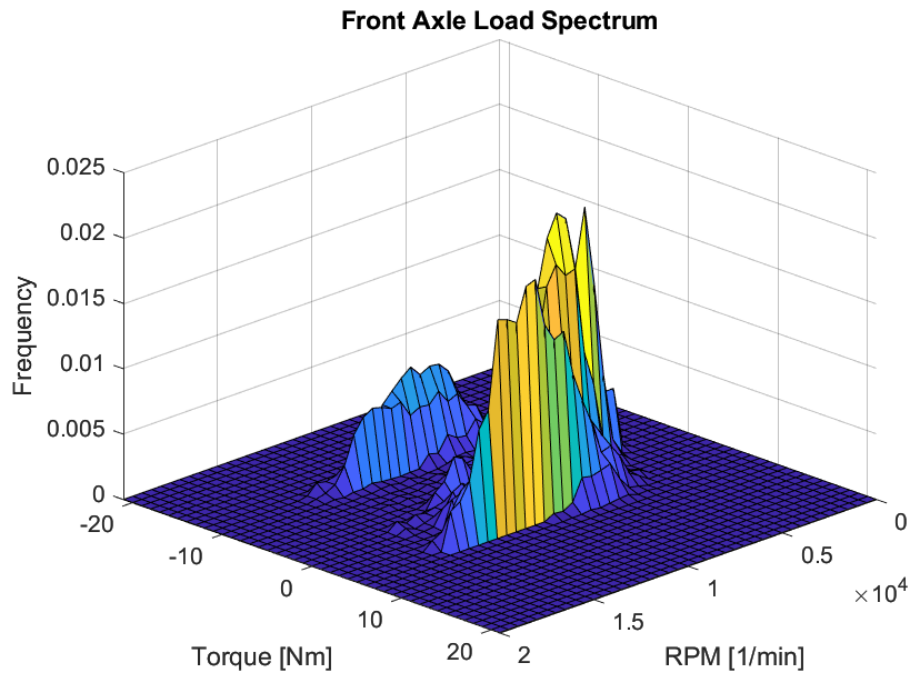


Figure 3.7. Front transmission load spectrum

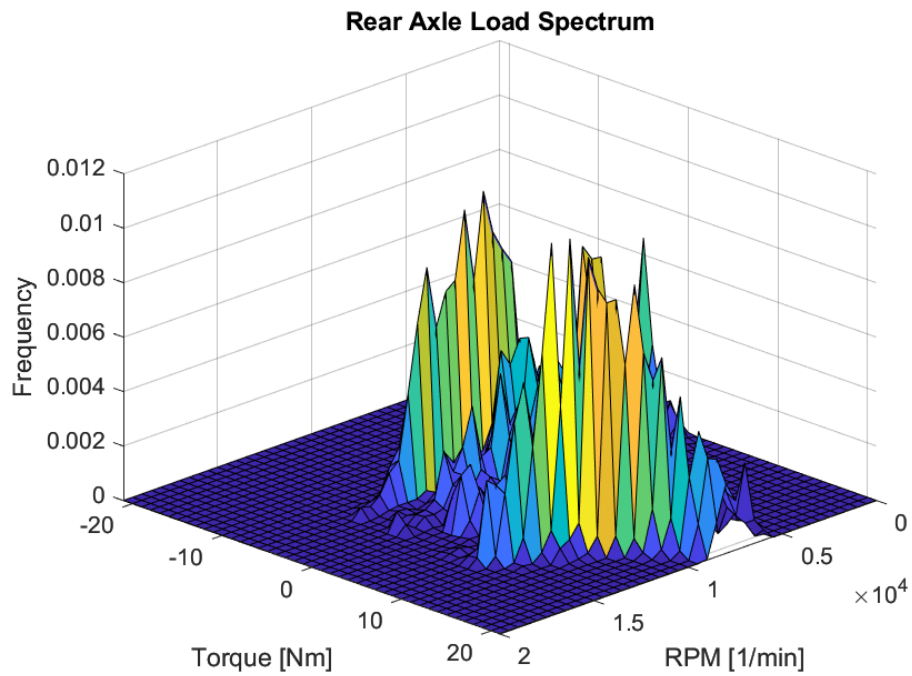


Figure 3.8. Rear transmission load spectrum

The required service life is estimated due to the unavailability of some log files of the SCdiciassette. Based on previous experiences and estimations a Formula Student vehicle life is subdivided in the following way.

- Races: 105 km (3 races each season, with an average of 35 km)
- Pre-seasonal test: 400 km;
- Mid-seasonal test: 300 km;
- Post-seasonal test: 600 km.

This results in an expected life that can be approximated to 1 500 km. Due to the fact that the average velocity of a Formula Student vehicle is around 40 km/h the required duty life expressed in hours is 37.5 h, being rounded up to 40 h for this project's purpose.

In conclusion, the whole gear set is sized on the iteration of a rear wheel load spectrum for 40 h.

### **3.8 Design flow**

After the targets are set, the transmission ration and the layout are chosen and the duty life with the load requirements are defined, the design of the gearbox can start. The process follows the logical path defined in the figure below.

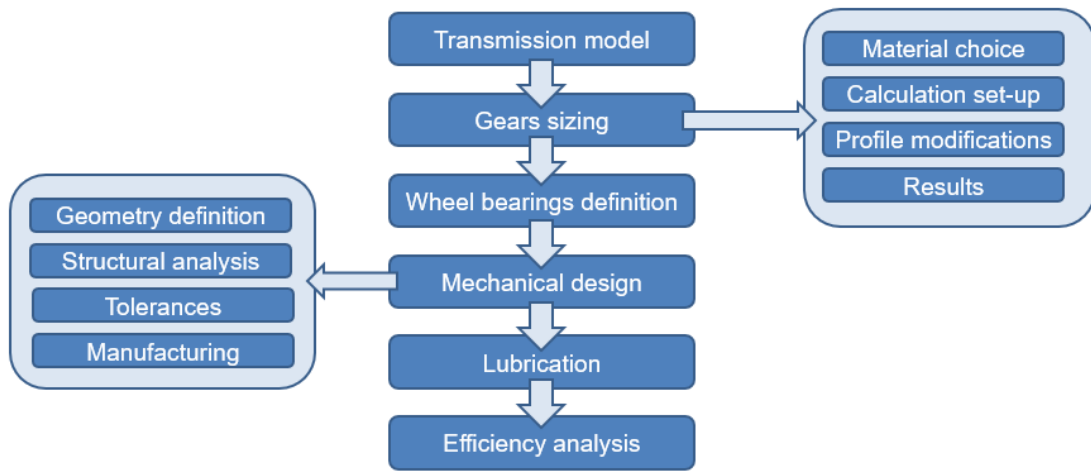


Figure 3.9. Design flow



# Chapter 4

## Transmission model

### 4.1 Introduction to KISSsys

The software used to model the transmission is KISSsys, that is a module of the software KISSsoft. KISSsoft is a popular software used for the sizing and the design of various mechanical components, from the a pair of meshing gears to shafts, bearings, springs and a lot of other components.

KISSsys is used to model more complex systems for example complete transmissions. In practice the full system is modelled into the KISSsys suite, while the calculations are performed by different KISSsoft sub-models recalled by the main KISSsys model. The common planetary geartrain has a devoted module in the KISSsoft suite with the characteristics of the gearbox are effectively modelled. A dual stage layout like the one described in the previous section should be then modelled in the KISSsys suite.

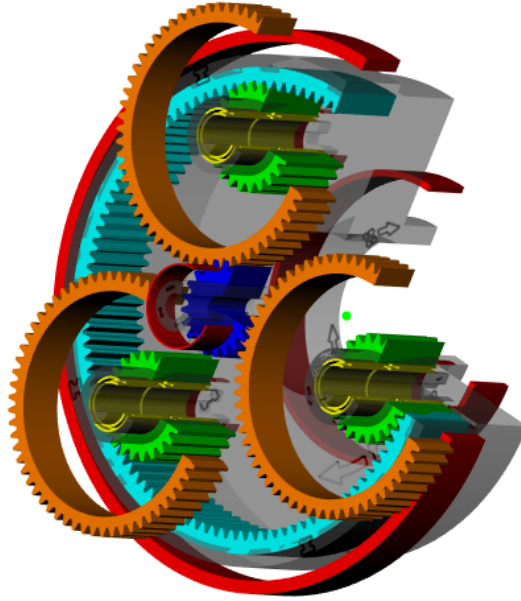


Figure 4.1. KISSsys model 3D view

## 4.2 SC18integrale transmission model

As already described in the previous section, the transmission layout is dual stage, with input on the pinion shaft, output on the planetary carrier and the ring gear fixed.

Below is described how this sort of gearbox is modelled in KISSsys suite.

### 4.2.1 Elements involved

In this section all the elements involved in the SC18integrale gearbox model are described briefly. In the following section the model build with all the specifications will be described in detail.

- Coaxial shafts: assembly of shafts sharing the same rotation axis;
- Shaft: general shaft, can be the support for different elements;

- Helical gear: representing a meshing gear (not bevel);
- Support: general support, constrains one of more degrees of freedom;
- Coupling: general coupling between different elements;
- Planet carrier coupling: coupling devoted to planetary gears;
- Speed or force constraints: constrains the speed, the torque or both of an element;
- Carrier-pin connection: connection between the planetary carrier and the planet pin shaft of an epicycloidal gear system;
- Connection roller bearing: bearing connecting two elements involved in the model, two parameters must be specified as an input, the inner and the outer race of the bearing;
- Coaxial shaft calculation module: sub-module in KISSsoft suite that carries the shaft calculation in terms of resistance, deformation, etc. . . ;
- Gear pair calculation module: sub-module in KISSsoft suite that carries the gear pair calculation.

### 4.2.2 Model build

First of all, the main gearbox folder is created, named “GB” in the tree [10]. After the main group is created, all the shafts needs to be added to it before adding bearings and cylindrical gears.

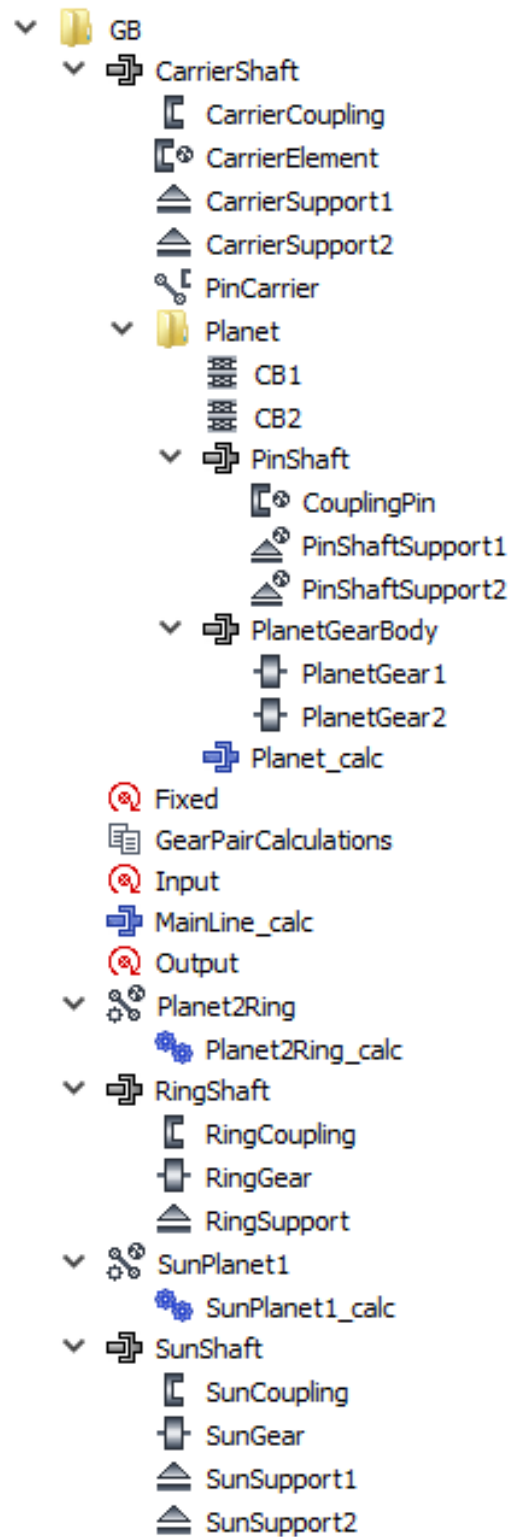


Figure 4.2. KISSsys model tree

The first coaxial shafts to be created are: the sun shaft (“SunShaft”), the carrier shaft (“CarrierShaft”) and the ring gear shaft (“RingShaft”). The subgroup “Planet” containing the model of the planet shaft needs then to be created and contained in it the two coaxial shaft representing the pin shaft (“PinShaft”) and the two planetary gears (“PlanetGearBody”).

At this point the various sub-elements must be added to each coaxial shaft.

Starting from “SunShaft” coaxial shaft the following machine elements must be added:

- One coupling (“CouplingSun”);
- Two supports (“SunSupport1”, “SunSupport2”);
- One helical gear (“SunGear”).

“RingShaft” coaxial shaft:

- One coupling (“CouplingRing”);
- One support (“RingSupport”);
- One helical gear (“RingGear”).

The coupling between the pin shafts and the planetary carrier occurs without velocity slipping and has a devoted type of element in KISSsys suite, the “planet carrier coupling”.

“CarrierShaft” coaxial shaft:

- One coupling (“CarrierCoupling”);
- One planet carrier coupling (“CarrierElement”);

- Two supports (“CarrierSupport1”, “CarrierSupport2”).

“PinShaft” coaxial shaft:

- One planet carrier coupling (“CouplingPin”);
- Two carrier-pin connection (“PinShaftSupport1”, “PinShaftSupport2”).

“PlanetGearBody” coaxial shaft:

- Two “helical gears” (“PlanetGear1”, “PlanetGear2”).

After all the elements have been created, the next step is to define the constraints between those elements:

- Gear meshing constraints between the sun and the first stage planet gear and the second stage planet gear and the ring gear;
- Needle roller bearings connecting the pin shaft to the planet gears;
- Coupling between the planetary carrier and the planet pin shaft.

The element involved in the gear meshing constraint is the “planetary gear pair constraint”. It is important to use it instead of the normal “gear pair constraint” because it considers the fact that the sun gear and the ring gear sustain three load cycle per each load cycle of a planet gear. In the three the first stage “planetary gear pair constraint” between the sun and the planet is called “SunPlanet1” while the second stage one is called “Planet2Ring”. In the coupling interface the user can choose the configuration of the coupling (sun/planet, planet/ring and planet/planet), gears involved in the coupling, the number of planets and the efficiency of the coupling.

The element used to represent the needle roller bearings between the pin shaft and the planet gears shaft is called “connection roller bearings” and it

allows to choose the two elements to be connected (“CB1” and CB2” in the model tree).

Finally, the coupling between the planetary carrier and the planet pin shaft is modelled with the coupling constraint. The latter allows to connect without slip the in shaft with the planetary carrier.

In order to define the kinematics of the gearbox, it is needed to define the input element, the output element the element fixed to the case. For all of them the element to be selected is the “speed or force input”. This element allows to choose an element belonging to a coupling a constraining its speed, its torque, or both to a certain amount and it allows to precise if the element is an input one (driving) or an output one (driven).

In this transmission’s case the input is via the sun shaft that is so constrained in speed and in torque. It is important to precise that the speed and the torque entity must be the peak ones, they will be scaled in the calculation module according to the load spectrum. Clearly the sun shaft is the driving element.

The ring gear is fixed, so its speed must be constrained to 0 rpm. Finally, the output is on the planetary carrier shaft so it must be a non-constrained driven element.

Below is shown how the diagram appears at this stage of the model, with all the element and constraints described up to now that can be visualized.

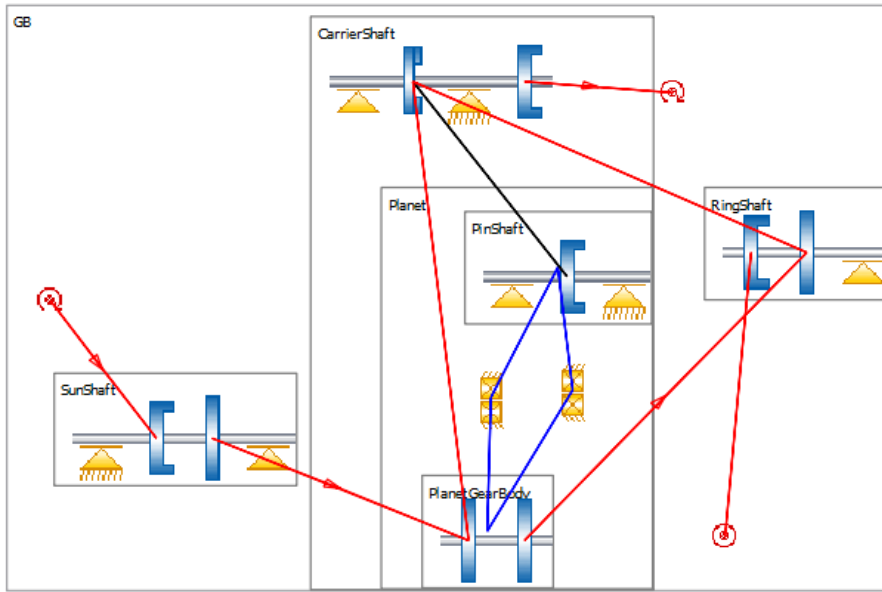


Figure 4.3. Diagram of the transmission model

## 4.3 Calculation modules

Different calculation modules can be linked to KISSsys transmission model. For this project the ones involved are described below.

### 4.3.1 Coaxial shafts calculation

This module offers an interface to model a system of coaxial shafts. Geometrical parameters, materials and load cases can be defined here. It is associated to each coaxial shafts system present in KISSsys model.

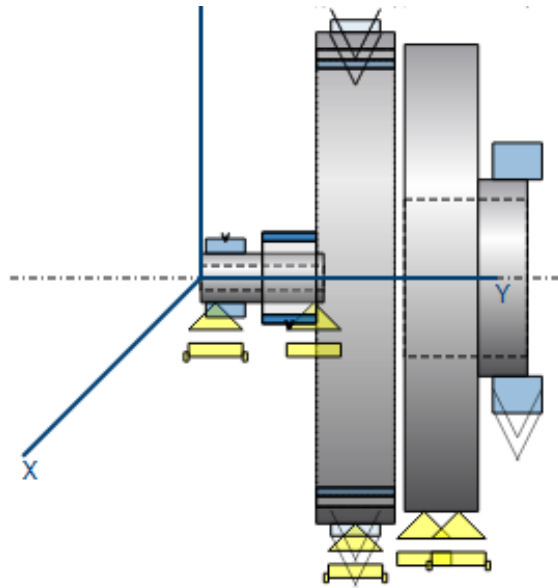


Figure 4.4. Main line calculation module

After running the calculation the maximum deflection and the maximum equivalent stress can be visualized along with the bearing data like the static safety factor, the minimum service life and the reaction forces. A more detailed post-process interface is also present in order to have a more complete overlook on the results both for the shafts and the bearings. Here different plots are generated: displacement, bending angle, equivalent stress and so on.

In this model, two systems of coaxial shafts are present:

- Main line: including the sun gear, the planetary carrier and the ring gear
- Planet shaft: including the planetary gears and the pin shaft

### 4.3.2 Gear pair calculation module

The shaft calculation module offers a tool to model a meshing gear pair by mean of its geometry, the production tolerances and the load ratings.

It is associated to the Gear Pair Constraint present in the KISSsys suite. It carries the constraints and the boundary conditions present in the overall transmission model, for example the number of load cycles per each gear.

Further detail will be discussed in the following section, dedicated entirely to the gear calculation.

# Chapter 5

## Gear life calculation

### 5.1 Introduction to KISSsoft

KISSsoft is a software tool able to perform different kinds of calculations regarding various mechanical components. Just to mention some of them: cylindrical gear pairs, bevel gear pairs, planetary gears, shafts, bearings, splines, etc. All the calculations are carried in an analytical way.

The "cylindrical gear pair" module allows to determine the geometry and verify the resistance to loads of a gear given as an input some geometrical parameters like the centre distance, the number of teeth (so the transmission ratio) and so on. Through different sections of the interface, all the needed input parameters can be specified.

KISSsoft allows also to find a solution of gear pair size given the load rating as an input and geometrical boundary constraints. For example the range of normal module or the range of centre distances amongst which the solution must lie.

Below the main sections of the "cylindrical gear pair" calculation model are explained in better.

### 5.1.1 Basic data

In the “Basic data” section the gear geometrical parameters are given as an input or they are calculated by the software. Here the normal module, the helix angle (if any), the centre distance, the number of teeth, the facewidth and the profile shift coefficients can be partially an input for the user and partially they can be determined by the calculations performed by the software to match the user requirement.

Other parameters that must be given as input in this section are the gear quality according to ISO 1328:1995, the gears material, the lubricant and the type of lubrication and are used by the software to perform the calculation.

In general in this section all the main parameters that define the gear are present.

### 5.1.2 Reference profile

In the “Reference profile” sections, as the name suggests, the parameters defining the reference profile are present. The reference profile can be chosen amongst different norms, one of the most common is the ISO 53:1998 Profile A, where the dedendum coefficient is set to 1.25, the addendum coefficient is set to 1.00 and the root radius coefficient is set to 0.38. From a manufacturing point of view, the “Reference profile section” allows also to generate the profile of the tool (hobbing cutter or pinion cutter) to be used.

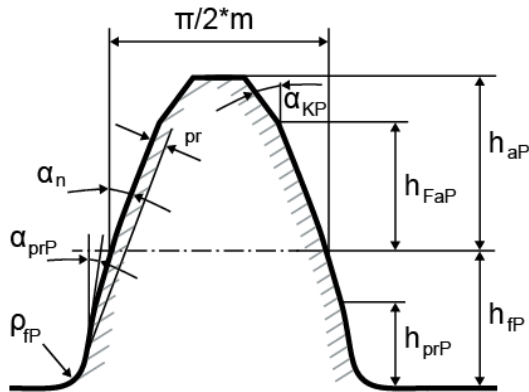


Figure 5.1. Reference profile [9]

### 5.1.3 Tolerances

In the “Tolerances” section, the tolerance class of the gears can be chosen amongst different norms and the centre distance tolerance can be specified. Care must be taken because the tolerance class impacts the calculation.

### 5.1.4 Rating

In the “Rating” section all the data regarding the load cases of the gear pair is present. Power, torque, speed, required service life and application factor  $K_a$  can be given as input. There is also the possibility to select a load spectrum or to insert a custom load spectrum.

The calculation method can be selected between ISO, DIN, AGMA standards and so on.

### 5.1.5 Factors

Finally, in the “Factors” section the user can modify the factors involved into the calculation. Just to mention some:  $K_A$ ,  $K_{H\beta}$ ,  $K_{H\alpha}$ ,  $Z$ ,  $Y$  factors.

### 5.1.6 Output plots

Various output plots can be generated after the calculations have been performed. The following figure is helpful to understand the main dimensions of a cylindrical gear and gives a representation of the main points present of the contact line (A, B, C, D, E) that are often indicated in the output plots.

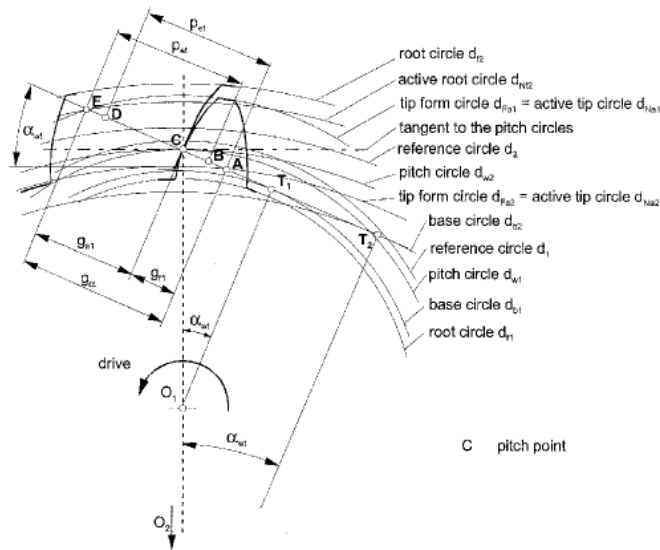


Figure 5.2. Length of path of contact for a cylindrical gear [9]

## 5.2 ISO 6336:2006 Standard

ISO 6336:2006 Standard was published in 1997 and updated in 2006 and provides a system for the calculation of the load capacity of cylindrical involute gears with external or internal teeth. In the formulae used for load capacity calculations factors influencing gear pitting and fractures at tooth fillet are present, by modifying those factors or adding other factors new knowledge can be implemented in the formulae [2].

The load capacity is evaluated both from a pitting point of view and from

a tooth breakage point of view. Consequently two different safety factors are considered:  $S_H$  is the one relative to pitting and  $S_F$  the one relative to tooth breakage. The safety factor is defined as:

$$Safety\ factor = \frac{Modified\ allowable\ stress\ number}{Calculated\ stress} \quad (5.1)$$

The allowable stress number is "modified" due to the corrective factors discussed before.

Three different calculation methods are considered by this standard [2]:

- Method A: factors involved in the calculations are derived from full-scale load tests, precise measurements or comprehensive mathematical analysis of the transmission system on the basis of proven operating experience, or any combination of these. This method can be the most accurate one but it is seldom used due to less research with respect to methods B and C and a large and costly experimental plan is required;
- Method B: factors are derived with sufficient accuracy for most applications, assumptions involved in their determination are listed. In each case, it is necessary to assess whether or not these assumptions apply to the conditions of interest. This is the most commonly used method;
- Method C: calculation based on simplified assumptions for some factors, assumptions under which they are determined are listed. On each occasion an assessment should be made as to whether or not these assumptions apply to the existing conditions. Its accuracy is lower with respect to method B.

"Experimental investigations ([5] and [6]) has proven that ISO 6336 standard is not accurate for modules below 5mm because it tends to underestimate the strength of the tooth as the module is reduced. The calculation

method involves factors which purpose is to take into account the size of gears only if the module is increased, but no standard rules are defined for module decrease. Cited research have proven that teeth in gears with fine module may be even 30% stronger than predicted by the calculation and even a correction factor of 1.29 has been proposed in [6] for carburized gears with  $m_n=1.0$  mm" [21].

The standards is not updated at the moment of writing and since the calculation is based on it, the results obtained can be considered rather conservative.

### 5.2.1 Pitting load capacity

The pitting stress is in general given by [2]:

$$\sigma_H = A_1 \sqrt{\frac{F_t}{d b} \frac{u+1}{u}} \quad (5.2)$$

From this, the permissible contact stress can be computed:

$$\sigma_{HP} = A_2 \frac{\sigma_{Hlim}}{\sigma_{Hmin}} \quad (5.3)$$

Where:

- $A_1, A_2$  are products of various factors;
- $u$  is the gear ratio;
- $b$  is the facewidth;
- $d$  is the gear reference diameter;
- $F_t$  is the nominal tangential load;
- $\sigma_{Hlim}$  is the maximum allowable pitting stress;
- $\sigma_{Hmin}$  is the minimum required pitting safety factor.

### 5.2.2 Fracture load capacity

The fracture stress is in general given by [2]:

$$\sigma_H = B_1 \frac{F_t}{b m_n} \quad (5.4)$$

From this, the permissible fracture stress can be computed:

$$\sigma_{FP} = B_2 \frac{\sigma_{Flim}}{\sigma_{Fmin}} \quad (5.5)$$

Where:

- $B_1, B_2$  are products of various factors;
- $m_n$  is the normal module;
- $b$  is the facewidth;
- $F_t$  is the nominal tangential load;
- $\sigma_{Flim}$  is the maximum allowable fracture stress;
- $\sigma_{Fmin}$  is the minimum required fracture safety factor.

## 5.3 Material choice

The main target of this project is to reduce the weight and the volume of the gearbox. One way to drastically reduce the weight is to change material with respect to SCdiciassette transmission so switching from steel alloys to aluminium or titanium alloys or even to plastic gears.

An analysis regarding the usage if aluminum alloys was performed on the first stage gears (meshing between the sun gear and the first planet gear)

giving the load rating conditions as an input and evaluating the various solutions proposed.

The material chosen for this analysis is the only aluminum alloy present in the software database, whose main properties are listed in the table below.

EN AW AlSi1MgMnT4	
Material type	Wrought aluminum
Type of treatment	Untreated
Surface hardness	65.0 HBW
Core hardness	65.0 HBW
$R_m$	205.0 MPa
$R_p$	205.0 MPa
$E$	80000.0 MPa
$\sigma_{Flim}$	160.0 MPa
$\sigma_{Hlim}$	260.0 MPa

Table 5.1. EN AW AlSi1MgMnT4 properties [2]

Below two scatter plots are shown: on both plots  $SH_{min}$  (minimum root safety between the two gears) is represented on the X axis and  $SH_{min}$  (minimum flank safety between the two gears) is represented, while in the first plot the normal module is color scaled and in the second plot the centre distance is color scaled.

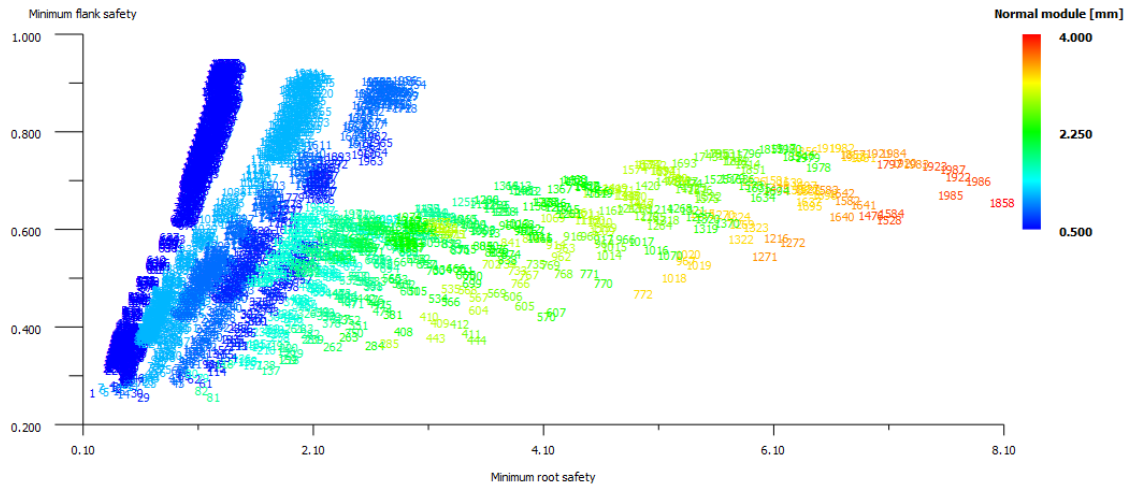


Figure 5.3. Solutions for aluminum gears scattered as a function of the normal module

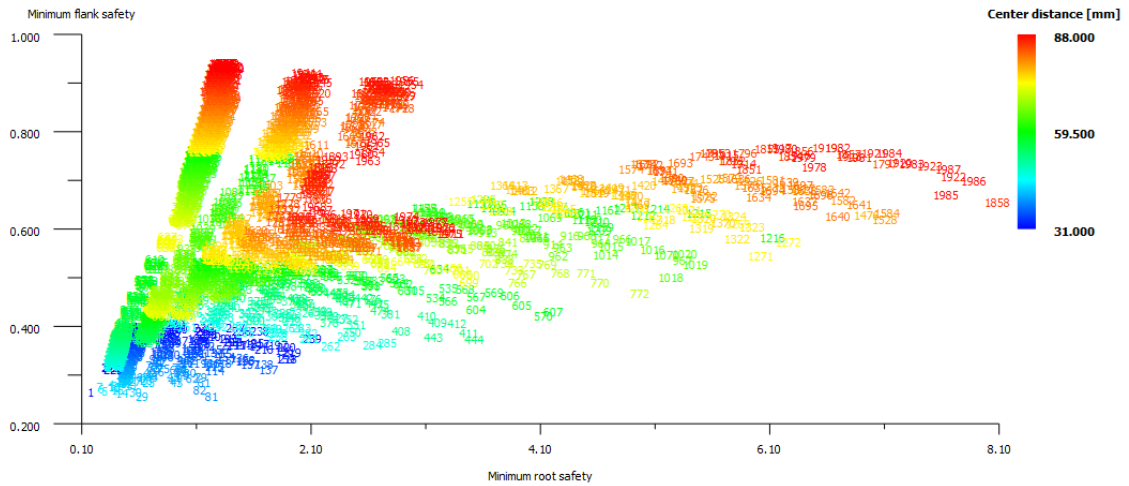


Figure 5.4. Solutions for aluminum gears scattered as a function of the centre distance

In order to achieve both  $SH_{min}$  and  $SH_{min}$  close or equal to 1 it is apparent that the volume of the transmission resulted even larger with respect to SCdiciassette one, becoming unacceptable for the project. Clearly with plastic gears, this situation is even worse.

Moreover, the gear manufacturer involved in the project has a large experience with steel alloy gears and heat treatments thus driving the material choice amongst steel alloys.

Having chosen to use steel alloys to produce the gears, it is beneficial to use the most performing alloy available in order to maximize the resistance of the components and consequently to minimize the material in the gear.

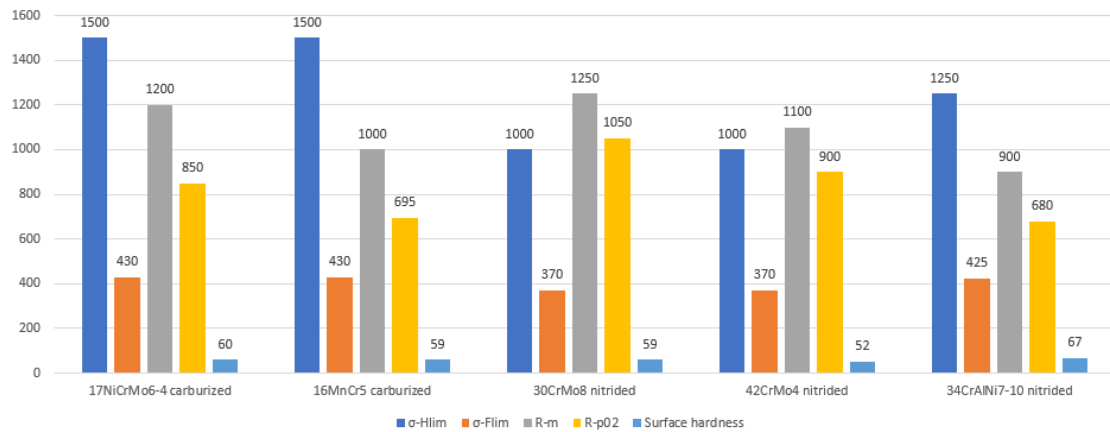


Figure 5.5. Properties comparison of case-hardening steels commonly used for gears manufacturing

EN 17NiCrMo6-4 (UNI 18NiCrMo5) carburized is chosen for all the external gears (pinion, planet gears) because of its properties and because is largely available between gears suppliers. In the table below its properties are shown.

17NiCrMo6-4	
Material type	Case-hardening steel
Type of treatment	Case-hardened
Surface hardness	61.0 HRC
Core hardness	325.0 HBW
$R_m$	1200.0 MPa
$R_p$	850.0 MPa
E	206000.0 MPa
$\sigma_{Flim}$	460.0 MPa
$\sigma_{Hlim}$	1500.0 MPa

Table 5.2. 17NiCrMo6-4 properties [2]

As shown in the graph reported below, the temperature at which the external gears are case-hardened is elevated (around 870 °C in this example), thus causing substantial distortions of the material and requiring consequently to be grinded after the heat treatment in order to make to tooth profile respect the tolerances imposed.

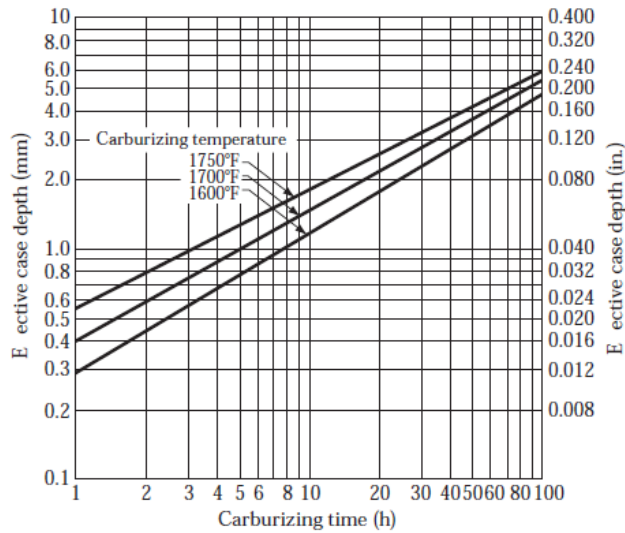


Figure 5.6. Nominal time and temperature requirements for different case depths [3]

It is apparent that in order to have a uniform durability of the gears in terms of pitting safety factor, it is necessary to have all the gears with a similar surface hardness. Not all the manufacturers are indeed capable to grind an internal gear, in this case, this process was impossible to be executed on the ring gear.

Nitridation instead is a process that occurs at lower temperatures, avoiding the gear to be grinded after the heat treatment. As a reference in the table below the parameters regarding AISI 4140 steel (EN 42CrMo4) are shown, the nitriding temperature (around 524 °C) is substantially lower with respect to the carburizing temperature.

Steel	Nitriding temperature	Case hardness	Core hardness
AISI 4140	975 °F	49-54 HRC	27-35 HRC

Table 5.3. Nominal temperatures used in nitriding and hardness obtained [3]

For the reasons mentioned above, the ring gear is decided to be nitrided after cutting without being grinded after the heat treatment. Clearly the same quality and the same tolerances of the grinded gears cannot be achieved for the ring gear.

Initially 34CrAlNi7-10 was chosen because the surface hardness reachable after the heat treatment is very high and it is really similar to the other gears. Below the properties of the mentioned material are shown.

34CrAlNi7-10	
Material type	Nitriding steel
Type of treatment	Gas-nitrided
Surface hardness	950.0 HV
Core hardness	950.0 HV
$R_m$	800.0 MPa
$R_p$	600.0 MPa
E	206000.0 MPa
$\sigma_{Flim}$	425.0 MPa
$\sigma_{Hlim}$	1250.0 MPa

Table 5.4. 34CrAlNi7-10 properties [2]

Although optimal for the calculations carried, this material was unavailable for the manufacturer of the gears so the choice was forced on 42CrMo4 steel nitrided. In the table below its properties are shown.

42CrMo4	
Material type	Through hardening steel
Type of treatment	Nitrided
Surface hardness	550.0 HV
Core hardness	210.0 HBW
$R_m$	1100.0 MPa
$R_p$	900.0 MPa
E	206000.0 MPa
$\sigma_{Flim}$	370.0 MPa
$\sigma_{Hlim}$	1000.0 MPa

Table 5.5. 42CrMo4 properties [2]

## 5.4 Calculation set-up

As seen in 5.3, the material chosen is 17NiCrMo6-4 carburized for all the external gears and 42CrMo4 nitrided for the ring gear.

It was chosen to have a pressure angle of  $20^\circ$  (SCdiciassette gears had a pressure angle of  $25^\circ$ ) because it is beneficial both for efficiency and manufacturing reasons. It must be noticed that it was decided to increase by the facewidth of the driving wheels (and also the smaller ones), i.e. the sun gear and the second stage planet gears, with respect to the driven gears. This aiming to ensure that the minimum facewidth computed is always in contact in order to avoid a reduction of the contact surface under load.

The quality level according ISO 1328:1995 is set to 5 for all the external gears, having discussed with the manufacturer that is possible to achieve this level of quality for grinded gears. The ring gear cannot be grinded with the manufacturer's equipment, so its quality level is set to 7. This parameter must be chosen carefully after knowing what the capabilities of the manufacturer are because its impact on the calculation is significant.

The oil chosen is the ISO-VG 68 (the lubrication topic will be dealt in more detail in Section 9) and the lubrication is set to be “oil bath lubrication” according to the real working condition of the gearbox.

The reference profile chosen is the ISO 53:1998 Profile A, where the dedendum coefficient is set to 1.25, the addendum coefficient is set to 1.00 and the root radius coefficient is set to 0.38.

The tooth thickness tolerance is set according to the class 3967 cd25, that according to Niemann proposal is suitable for standard machine parts with a module  $0.5 \text{ mm} < 3 \text{ mm}$ .

For this project the load condition is given by the load spectrum discussed in Section 3.7 that scales the peak input values of 21 Nm torque and 20000 rpm speed per each time step. The required service life has been set to 40 h.

Moreover, due to the detailed knowledge of the load history of the gearbox and due to its low possibility to vary from those conditions, the application factor  $K_A$  has been set to 1.0.

Finally, the following considerations has been made regarding the corrective coefficients:

- Dynamic factor  $K_V$ : calculated by the software through the load spectrum data per each voice of the latter;
- Transverse load factor  $K_{H\alpha}$ : calculated by the software through the load spectrum data per each voice of the latter;
- Face load factor  $K_{H\beta}$ : calculated according to ISO 6336 by the software giving as input the type of pinion shaft and the tooth trace modification (if any);
- Alternating bending factor (mean stress influence coefficient)  $Y_M$ : calculated for an oscillating stress.

Regarding  $K_{H\beta}$  coefficient calculation, the pinion type is different between the two stages. In particular, according to Figure 5.7:

- 1<sup>st</sup> stage: C;
- 2<sup>nd</sup> stage: E.

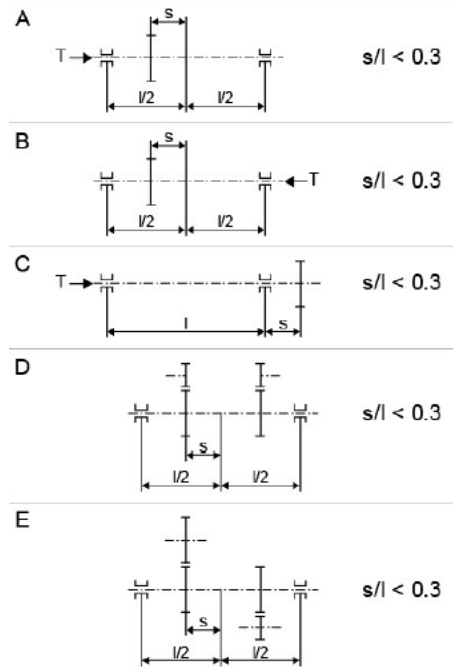


Figure 5.7. Type of pinion shaft according to ISO 6336 Picture 13e [2]

Also, all the gears are manufactured with an end relief. In Section 5.5 the purpose of this tooth modification is shown.

ISO 6336-1:2006		KISSsoft
1	None	None
2	Central crowning only [ $C_\beta = 0.5 \cdot f_{ma}$ ]	Slight crowning [ $C_\beta = 0.5 \cdot f_{ma}$ ]
3	Central crowning only [ $C_\beta = 0.5 \cdot (f_{ma} + f_{sh})$ ]	Crowning [ $C_\beta = 0.5 \cdot (f_{ma} + f_{sh})$ ]
4	Helix correction only	Helix angle modification
5	Helix correction plus central crowning	Crowning with helix angle modification
6	End relief	End relief
	Full helix modification [Eq. (56)]	Optimal tooth trace modification

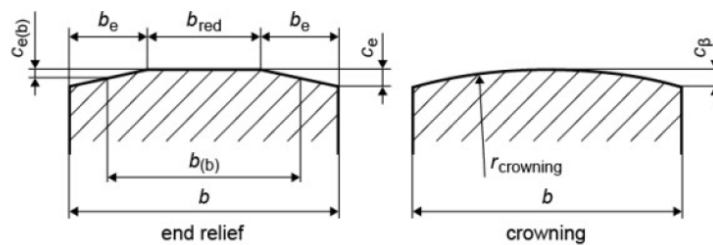


Figure 5.8. Tooth trace modification [2]

Regarding the alternating bending factor calculation  $Y_M$ , with reference to Figure 5.9 and considering an average oscillating cycles number of 210 per the sun gear and of 70 for the second planet gear the following equation is used [7].

$$Y_M = 0.85 - 0.20 \frac{\log(N_{rev})}{6} \quad (5.6)$$

Giving the following results:

- $Y_M = 0.773$  for the first stage;
- $Y_M = 0.788$  for the second stage.

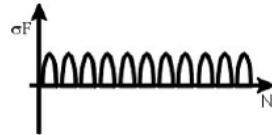
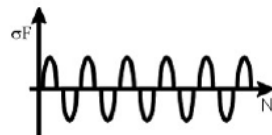
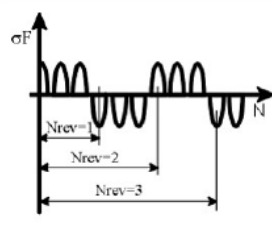
Operating Mode	Alternating Bending Factor (Mean Stress Influence Factor) $Y_M$	Load Direction
Pulsating	1	
Alternating	0.7 <sup>(1)</sup> 0.65 <sup>(2)</sup>	
Oscillating	$0.85 - 0.15 \cdot \frac{\log N_{rev}}{6}$ <sup>(1)</sup> $0.85 - 0.20 \cdot \frac{\log N_{rev}}{6}$ <sup>(2)</sup> ( $1 \leq N_{rev} \leq 10^6$ ) 0.7 <sup>(1)</sup> 0.65 <sup>(2)</sup> ( $N_{rev} \geq 10^6$ )	
(1) Linke, H.: Stirnradverzahnung, Carl Hanser Verlag, 1996. (2) Linke, H.: Stirnradverzahnung, Carl Hanser Verlag, 2010.		

Figure 5.9. Alternate load factor determination [9]

## 5.5 Results

### 5.5.1 Final geometry definition

After some calculation loops, the following solution resulted to be the one that matched more all the targets imposed.

First stage			
Normal module		$m_n$	0.8 mm
Pressure angle at normal section		$\alpha_n$	20°
Centre distance		a	33.8 mm
		Gear 1	Gear 2
Number of teeth	z	21	63
Facewidth	b	11.0 mm	10.0 mm
Profile shift coefficient	$x^*$	0.3500	-0.0945
Quality (ISO 1328:1995)	Q	5	5
Material		17NiCrMo6-4	17NiCrMo6-4

Table 5.6. First stage data

Under load the tooth is deformed and its profile is not an involute anymore, also the profile is changed from the ideal one due to manufacturing errors and the teeth in contact can be one or two (the latter for most of the time) [8].

Profile modifications tip relief aims to reduce the irregularity of the loads acting on the gear during meshing (i.e. the transmission errors), achieving a more regular meshing is beneficial both from noise and resistance point of view. One possible profile modification is the tip relief. Tip relief on the driven gear reduces the entry impact, whereas tip relief on the driving gear reduces the exit impact. Tip relief is therefore usually applied to both gears [9].

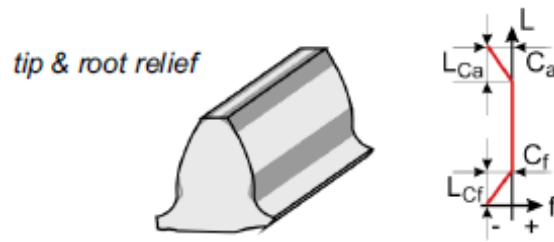


Figure 5.10. Tip and root relief [8]

The optimal tip relief can be computed by KISSsoft according to various methods, in this case the linear method has been chosen and the a tip relief of  $8\mu m$  ( $C_a$  in Figure 5.10) with a length of  $7\mu m$  ( $L_{Ca}$  in Figure 5.10) is obtained for the first stage gears, also a 0.2 mm chamfering of the tooth end is proposed. Below the plot of the normal forces acting on the tooth flank on the first stage gears both with and without end relief modification are shown, the smoothness difference is apparent.

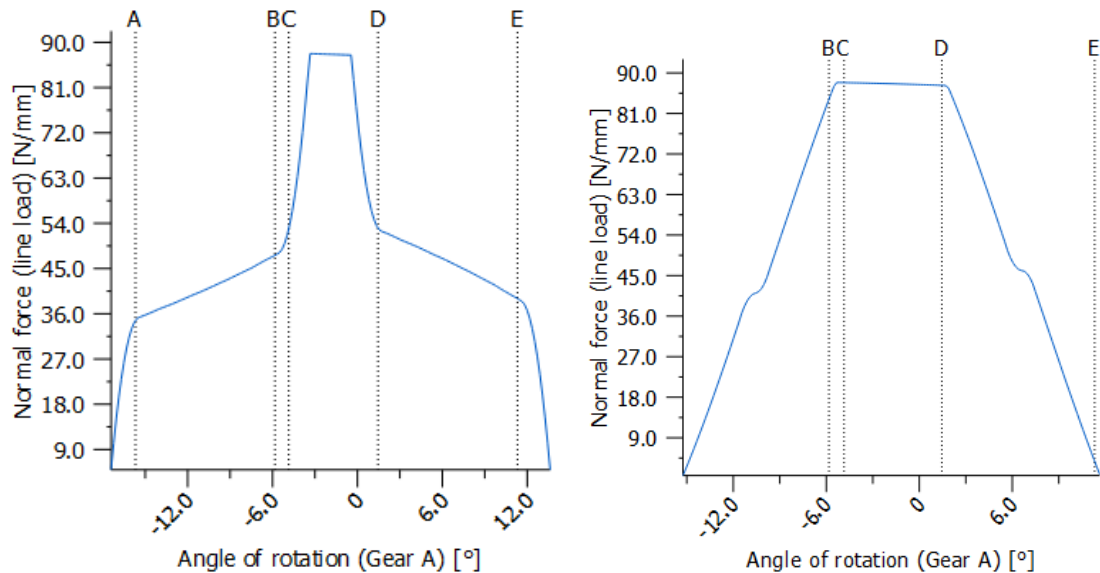


Figure 5.11. First stage without (left) and with (right) tip relief modification

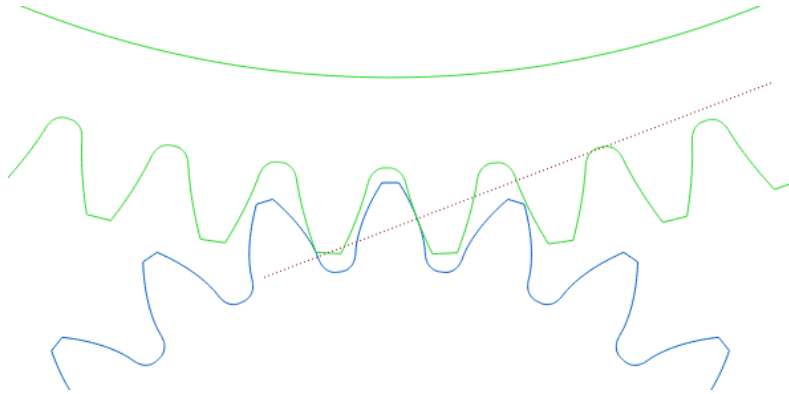


Figure 5.12. First stage meshing gears

		Second stage	
Normal module		$m_n$	0.8 mm
Pressure angle at normal section		$\alpha_n$	20°
Centre distance		a	-33.8 mm
		Gear 1	Gear 2
Number of teeth	z	24	-108
Facewidth	b	17.0 mm	16.0 mm
Profile shift coefficient	$x^*$	0.4976	-0.7531
Quality (ISO 1328:1995)	Q	5	7
Material		17NiCrMo6-4	42CrMo4

Table 5.7. Second stage data

Also for the second stage the linear method has been chosen and the a tip relief of  $11\mu\text{m}$  ( $C_a$  in Figure 5.10) with a length of  $10\mu\text{m}$  ( $L_{Ca}$  in Figure 5.10) is obtained, also a 0.2 mm chamfering of the tooth end is proposed. In the following, as for first the first stage, also for the second stage are shown the plots of the normal forces acting on the tooth flank both with and without end relief modification are shown.

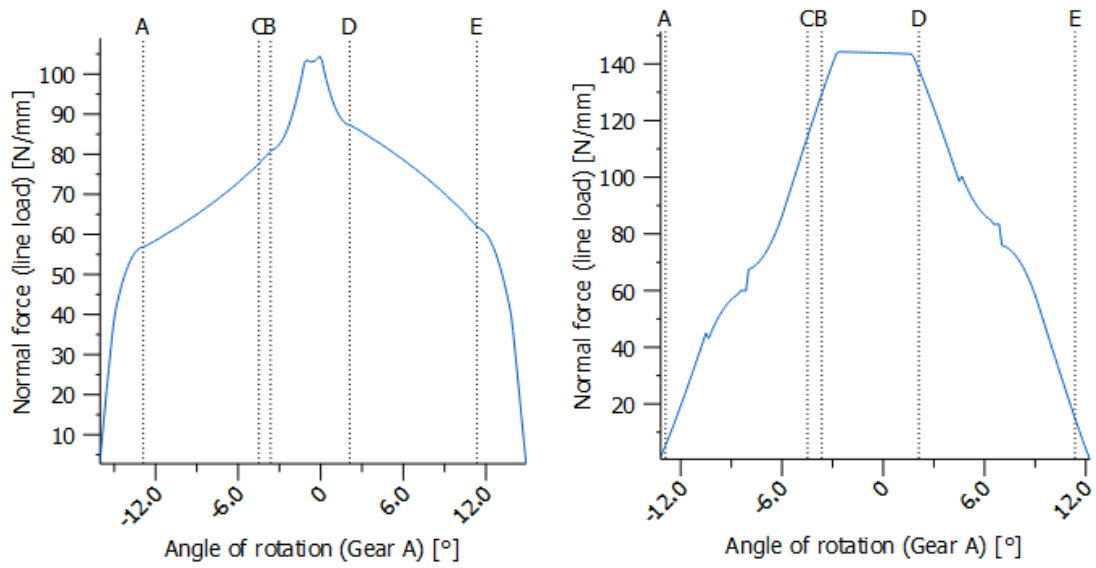


Figure 5.13. Second stage without (left) and with (right) end relief modification

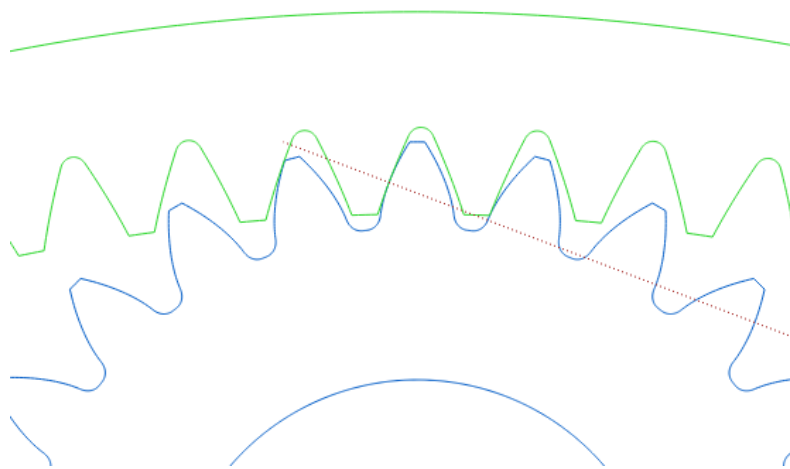


Figure 5.14. Second stage meshing gears

The transmission ratio obtained is 14.8:1, that is close to the target one of 15:1.

## 5.5.2 Life calculation results

### First stage

Below the safety factors for the first stage are shown. Even though in Section 5.2 it was explained that for small module gears ISO 6336:2006 calculation method is conservative, a safety factor above one is considered acceptable.

First stage safety factors		
	Gear 1	Gear 2
Root safety	2.7	2.3
Flank safety	1.5	1.8

Table 5.8. First stage safety factors

Below the specific sliding for the first stage is shown.

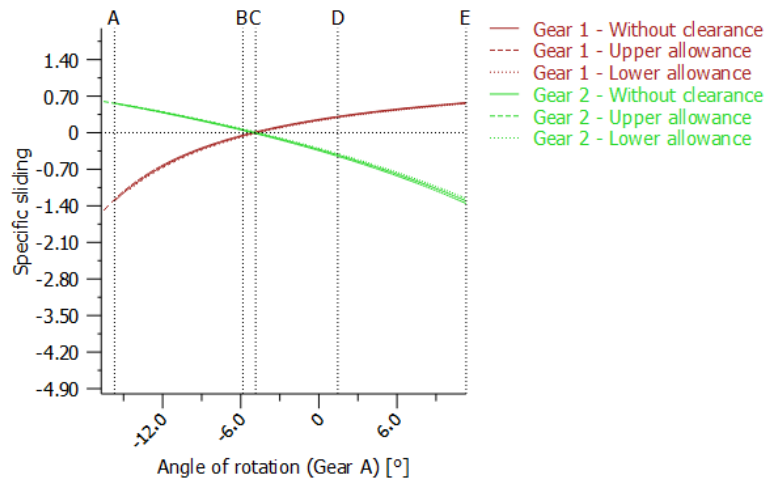


Figure 5.15. First stage specific sliding

Also the root stress plots under maximum torque are shown below for the first stage gears.

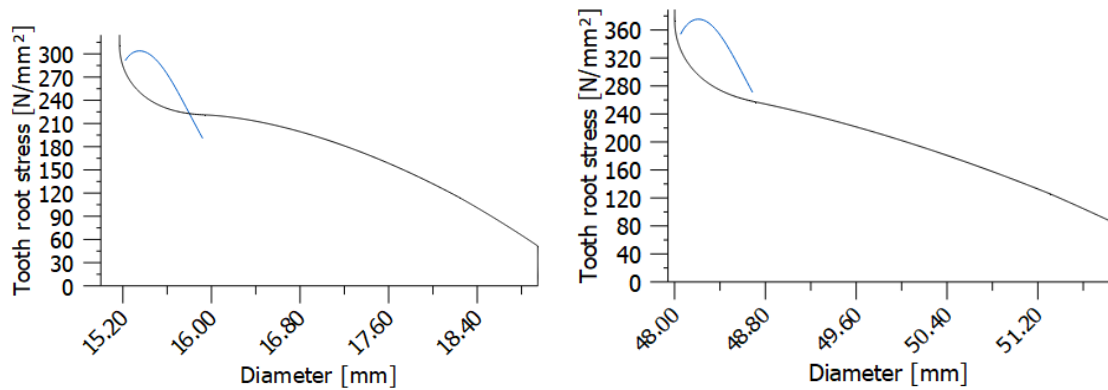


Figure 5.16. Root stresses for the sun gear (left) and for the first planet gear (right) under maximum torque

Finally, the hardness curve recommendation along the distance from the surface is shown.

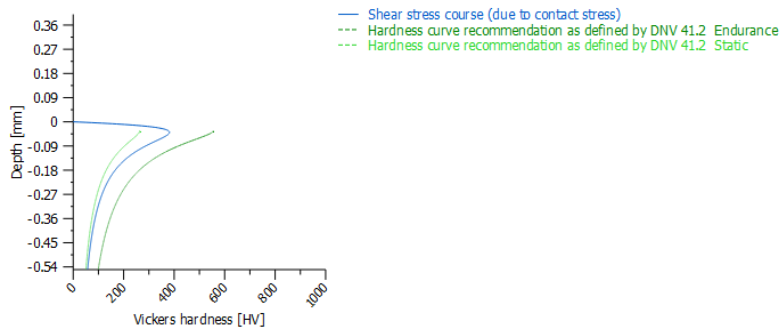


Figure 5.17. First stage hardness curve recommendation

## Second stage

Below the safety factors for the second stage are shown. The target was to have all the safety factors above 1 and the only gear that doesn't respect that condition is the ring gear, but due to the fact that its safety factor is quite close to 1 (0.9) and having said in Section 5.2 that the the normative is quite conservative, the result is anyway acceptable.

Second stage safety factors		
	Gear 1	Gear 2
Root safety	1.9	1.6
Flank safety	1.7	0.9

Table 5.9. Second stage safety factors

Below also the specific sliding for the second stage is shown. The condition is clearly less favourable with respect to the first stage one because being forced to maintain the same centre distance between the two stages doesn't allow to optimize the specific sliding for both the stages.

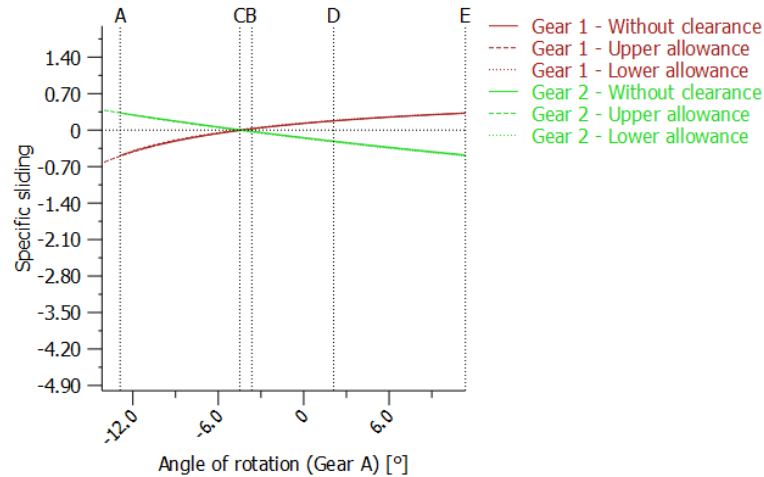


Figure 5.18. Second stage specific sliding

The root stress plots under maximum torque are shown below for the second stage gears.

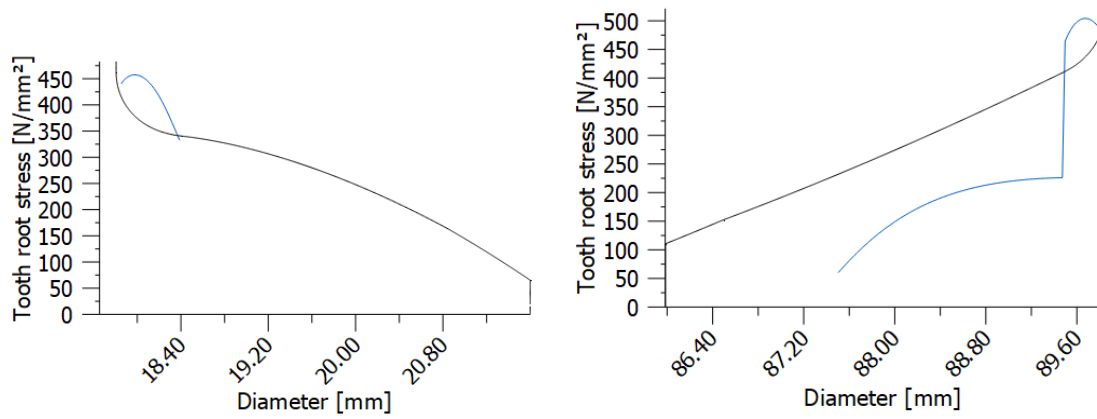


Figure 5.19. Root stresses for the second planet gear (left) and for the ring gear (right) under maximum torque

Finally, the hardness curve recommendation along the distance from the surface is shown.

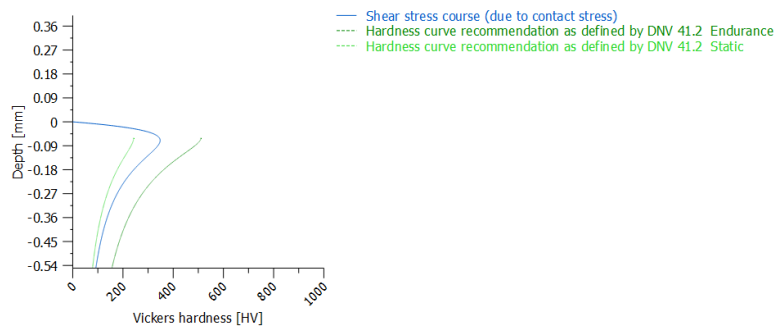


Figure 5.20. Second stage hardness curve recommendation



# Chapter 6

## Wheel bearings

### 6.1 Layout and bearing choice

As seen in Section 3.5 the planetary carrier and output shaft of the gear train is also the wheel hub. For this reason, the bearings connecting the planetary carrier to the upright (i.e. the transmission case) are indeed the wheel bearings. Obviously, a stiff assembly is ideal for the wheel operation, both in the radial direction and the axial direction.

As in most of wheel bearings application, two oblique bearings in the “O” mount configuration have been chosen. Oblique bearings can sustain large axial loads along with the radial loads. Moreover, due to the oblique ball raceways, the reaction points on the wheel axis are shifted with respect to the bearing mid plane. “O” mount bearings offers the stiffest mount because the reaction point on the wheel axis are more spaced with respect as if the bearings were common radial bearings.

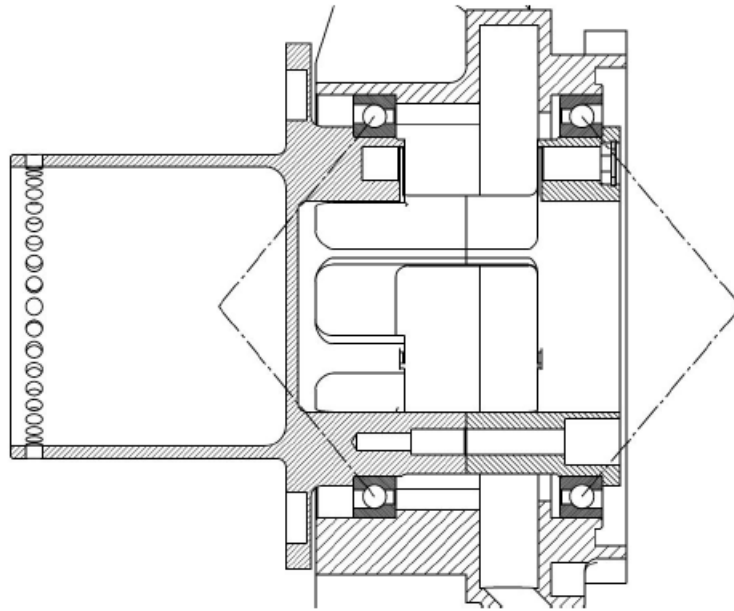


Figure 6.1. SC18 integrable wheel bearings layout

SC17 also features “O” mount oblique wheel bearings are 71820 CD/HCP4, manufactured by SKF. Below the characteristics can be seen with reference to Figure 6.2.

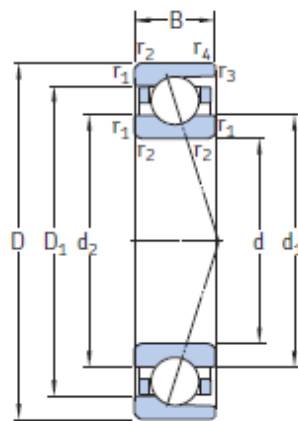


Figure 6.2. Main dimensions for bearings of the type ACD,CD [11]

Main dimensions			Load coefficients		Maximum velocity	Mass
d	A	B	C	C <sub>0</sub>	Oil-air lubrication	
mm			kN		rpm	kg
100	125	22.5	29	11	17 000	0.28

SKF 71820 CD/HCP4 bearing characteristics [11]

The bearings have a ceramic spheres that brings to a weight reduction of 30 g per each bearing with respect to the same bearing with steel spheres (71820 CD/P4). The ceramic spheres solution offers the possibility to operate at higher rotational speeds.

In the transmission discussed in this work the centre distance is 33.8 mm (as determined in Section 5.5) so the bearings external diameter can be significantly reduced from a package point of view. Dimensions-wise the smallest bearings compatible with this assembly is SKF 71816 ACD/P4. This bearing is taken from the Super-precision catalogue because in the common oblique bearings catalogue all the bearings have larger dimensions.

Main dimensions			Load coefficients		Max velocity	Mass
d	A	B	C	C <sub>0</sub>	Oil-air lubric.	
mm			kN		rpm	kg
80	100	10	13.8	17	17 000	0.15

SKF 71816 ACD/P4 bearing characteristics [11]

The same bearing with the ceramic spheres instead of the steel ones is called SKF 71816 ACD/HCP4 and it has the same load rating but a maximum admissible velocity of 20 000 rpm with oil-air lubrication and a mass of 0.14 kg.

For the SC18intergale project it was decided not to use the bearing with ceramic spheres because the hub peak rotational speed is around 1 350 rpm, so the steel spheres offers a speed rating that is more than enough and the weight reduction (10 g) is not significant for this application. The bearing with the steel spheres is available from the manufacturer with a much lower lead time.

With respect to SCdiciassette wheel bearings a weight saving of 0.13 kg per each bearing so 0.26 kg per vehicle corner is achieved.

## **6.2 Bearings life calculation**

The wheel bearings sizing has been done in collaboration with Squadra Corse's long partner and supplier SKF. The load spectrum at the tire contact patch has been supplied by Squadra Corse to SKF, that carried the bearings like calculation.

### **6.2.1 Load spectrum**

Below the load spectrum of the forces in all the three directions is shown. This load spectrum is extracted from a log file relative to an Autocross event, the most demanding in terms of required power and peak accelerations.

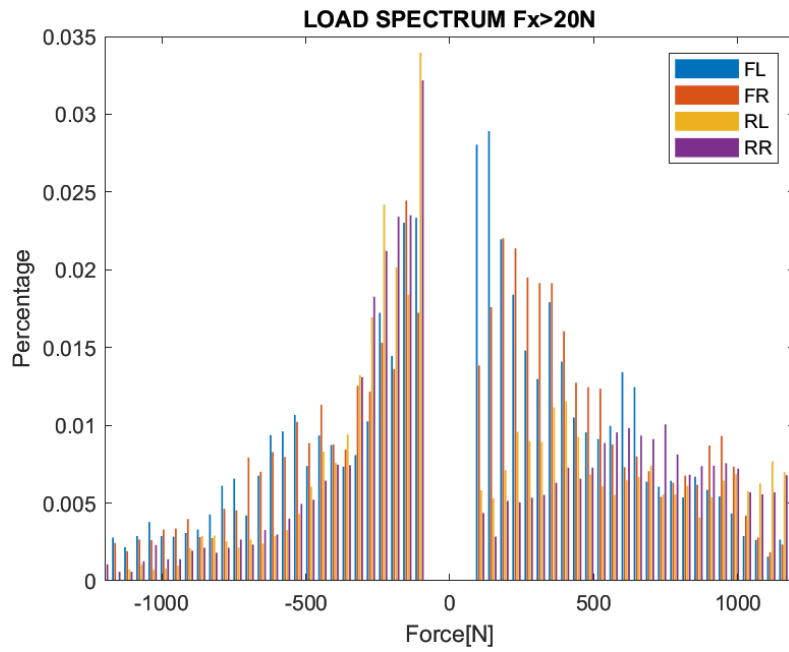


Figure 6.3. Fx load spectrum where  $F_x \geq 20$  N

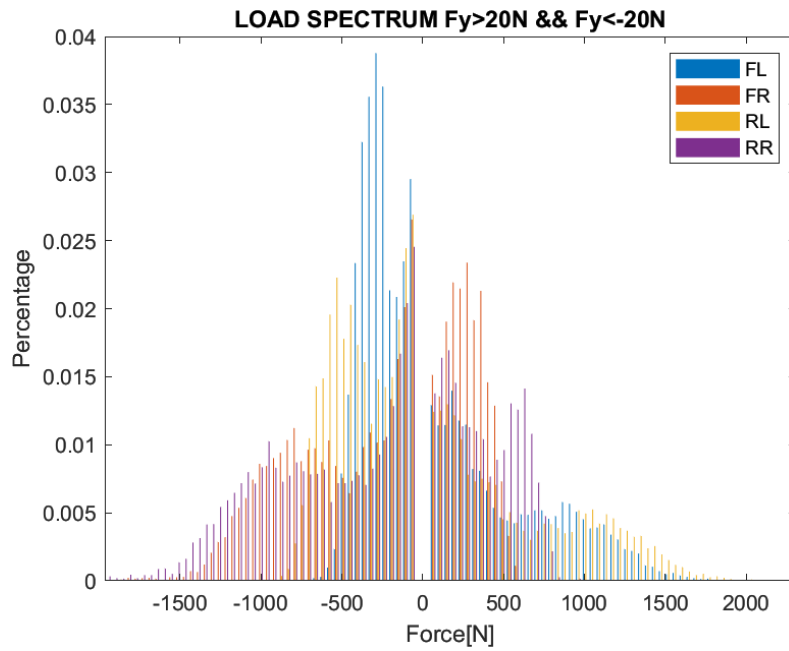


Figure 6.4. Fx load spectrum where  $F_y \geq 20$  N

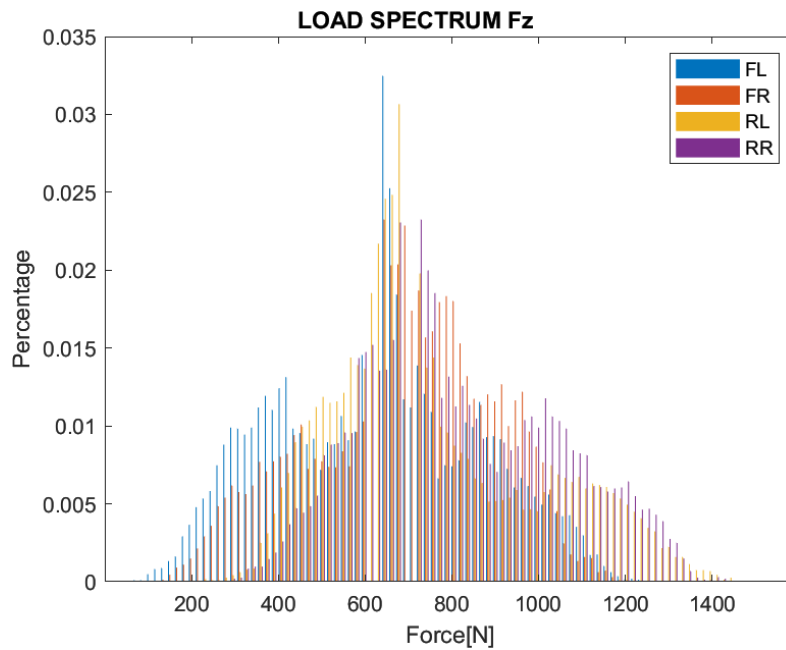


Figure 6.5. Fz load spectrum

## 6.2.2 Life calculation results

The purpose of the calculation carried is to determine the life of the bearings assembly and to determine which is the axial preload that maximizes the bearings' life. Obviously, the details of the calculation are not disclosed by SKF, for this reason below only the results are reported.

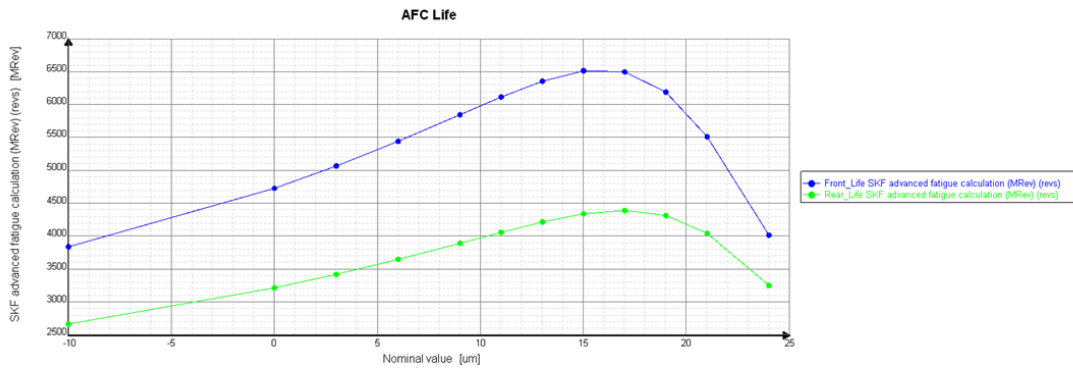


Figure 6.6. Wheel bearings life as a function of axial preload [14]

In the first plot the fatigue life versus the preload values is plotted. The most stressed wheel resulted to be the rear one with a life of around 4 300 Mrevs, while the predicted life of the front wheel is 6 500 Mrev. Considering the estimated life of 1 500 km (Section 3.7) and the loaded rolling radius of 236.5 mm, the required life for the wheel bearings is around 1 MRev, thus the predicted life of the wheel bearings is acceptable.

This plot underlines the importance that a proper preload has on the bearing's life. For this application a value of 15  $\mu\text{m}$  is chosen.

In the following plots the peak contact load is plotted for the internal and external bearings for both the front and the rear wheels, with 15  $\mu\text{m}$  preload.

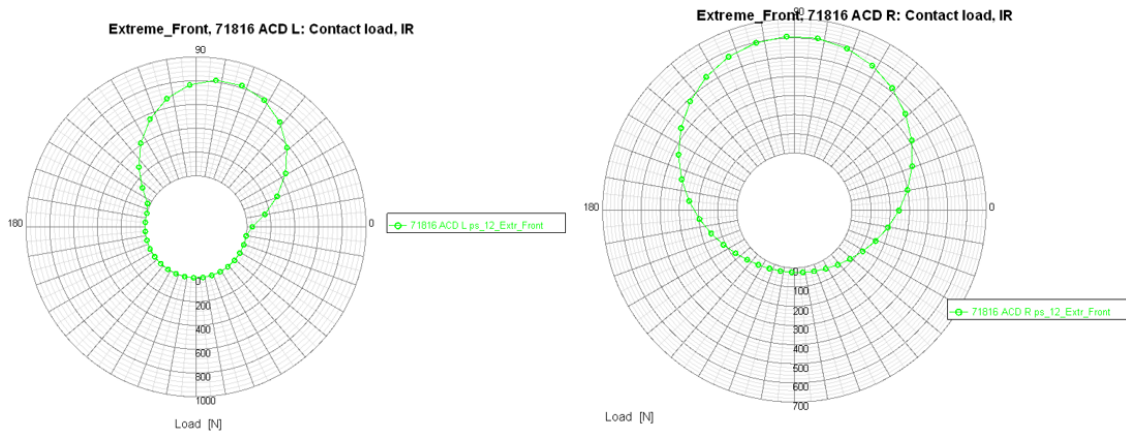


Figure 6.7. Front peak contact loads on the external bearing (left) and on the internal bearing (right) [14]

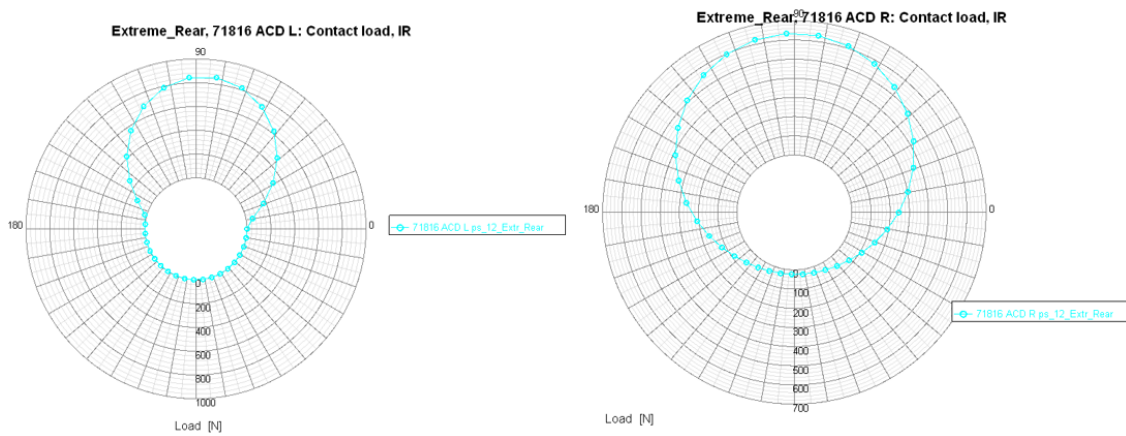


Figure 6.8. Rear peak contact loads on the external bearing (left) and on the internal bearing (right) [14]

## 6.3 Axial preload

In the previous section the large influence that the axial preload of a bearing assembly has on the bearings life has been showed quantitatively. It must be then carefully regulated because it can impact significantly on the bearing life.

One way to regulate the preload is to act on the axial displacement between the inner and the outer rings of the two bearings. For this reason, in this application the way to regulate the axial preload is to act on the thickness of a calibrated spacer.

In the SC17 the axial preload was regulated by mean of a calibrated spacer ring acting on the bearing internal raceway and a retaining locknut, labelled respectively as "1" and "2" in Figure 6.9.

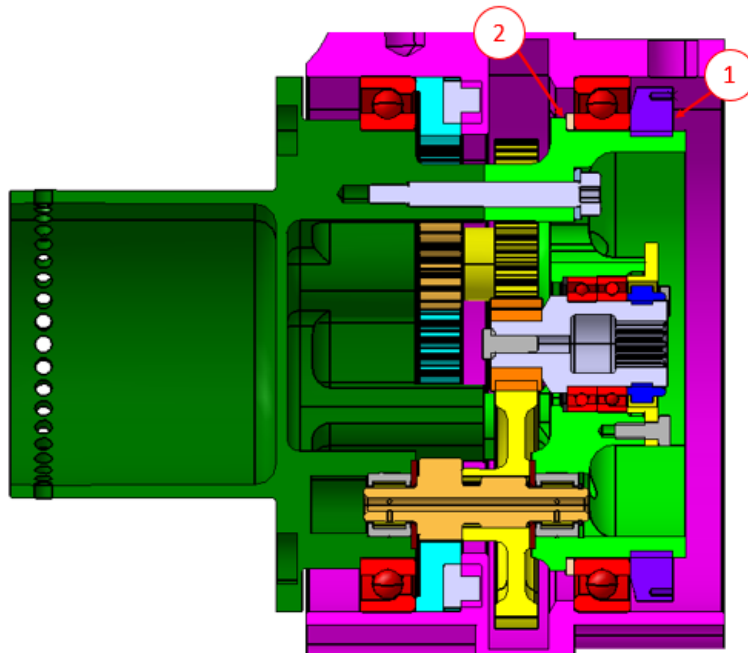


Figure 6.9. SC17 wheel assembly section

The disadvantages of this solution are mainly two:

- The locknut increases the overall weight of the gearbox and constraints its minimum axial length;
- Due to the fact that the external bearing outer raceway is in contact

with the ring gear, preloading the bearing assembly also gives an axial preload to the ring gear, thus fixing it and avoiding it to float. This is not beneficial for the meshing with the planetary gears, as it will be better discussed in Section 7.2.

In the SC18integrale layout, the locknut has been removed and the bearing is kept in position by the screws that retain also the planetary carrier to the hub, as shown in Figure 6.10. The preload ring is the one highlighted in orange in the same picture.

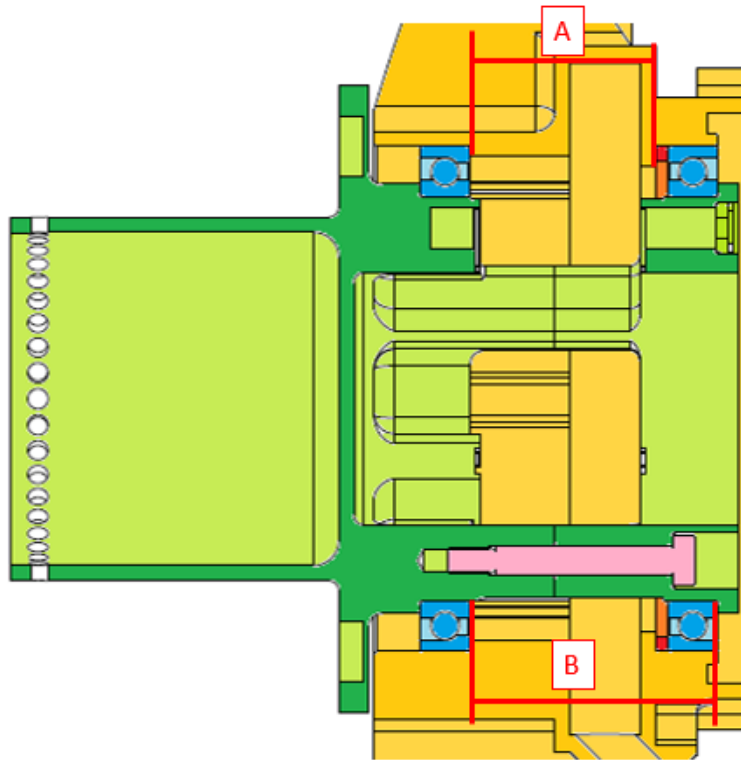


Figure 6.10. SC18 wheel bearings preload

The preload ring must be calibrated during the assembly of each corner because the bearing life is so sensitive to the variations in preload that any

chain of tolerances developed will result to be inadequate. In particular, referencing again Figure 6.10, the thickness of the preload ring is given by the following equation.

$$s = B - A - p \tag{6.1}$$

Where:

- B, A are measured during the assembly
- p is the target preload, determined in Section 6.2



# Chapter 7

## Mechanical design of gear train components

### 7.1 Sun gear

#### 7.1.1 Component engineering

Below a section view of the SCdiciassette geartrain pinion shaft.

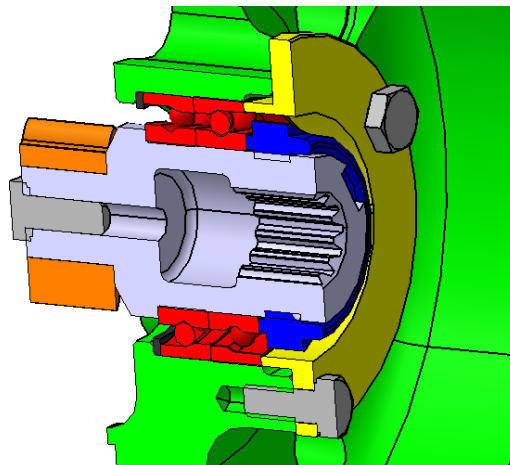


Figure 7.1. SC17 sun shaft

As it can be noticed, the axial width of the components is relevant mainly due to the two angular contact bearings, the locknut used to regulate their axial preload and the spacer used to retain the bearing external ring. Removing those bearings system is a way to reduce drastically the axial package the transmission and to reduce the weight of the planetary carrier by removing its whole central part. The advantages described can be seen clearly in Figure 7.2. Also the spline is broached into a shaft where only in a second phase the gear wheel is mechanically coupled to it through press-fit.

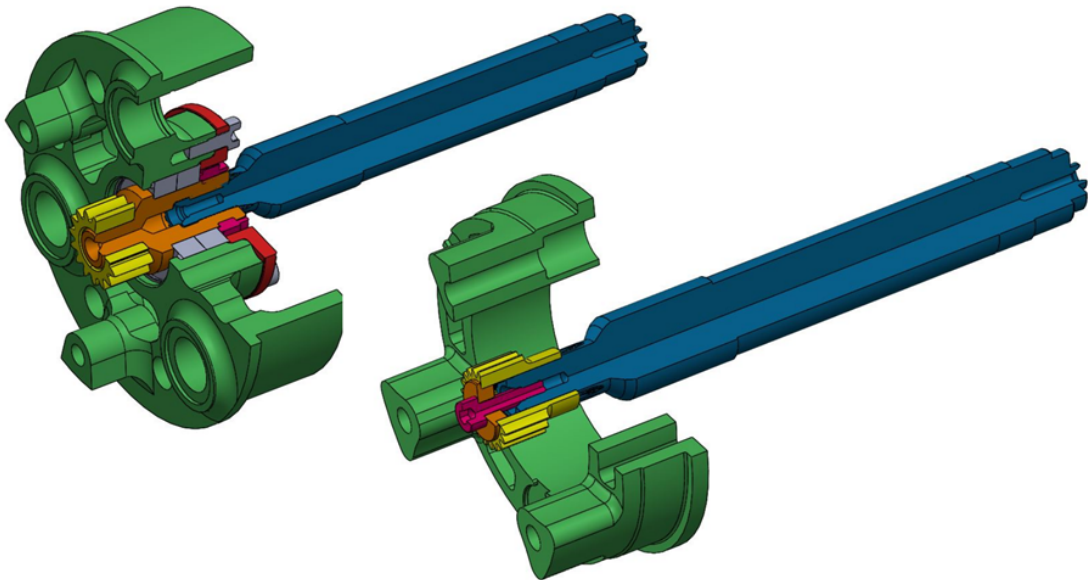


Figure 7.2. Comparison between the sun gear assembly of the SCdiciassette (left) and the sun gear assembly of the SC18integrale (right)

The situation must however be analysed with particular care because the bearings offer the advantage to couple sun shaft to the planetary gears with good precision and with a low oscillation of the shaft under load. The electric motor shaft though is already supported by two bearings so without admitting some degrees of freedom on the splined coupling, the system results to be hyperstatic.

In order to decide whether to maintain the bearings or not, a detailed analysis of the geometric oscillations of the motor output shaft due to production tolerances and an analysis of the oscillations under load has to be carried. Those aspects will be dealt in detail in Sections 7.1.2 and 7.1.3.

Removing the bearings means also to have the planetary carrier and the sun wheel closer to the motor mounting flange. Due to the proximity of the planetary carrier to the motor mounting flange, countersunk screws needs to be used to retain the motor to its mounting flange in order to avoid interferences.

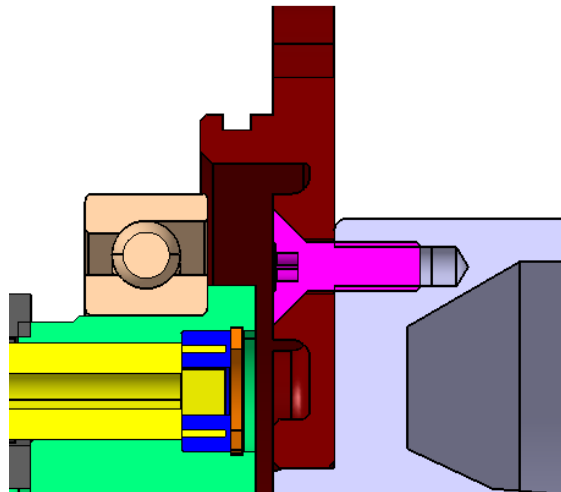


Figure 7.3. Motor mounting flange detail

The output of the electric motor shaft is a male spline (DIN 5480 - W11 x 0,8 x 30° x h8), schematically shown Figure 7.4. In order to reduce the volume of the component and consequently its weight the female spline in the SC18integrale layout is broached directly into the sun gear (differently from what shown in Figure 7.2 for the SCdiciassette layout).

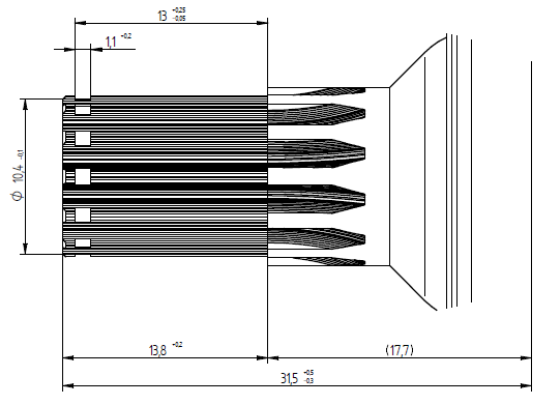


Figure 7.4. Motor output spline

Finally a retention model for the sun gear to the motor output shaft has to be found. This can be done in two ways: through a circlip (see Figure 7.4) or through a screw (see Figure 7.5).

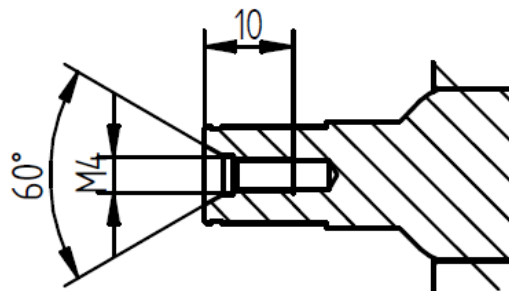


Figure 7.5. Motor output spline section view

In this application it was impossible to use a circlip due to excessive overhang of the sun gear, consequently a turned plug and a screw have been employed to this purpose, as shown in Figure 7.6. Due to the fact that all the torque in input and in output of the gearbox is carried by the spline, the screw tightening torque doesn't have to be sized to carry the transmitted torque but in any case it is tightened to the maximum sustainable axial load

for an M4 screw and some threadlocker is used.

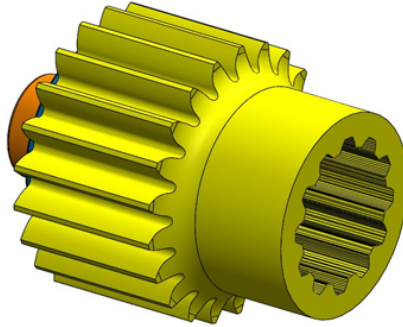


Figure 7.6. Sun gear

### 7.1.2 Geometric oscillations of the motor output shaft

In order to evaluate the precision with which the motor output shaft is manufactured, two type of measures have been performed: oscillation of the spline root radius and of the spline top radius from the nominal one, maximum oscillation of the non-splined section.

The measures have been carried using a centesimal dial gauge in a temperature-controlled chamber (Figure 7.7). The gauge is set on the first tip (or the first root), whose diameter has been previously measured and the motor shaft is rotated in order to measure the oscillation of all the other tips (or roots) with respect to the reference one. This process is repeated three times and the measured dimensions are averaged in order to minimize the errors in the reading of the measure.



Figure 7.7. Measurement set-up

Below the result of the performed measures is shown.

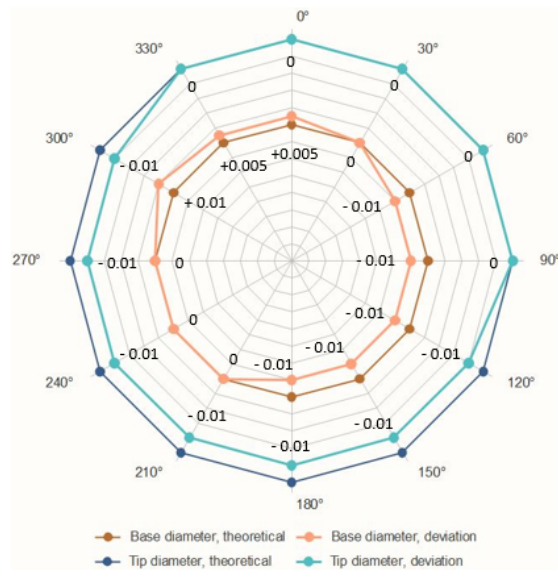


Figure 7.8. Oscillation of the motor output spline top and root diameters from their nominal value

Also the peak oscillation in the non-spline section has been measured for

reference, resulting to be equal to 0.012 mm.



Figure 7.9. Maximum oscillation of the motor output shaft non-splined section

### 7.1.3 Analysis of the motor output shaft under load

Theoretically there are not any forces that stress the sun gear shaft (and so the motor output shaft), this because in the layout with three planetary gears the three radial components of the contact forces should balance between each other and the center of mass of the sun gear lies exactly of the motor output shaft.

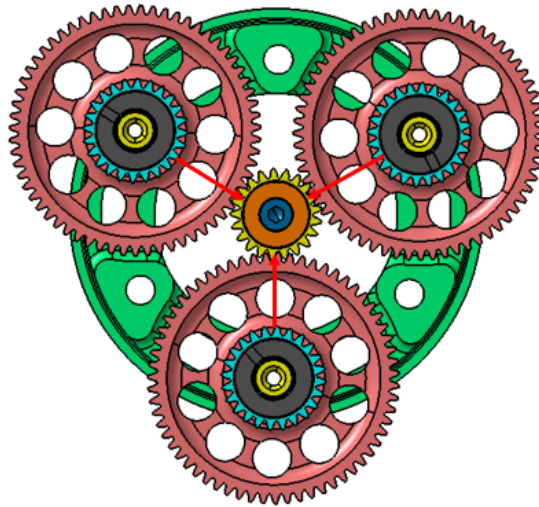


Figure 7.10. Radial forces due to meshing gear pairs acting on the sun gear

In the real application those two conditions are not necessarily guaranteed, so to verify the peak deflection of the motor shaft it was assumed that the radial force coming from one meshing pair is totally sustained by the sun shaft and that the centre of mass of the sun shaft has a radius of 0.5 mm with respect to the motor axis, the latter assumption being conservative because the sun gear is balanced after being manufactured. Due to the fact that, as shown in Figure 3.2, at the maximum motor speed of 20 000 rpm the torque available is around 14 Nm and that the peak torque of 21 Nm is available up to 13 000 rpm, the worst between the following two cases must be analyzed:

- Maximum motor speed: 134 N of radial force;
- Maximum motor torque: 388 N of radial force.

The worst case scenario is the one at maximum radial torque, so 388 N is the load against which the motor shaft has to be verified. The system is modeled in KISSsoft suite.

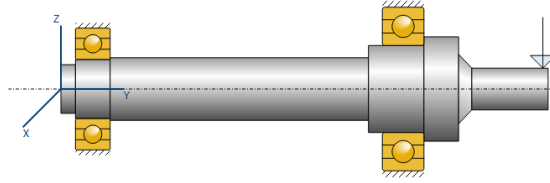


Figure 7.11. Model of the motor output shaft in KISSsoft

The resulting peak deflection is 0.036 mm. The deflection plot along the shaft length is shown below.

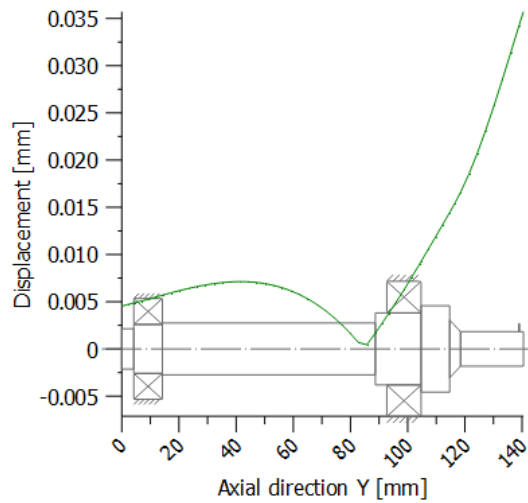


Figure 7.12. Motor shaft deflection

#### 7.1.4 Manufacturing

The material chosen for the sun gear is 18CrNiMo5 (Section 5.3).

After the rough shape of the component has been turned, the sun gear is hobbed, then the part is carburized. Finally the the gear is finished through grinding.

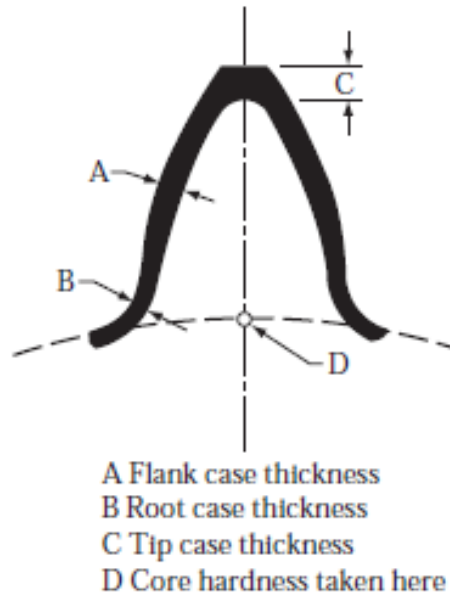


Figure 7.13. Carburized case pattern

The case hardening depth is set to 0.3-0.4 mm, this being larger than the minimum one given by the output of the calculation (0.15 - 0.18 mm) and lower with respect to the maximum one given by Equation 7.1. Some extra-material is added in order to take into account the material removed during grinding, that is expected to be 0.05-0.1 mm.

$$h_{em} = 0.40 * m_n = 0.40 * 0.8mm = 0.32mm \quad (7.1)$$

Where:

- $h_{em}$  is the maximum case hardening depth;
- $m_n$  is the gear normal module.

The latter equation refers to the maximum allowable case depth in the region C of Figure 7.13 because a too deep case in this region may cause the whole top of the tooth to break off.

## 7.2 Ring gear

### 7.2.1 Component engineering

In the planetary gear train studied the ring gear is fixed to the case (i.e. the upright) in order to be able to work as a reducer.

The SCdiciassette ring gear is retained to the fixed case by mean of a cam. In order to fit the cam the external ring gear diameter needs to be significantly larger with respect to the gear pitch diameter (as shown in Figure 7.14) thus implying the ring gear to be heavy and to require large radial room to be installed.

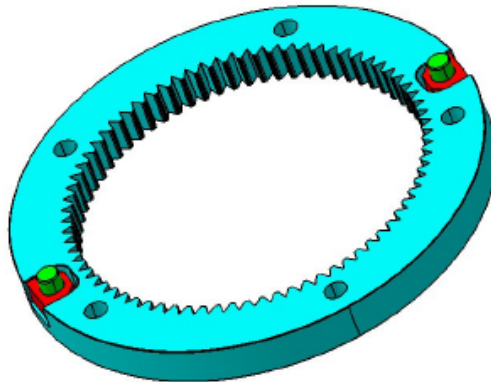


Figure 7.14. SCdiciassette ring gear retention system [22]

In order to avoid those issues, the solution adopted is to machine external teeth on the ring gear external profile. Two different kinds of tooth profiles have been investigated: curved flank teeth (Figure 7.15), straight flank teeth (Figure 7.17).

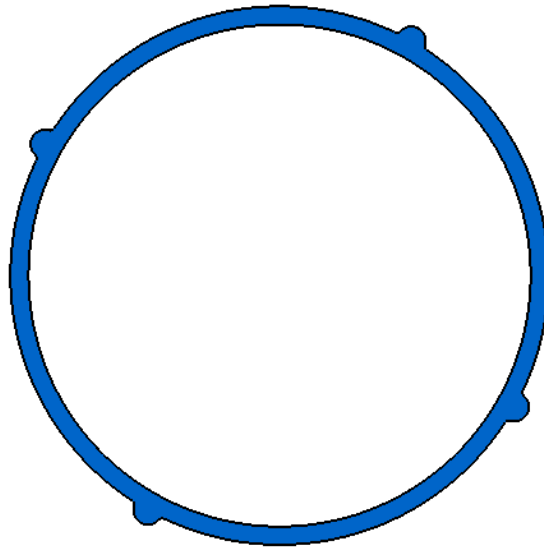


Figure 7.15. Curved flank teeth solution

In order to guarantee a better contact, the curved flank tooth profile needs relief grooves to be machined at the tooth root. After some preliminary FEA analysis it is apparent that this solution causes the external profile stresses to be significantly high.

Therefore, the straight flank teeth solution has been chosen. The straight flank offers a better contact area with the upright. Moreover, there is no more need for a relief groove since the contact can occur on the straight flank so at the tooth base a fillet can be present. Obviously, the stresses observed as output of the FEA analysis are drastically lower, the teeth number was also increased to reduce further the peak stresses.

Finally, three radial screws with custom calibrated end diameter constrain the ring gear axially to the upright (Figure 7.16).

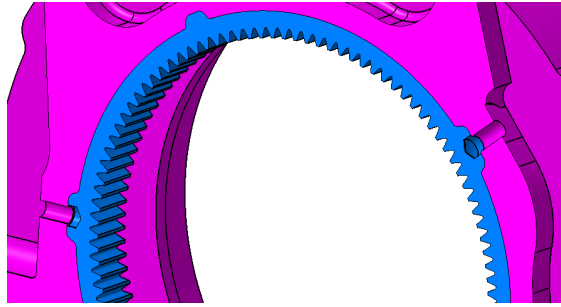


Figure 7.16. SC18 integrale ring gear retention system

The external diameter of the ring gear (not the teeth external diameter has a nominal value of 96 mm (as the mating bore in the upright) and the coupling between it and the mating bore is d7-H7, thus a significant radial backlash exists. This is made to keep the ring gear slightly floating thus accommodating better production tolerances.

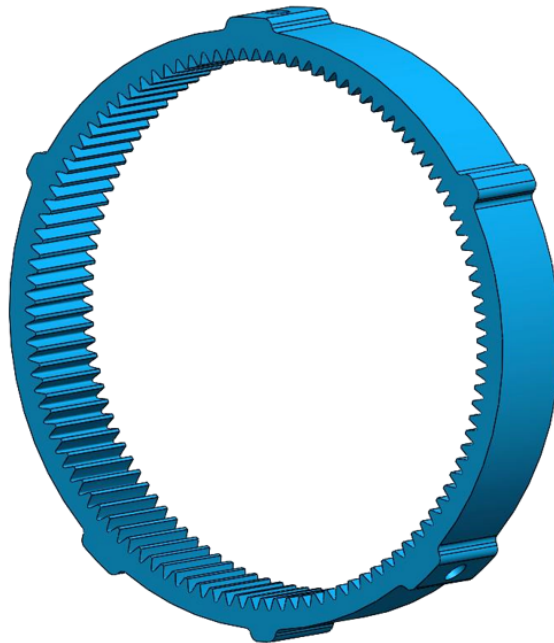


Figure 7.17. Ring gear

## 7.2.2 Structural analysis

Along with the ring gear, also the bore in which the ring gear is modeled and meshed for this analysis in order to check for potential strains in the upright. A simplified version of the ring gear with only the teeth where the force is applied is meshed, in order to reduce the computational times.

The bore in which the ring gear fits is fixed in all its degrees of freedom, while the ring gear is allowed to rotate only on its axis. The load transmitted by each gear in peak torque condition is applied to three teeth meshed. Contact surfaces without slip are defined at the contact point between the ring gear and the upright in the direction opposing to the load applied.

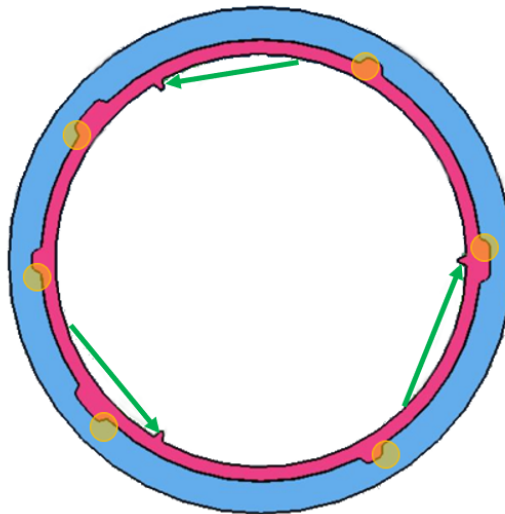


Figure 7.18. Ring gear FEM model

The most stressed point resulted to be the fillet of a tooth near the load application. Below its contour plot is shown.

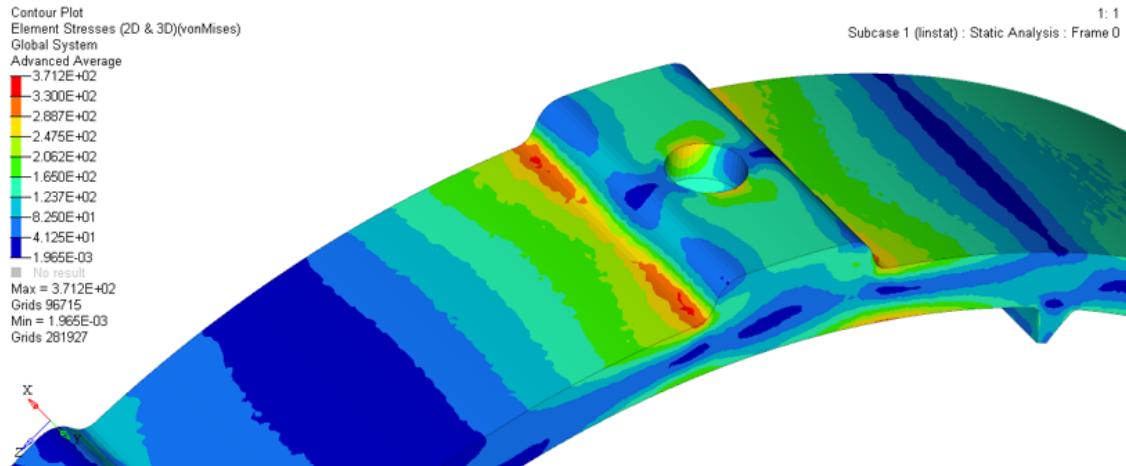


Figure 7.19. Ring gear stress contour plot

The static safety factor against strain is given by the following expression.

$$SF = \frac{R_p}{\sigma_{max}} = \frac{900MPa}{371.2MPa} = 2.4 \quad (7.2)$$

The latter being acceptable for this purpose.

### 7.2.3 Manufacturing

The gear tothing is the first machining process to be performed on the ring gear, the outer profile is kept circular from the raw material.

After gear cutting, the ring gear external profile (the one used to constrain its rotation to the case) is machined. The ring gear in this stage is constrained to the mill plate through four cylindrical rollers that lies on the gear teeth. The phase that the external teeth have with respect to the internal ones is not relevant but it is fundamental that the external diameter is concentric with respect to the pitch diameter.

Finally, the ring gear is case hardened. As already mentioned, the ring gear is case hardened through nitridation with a case depth of 0.15 mm. The latter case depth being the minimum one imposed by the calculation because keeping the depth minimum reduces the heat treatment time as shown in Figure 7.20.

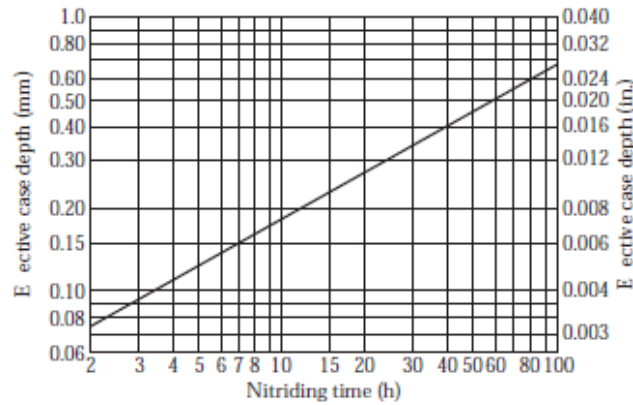


Figure 7.20. Nominal times required for different nitride case depths [3]

Reducing the heat treatment time is helpful to minimize the distortion of the component because the ring gear is not reworked after case hardening.

## 7.3 Planetary gears assembly

### 7.3.1 Components engineering

In the picture below, a section view of the planet gear assembly can be seen.

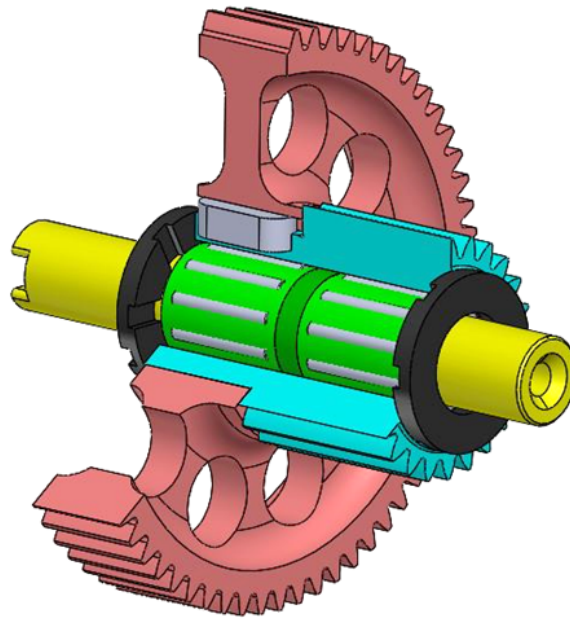


Figure 7.21. Planetary gears assembly

The two planetary gears (light blue and pink in Figure 7.21) are separately cutted and then assembled together. This solution is adopted because it allows to minimize the axial dimension of the planetary gears. By making them from a single piece the room taken by the component would be significantly higher because the smaller wheel would need some axial relief in order to allow the tool passage during the gear cutting and the grinding.

In order to have a proper meshing of the gears, the assembly needs all the planetary gears to be equal to each other, the latter condition coming from the meshing requirements discussed in Section 3.6. If not one or two gears may not have a proper meshing or worse, they cannot be assembled, the tight axial backlash between the teeth makes this situation even more critical and requires more precision in the assembly. The assembly procedure will be explained better in Section 7.3.6.

The purpose of the keyway (grey in Figure 7.21) is not to transmit torque but to locate one gear with respect to the other, in fact its size is not suitable to transmit the torques involved. Therefore, all the torque transmitted by the planetary gears is transferred from one gear to the other by means of friction. This topic will be better investigated in Section 7.3.2.

The two planetary gears assembled are connected to the planetary carrier by mean of a shaft (yellow in 7.21) and they are supported onto this shaft through two needle roller bearings, axially located by mean of a plastic ring (dark green in 7.21).

The spacers coloured in black in Figure 7.21 are used to avoid that the carburized gears spin during operation against the planetary carrier and the hub surfaces, damaging them. To this purpose the spacers are retained with an anti-rotation pin (Figure 7.22) to the hub and the planetary carrier by one side, while from the other side they slide against the planetary gears. In order to avoid the spacers to damage during operation, their material and the heat treatment has been properly chosen and some oil passages have been worked onto their surface. The latter aspect is useful also for needle bearings lubrication purposes.



Figure 7.22. Anti-rotation pin in the carrier (left) and spacer (right)

One axial hole and two rows of radial holes are drilled into the planet pin shaft in correspondence of the needle roller bearings midplane. This solution is aimed to guarantee an oil flow from the case to the bearings along with the previously described spacers.

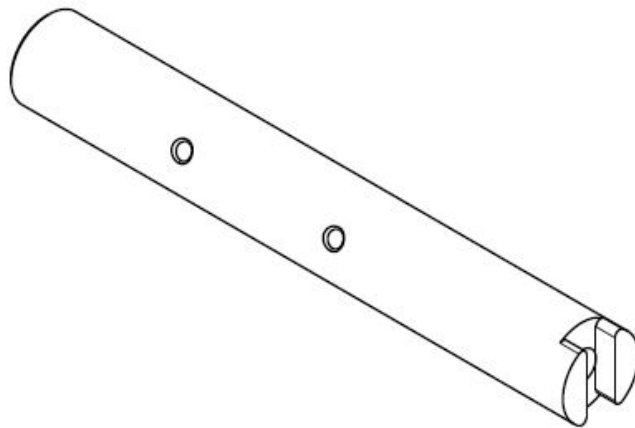


Figure 7.23. Planet pin shaft

Finally the planet pin shaft rotation is prevented by the fact that the groove into the pin shaft visible in Figure 7.23, couples with an H-shaped bushing that is press fitted into the planetary carrier and axially retained by a circlip.

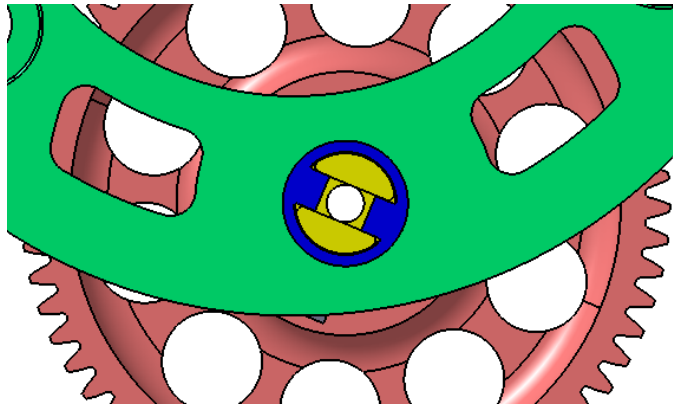


Figure 7.24. Planet pin shaft rotational constrain

### 7.3.2 Torque transmission

The torque transmission between one gear and the other as already mentioned occurs by friction. This solution has been already successfully adopted in the previous year's transmission and it avoids using a keyway that takes a lot more space. Also, it avoids using splines or other profiles that are difficult to manufacture.

The type of pressure fit has been studied by means of a devoted KISSsoft sub-module. Giving as an input the dimensions of the two components, the joint diameter, the length of the fit, the materials of the coupled components, the operational torque and rotational velocity, the friction coefficients, the service temperatures, the surface finish and the tolerances of both the shaft and the hub, the software is able to calculate the safety against sliding and the safety against the fracture of both the shaft and the hub.

The diameters with their tolerances of the components involved are:

- Shaft: 17.5 (+0.030/0.035 mm);
- Hub: 17.5 H6 (0/+0.011 mm).

Below the allowances are shown.



Figure 7.25. Left display: tolerance field only takes allowances into account, centre display: tolerance field takes into account temperature and centrifugal force (without pressure), right display: tolerance field takes into account temperature, centrifugal force and pressure

Below is shown also the plot of the stresses involved into the press fit.

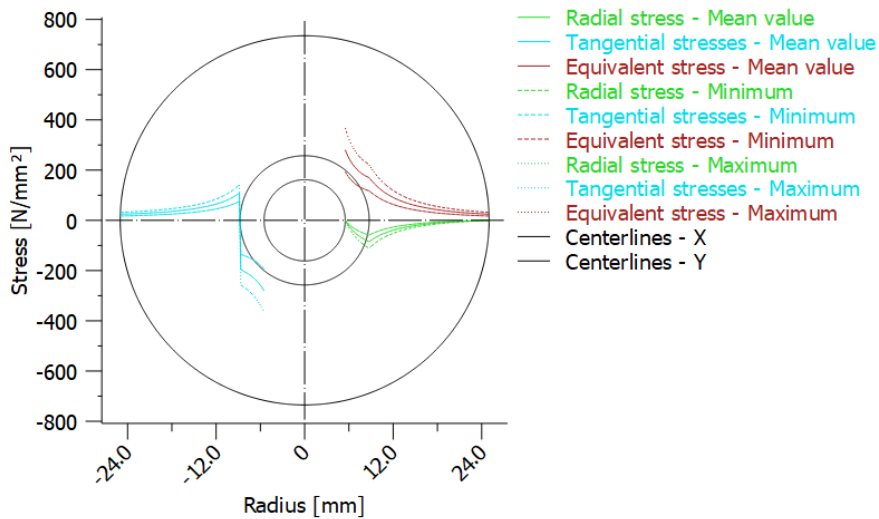


Figure 7.26. Plot of the stresses of the press fit in the shaft and in the hub

### 7.3.3 Pin shaft structural analysis

#### KISSsoft model

The deflection and the stresses on the pin shaft have been evaluated in a first stage using the KISSsoft suite. A coaxial shafts model has been developed in KISSsys suite as a part of the main transmission model, where the pin shaft is modelled with two supports in the contact points with the planetary carrier and the hub.

In this case the two assembled gears were modelled as it was single shafts. As a connecting element between the two shafts, rolling bearings has been used in order to minimize the radial dimension.

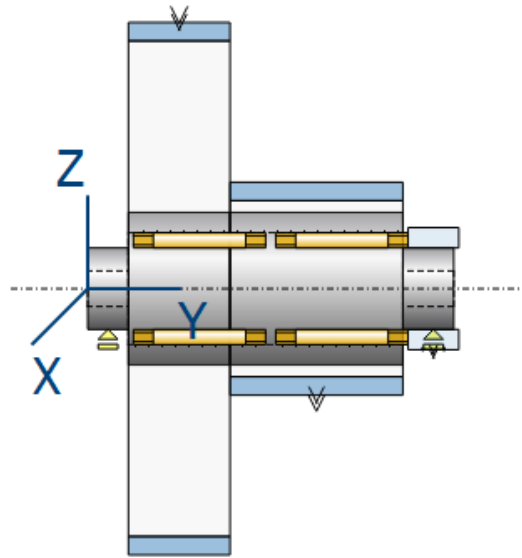


Figure 7.27. Planetary gear assembly model in KISSsoft

The two connecting needle roller bearings are K 8x11x13 TN supplied by SKF. They have 1.5 mm diameter needle rollers and a length of 13 mm [12]. The model of those bearings can be found in KISSsoft database so they are easily added to the calculation.

The calculation is performed under maximum torque conditions, below the results in terms of displacement and stresses are shown.

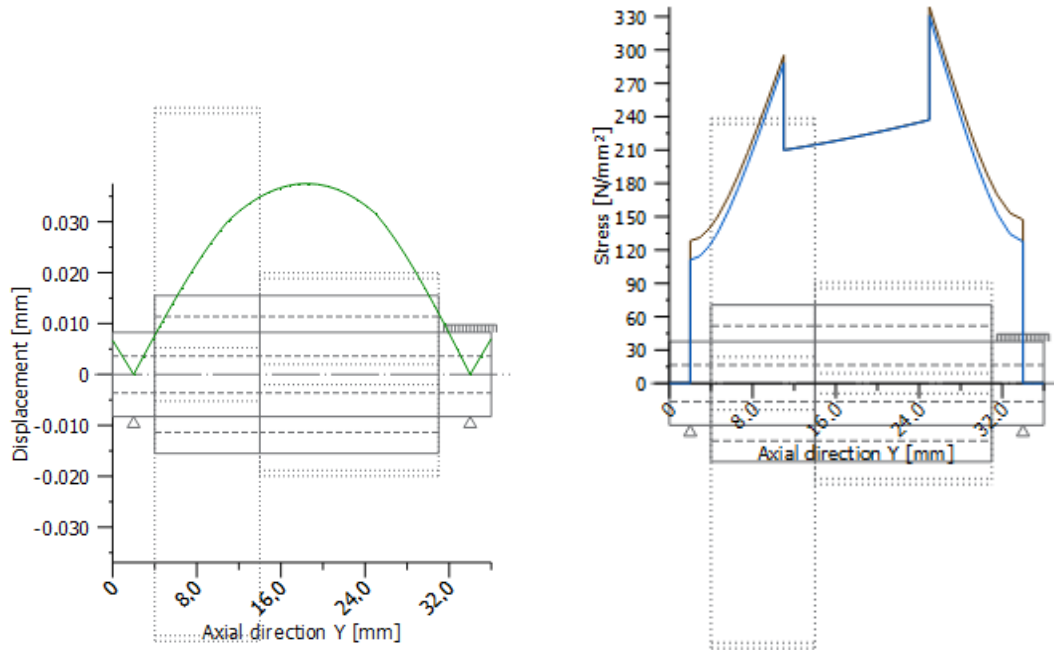


Figure 7.28. Planet pin shaft displacement (left) and stresses (right)

The peak deflection resulted to be 0.037 mm and the peak stress 331 MPa, both acceptable for this purpose.

The minimum static safety for the two needle roller bearings is  $S_0 = 3.4$  with an expected service life of  $L_{nh} = 87h$ . Those values are acceptable for the application.

### 7.3.4 Planet gear structural analysis

A proposal with 10 circumferential holes have been model aiming to reduce the weight of the second stage planetary gears. Care has been taken to leave a

minimum of 3/4 mm of material everywhere, the latter being a rule of thumb in order to avoid too large distortions during the case hardening, even if the stresses and displacement calculated through the FEM model are acceptable. A FEM model was developed in order to evaluate the feasibility of the drilled circumferential holes.

In this model, the rotations and the translations of the planet gear were constrained, while on the tooth flank through RBE3 elements, a force of around 2 540 N is applied, corresponding to the peak torque condition. The analysis performed is linear static.

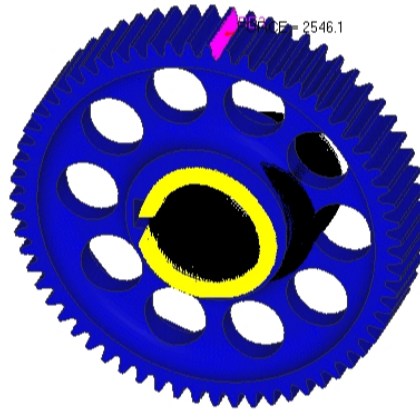


Figure 7.29. Planetary gear FEM model

It must be stressed that the purpose of this model is to evaluate the consistency of the weight reduction and not to simulate the details of the tooth stress and of the tooth resistance, that were already calculated with KISSsoft tool.

Apart from the teeth closest to the one where the load application occurs, all the displacements are lower than 0.22 mm, the latter being an acceptable value.

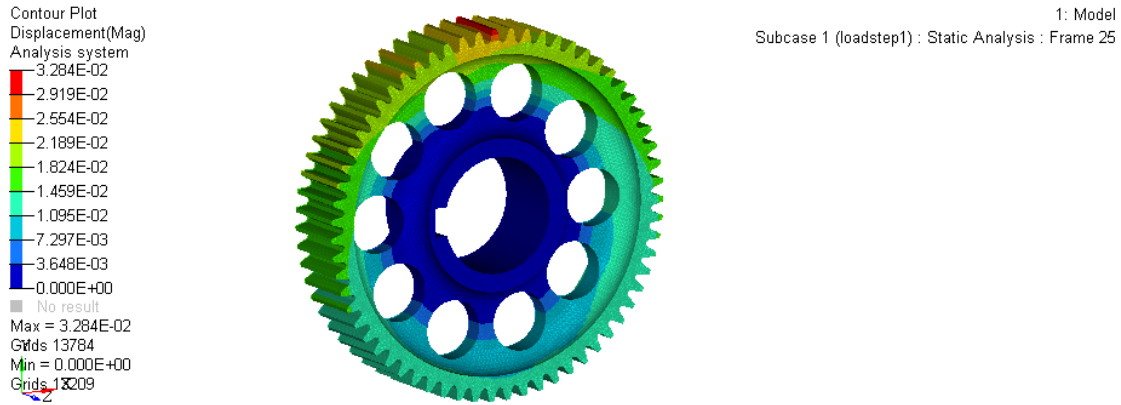


Figure 7.30. Planetary gear displacement

The stress contour plot is shown for a section of the mesh, this to show the stress along the whole section of the gear and not only on its surface. It's important to evaluate stresses also far from the surface because the strength of the material decreases progressively when the distance from the surface increases.

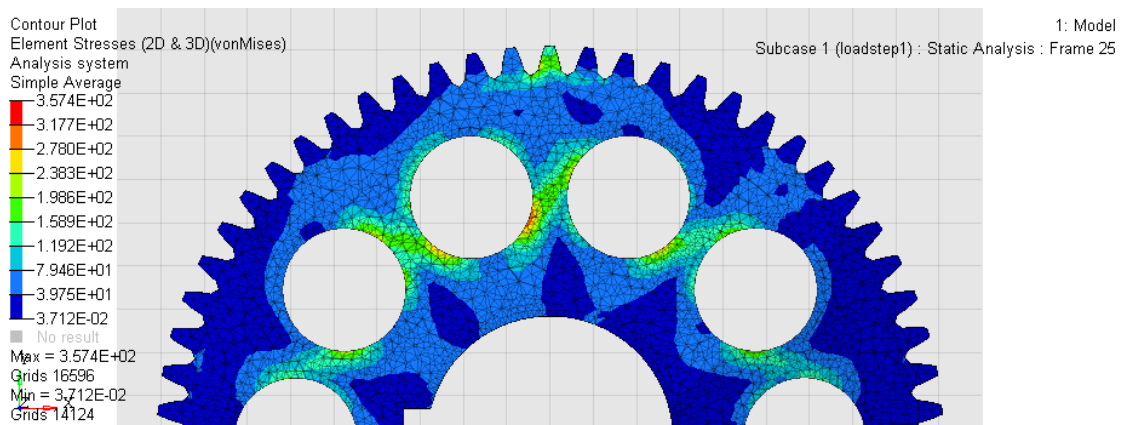


Figure 7.31. Planetary gear stress on a mid-plane section

Given the mesh size of 0.5 mm, all the elements deeper than 0.5 mm from the surface are characterized by a stress lower than 240 MPa.

Considering the peak stress of 318 MPa in an area that is not the tooth one, the following safety factor is obtained.

$$SF = \frac{R_p}{\sigma_{max}} = \frac{850MPa}{240MPa} = 3.5 \quad (7.3)$$

The latter being acceptable.

The holes in the planetary gear allow a reduction of 10 g per gear, so 30 g per each transmission.

### 7.3.5 Assembly tolerances

In KISSsoft suite is possible to change manually the centre distance between the gear in order to input different values with respect to the calculated one and check for interferences during meshing. The meshing of the first with the correct centre distance of 33.8 mm is shown in Figure 5.5.1.

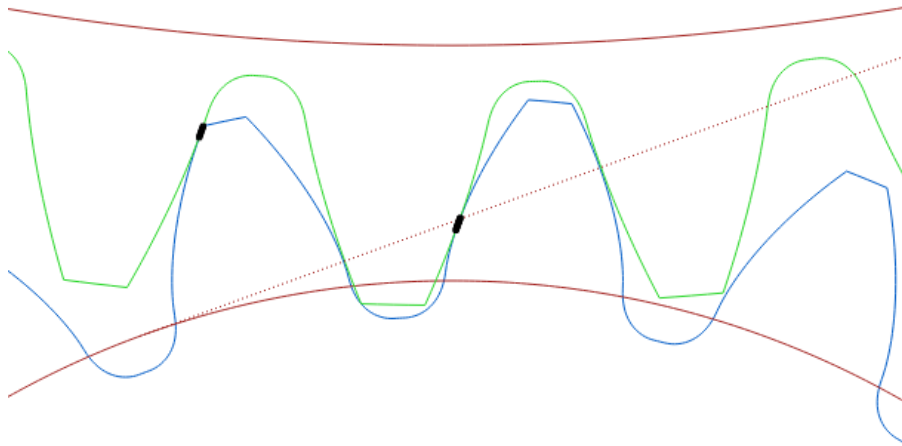


Figure 7.32. First stage meshing profiles with 33.6 centre distance

In Figure 7.32 the meshing gear pair with the centre distance reduced by

0.2 mm is shown. In this condition the contact starts to occur on a line instead of on a single point, clearly indicating an interference between the two profiles. Moreover the tip of the first stage planet gear is very close to the root of the sun gear. For the reasons listed, this condition will be considered the lowest boundary of the centre distance.

It must be assured that this condition is never reached during the gearbox operation. The factors influencing the centre distance are both static and dynamic and they are listed below.

- Centre distance tolerance on the pin shaft position;
- Precision of the coupling between the pin shaft and the planetary gears;
- Sun gear addendum radius tolerance;
- First stage planet gear addendum radius tolerance
- Peak deflection of the motor output shaft;
- Peak deflection of the pin shaft in the first stage planet gear area.

The following tolerances hold for the addendum diameters:

- Sun gear addendum diameter:  $\phi$  18.92 mm h9 (0/-0.052 mm);
- First stage planet gear addendum diameter:  $\phi$  51.84 mm h8 (0/-0.046 mm).

The needle roller bearings diameter tolerance is  $-1/-3 \mu\text{m}$  and the suggested tolerances for the internal and external raceways are H6 for the 11 mm bore into the planetary gears (0/+0.011 mm) and g5 for the 8 mm pin shaft (-0.005/-0.011 mm) [12]. The maximum allowance permitted by this coupling is given by:

$$a_{max-pin} = 0.011mm + 0.011mm + 0.003mm = 0.025mm \quad (7.4)$$

The position tolerance of the pin shaft with respect to the planetary carrier is 0.01 mm, while the coupling between the pin shaft and the bore in the planetary carrier is  $\phi 8$  mm H6 (0/+0.009 mm)/g5 (-0.005/-0.011 mm). The maximum allowance permitted by this coupling is given by:

$$a_{max-carr} = 0.01mm + 0.011mm + 0.009mm = 0.03mm \quad (7.5)$$

The following deflections exists:

Pin shaft deflection  $f_{pin}$ : 0.035 mm;

- Motor output shaft  $f_{mot}$ : 0.036 mm.

The following relation must hold:

$$a - a_{max-pin} - a_{max-carr} - f_{pin} - f_{mot} > 33.6mm \quad (7.6)$$

The sun gear and planet gear addendum diameters have respectively the tolerances classes h9 and h8, for this reason in the worst case scenario for this analysis their diameter is equal to to the nominal one, so their contribution is equal to zero in the current calculation (this is the reason why they do not appear in the abovementioned relation).

Substituting the values previously obtained:

$$33.71mm > 33.6mm \quad (7.7)$$

It can be concluded that all the deflections are acceptable with the specified tolerances.

### 7.3.6 Manufacturing

In order to be able to assemble the gearbox the three planetary gears must be as equal to each other as possible. The easiest way to translate this requirement into manufacturing indications is to specify that one tooth of the smaller and one of the larger gear must be precisely in phase (the same consideration can obviously be made about two vanes).

In order to obtain the tightest manufacturing tolerances through this process, the solution developed follows those steps:

1. The smaller gear is toothed and grinded alone;
2. The second gear is toothed;
3. Through a locating keyway (smaller with respect to a keyway sized to transmit torque) the second gear is assembled to the first one in a proper position;
4. The larger gear is grinded after the assembly in order to correct the errors in the assembly.

This manufacturing process is difficult to achieve, so all the parts were verified through coordinate measurement machine inspection.

Also, due to the fact that the three planetary gear couples must be phased equally (as discussed in Section 3.6), the phased tooth is marked in order to facilitate the assembly.

The two gears are manufactured in 18CrNiMo5 (Section 5.3) carburized with a case depth of 0.3 mm - 0.4 mm, higher than the minimum prescribed by the calculation output (0.15 - 0.18 mm) and lower than the maximum one

imposed by Equation 7.1.

Moreover, this material permits to reach surface hardness of 60 HRC thus respecting also the requirement coming from the SKF catalogue to have an hardness of 58-64 HRC [12] in order fully exploit the load carrying of the needle roller bearing.

Also the pin shaft has been manufactured in 18NiCrMo5 in order to have a great strength and a proper hardness onto its surface, while maintaining in the core a behaviour suitable to sustain bending loads for long cycles without the risk of breaking.

The spacers are manufactured in 100Cr6 and they are milled with the material not heat treated. After the first machining process the spacers are heat treated and finally they are honed in order to maintain the thickness tolerances.

# Chapter 8

## Planetary carrier mechanical design

### 8.1 Layout

Once the bearings (Section 6), the shaft seal (Section 9) are chosen and the gears geometry is defined (Section 5), the definition of the carrier assembly can start along with the already described mechanical design of the gear train components (Section 7).

The assembly procedure is already explained in detail in Section 11. Anticipating the topics dealt in the section dedicated to the assembly, the planetary carrier of the gearbox is composed by two separate parts bolted together in order to allow the assembly of the gearbox. With reference to Figure 8.1 the two parts bolted together are called in this work "hub" (A) "carrier" (B). Although it is always the same component but this distinction can be useful because the part called "hub" is actually where the wheel is coupled. The hub and the carrier are coupled together with three calibrated screws (UNI ISO 7379).

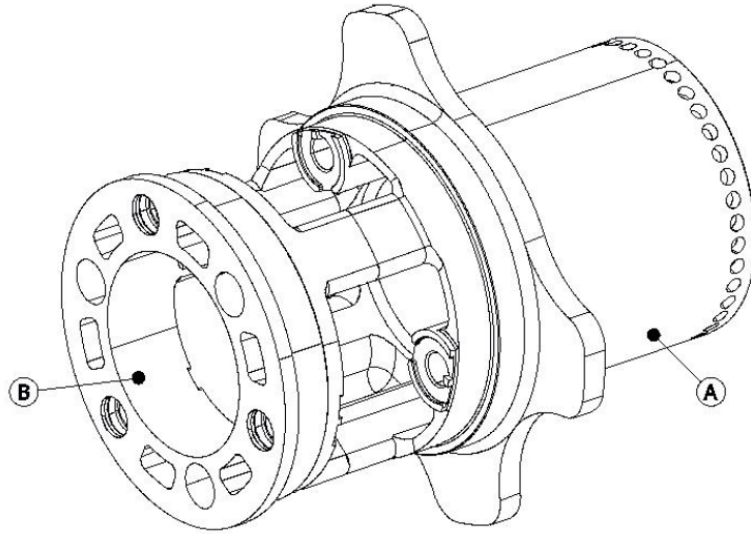


Figure 8.1. Planetary carrier

The carrier is a crucial part of this transmission because it integrates the upright, all the gears and the wheel. The raw parts are firstly modelled respecting all the interfaces and the dimensional constraints. Those geometries are then optimized and once obtained the final model it is checked through FEA analysis.

## 8.2 Wheel locknut

The tightening torque is a crucial parameter to be sized because it is the major contributor to the the axial load on the hub. As already seen is Section [3.3.2](#) the wheel is retained to the wheel hub by mean of a single locknut.

Aiming to minimize the wheel tightening torque a first analysis has been done in order to investigate the possibility to carry the wheel torque by mean of pins machined onto the wheel coupling flange of the hub. This would have required to impose severe production tolerances in order to assure that the

wheel would not loose during the vehicle operation. The tighter are the coupling tolerances the harder is to install the wheel. Unfortunately the tolerance on the diameter of the holes in the rim is loose for this purpose (0/+0.1 mm) and the rim is a standard part so it was impossible to change that tolerance.

For all those reasons, the idea to have the torque carried by the pins was abandoned in favour of transmitting it totally by friction to the hub through the threaded coupling.

As shown in Figure 8.3 the highest accelerations are negative, thus the maximum force in X direction applied at the tire contact patch is due to braking on the front wheels. For this reason it was decided to size the tightening torque on the maximum force in X direction due to traction, consequently to have the tractive torque that works as an "unscrewing" torque and the opposite for the breaking torque. For this reason the left locknuts have left-handed thread and the right locknuts have right-hand thread.

In Appendix C the wheel locknut tightening torque calculation is discussed in detail.

## 8.3 Materials choice

The initial idea was to manufacture both the planetary carrier and the hub in an aluminum alloy like 7068-T6511 or 7075-T6, but after the first FEM analysis were performed the average stress (around 200 MPa) caused by the wheel locknut tightening on the hub-rim coupling flange raised large concerns regarding a potential fatigue failure of the hub itself.

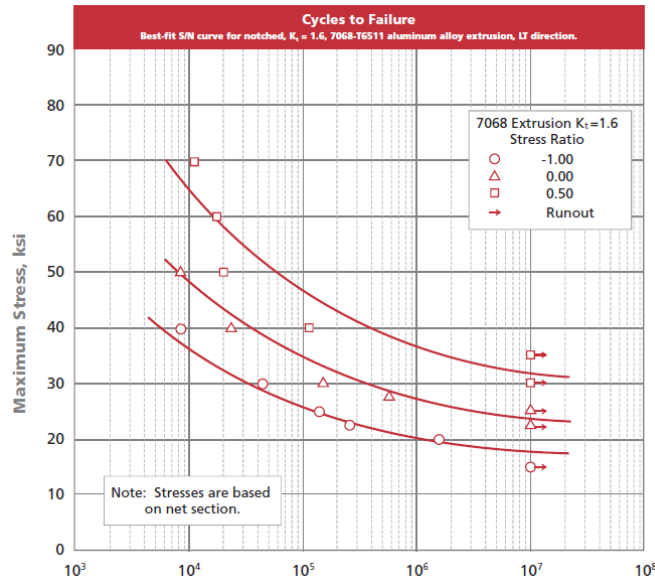


Figure 8.2. Maximum stress vs fatigue life for 7068-T6511 aluminum alloy [25]

In order to be able to sustain larger stresses and to minimize the weight, a titanium alloy is chosen for the hub: Ti6Al4V, Grade 5. In the table below its properties are shown.

Titanium Ti-6Al-4V (Grade 5), Annealed	
Density	4430 $kg/m^3$
Hardness	36 HRC
Ultimate tensile strength	950 MPa
Yield tensile strength	880 MPa
Compressive yield strength	970 MPa
Module of Elasticity	113 800 MPa
Elongation at break	14%
Fatigue strength (unnotched $10^7$ cycles)	510 MPa
Fatigue strength ( $K_t=3.3$ $10^7$ cycles)	240 MPa

Table 8.1. Titanium Ti-6Al-4V (Grade 5), Annealed properties [24]

The planetary carrier instead, resulted to be far less loaded as it will be shown in Section 8.4.3 so it was possible to manufacture the component in

7075-T6 aluminum alloy. This solution was preferred with respect to 7068-T6511 although the latter has a higher yield strength because the stresses observed are acceptable also for 7075-T6 alloy and because the latter alloy is available in less time for the supplier that machines the planetary carrier.

Aluminum 7075-T6	
Density	2810 $kg/m^3$
Hardness	150 HB
Ultimate tensile strength	572 MPa
Yield tensile strength	503 MPa

Table 8.2. Aluminum 7075-T6 properties [26]

## 8.4 FEM analysis and optimization

In the first stage the raw (i.e. not optimized) CAD model is designed based on package constraints, assembly procedure and gears characteristics and size. Obviously from this stage this component's weight can be significantly reduced so this geometry has been optimized through a topological optimization. The output of the optimization shows the areas where the material is needed to achieve the target imposed. Based on that the final CAD model is then developed and verified through a final FEM analysis.

### 8.4.1 Loads

In the g-g diagram shown below (extracted always from log files of Autocross events) it can be observed that the worst case for combined accelerations is during an acc-in-turn manoeuvre. Due to the load transfer towards the rear axle during acceleration and the static weight balance slightly towards the rear axle too, the rear wheels turns out to be the most stressed, the structural verification is thus performed on the loads coming from an acc-in-turn manoeuvre on a rear wheel tire contact patch.

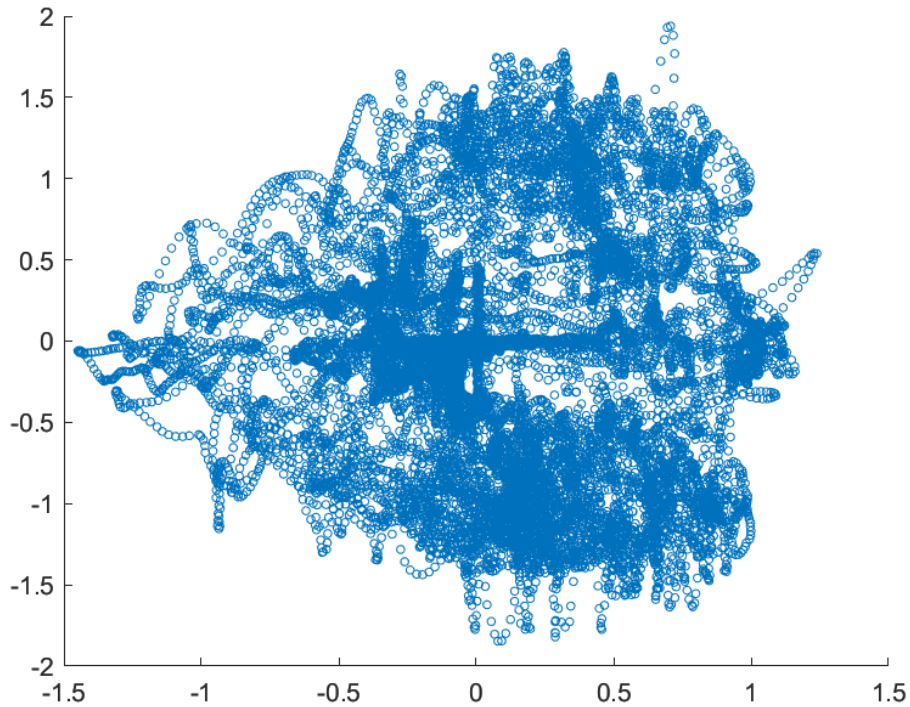


Figure 8.3. Autocross g-g diagram

The peak combined accelerations are 2 g in Y direction and 0.75 g in X direction. In addition to the tire contact patch loads, the axial load due to the locknut tightening must be added.

The loads used in the simulation are:

- Axial load due to tightening: 27 000 N;
- Tire contact patch X load: 1 150 N;
- Tire contact patch Y load: 3 075 N;
- Tire contact patch Z load: 1 540 N.

## 8.4.2 Optimization

Below is shown the 3D model of the planetary carrier and hub assembly before any optimization has been performed.

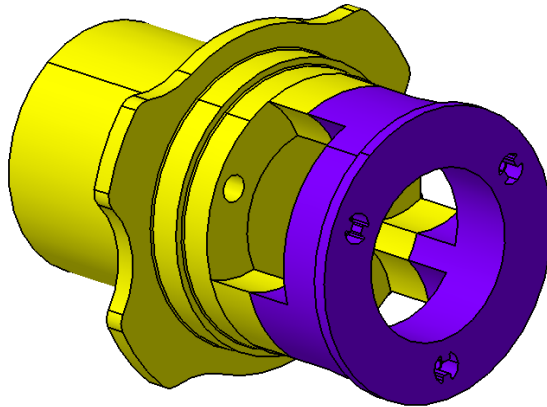


Figure 8.4. Hub-carrier assembly before optimization

The weight of the components is:

- Planetary carrier in aluminium: 192 kg
- Hub in aluminum: 0.560 kg
- Hub in titanium: 0.921 kg

### Optimization set-up

The model build in Hyperworks will be explained in detail in Section [8.4.3](#) where the whole model generation starting from the final geometry is detailed. In this section only the optimization set-up along with its targets and constraints is explained.

The most external elements constituting the hub-carrier group including the hub-rim coupling flange and the surfaces in contact with the bearings

raceways are set as non-design space (light blue in Figure 8.5), i.e. the elements density in those area is not modified during optimization. All the other elements are set as design space so during the optimization process, the solver will iteratively vary the density of the elements in those areas in order to match the targets and constraints imposed by the user.

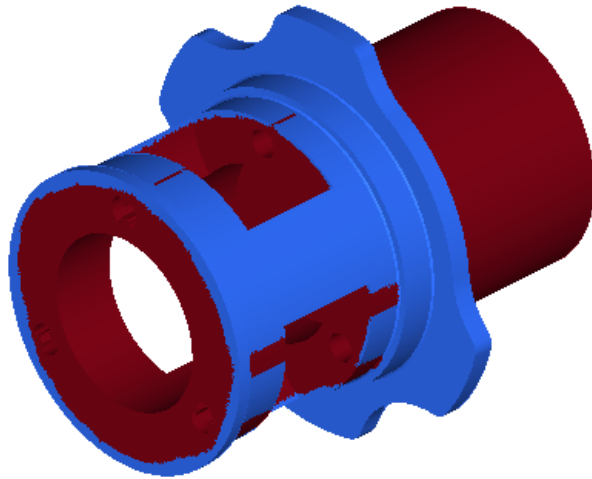


Figure 8.5. Optimization design and non-design spaces

A topological optimization is performed on the design space with the following parameters imposed.

- Constraint: maximum allowable stress 200 MPa
- Constraint: minimum volume 50% of the original one
- Target: minimize compliance (maximize stiffness)

### Optimization results

In what follows the contour plots of the required element densities computed by the solver is shown. Only the elements with density equal to at least 50% of the original one are shown.

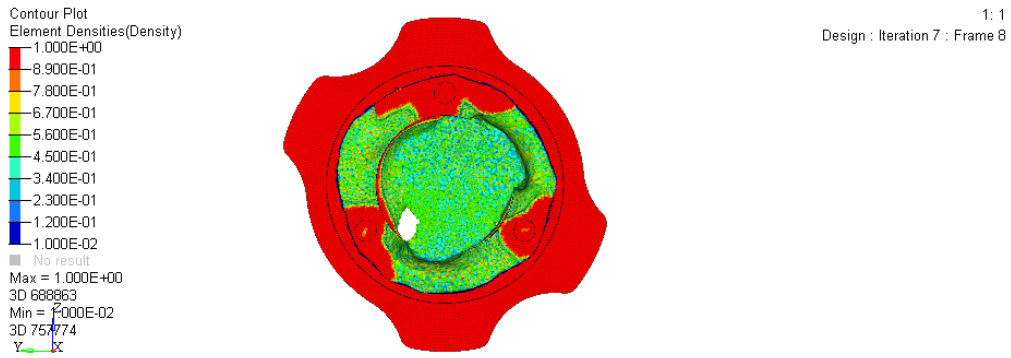


Figure 8.6. Element density contour, rear view

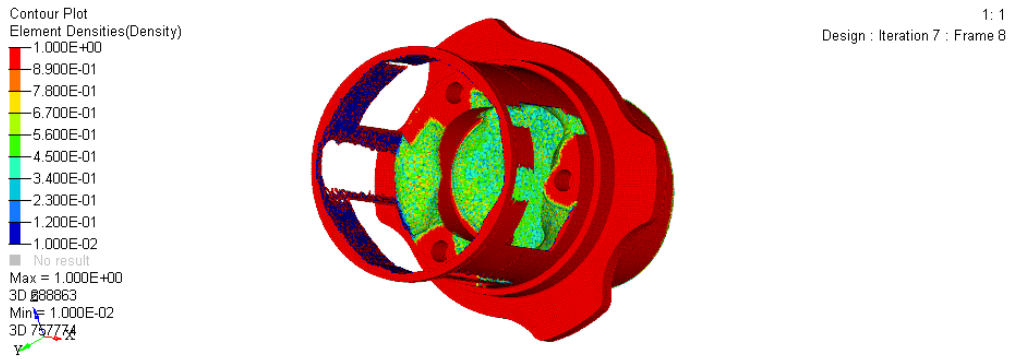


Figure 8.7. Element density contour, isometric view

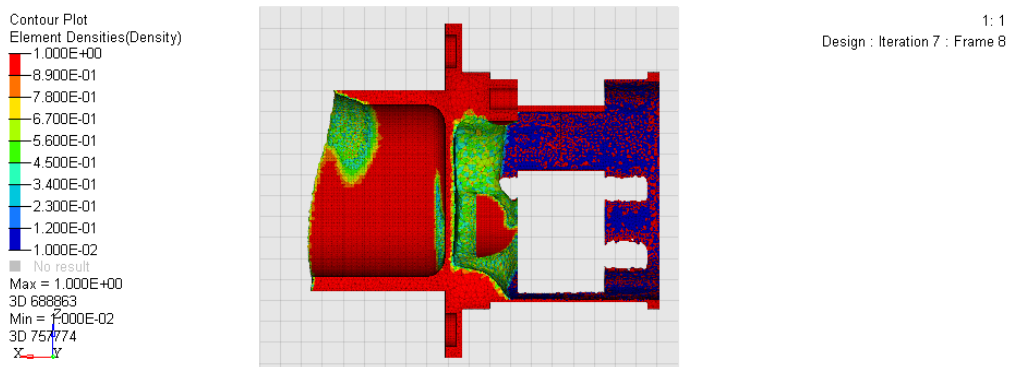


Figure 8.8. Element density contour, section view

### CAD post process

The geometry that is generated as an output from the optimization is obviously very rough because it is generated starting from the elements composing the mesh of the optimized component. Therefore, through CAD modelling, the material should be removed from the original raw component in order to ideally match the solver's output.

Below the raw 3D model of the planetary carrier and the hub is compared to the final one, generated basing on the optimization's output.

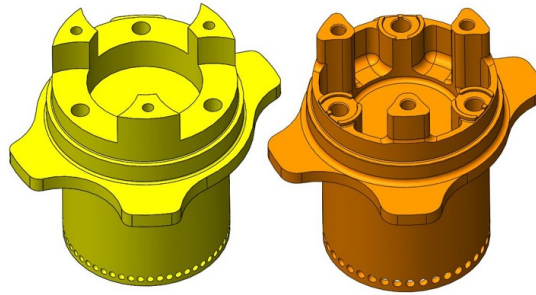


Figure 8.9. Hub before (left) and after optimization (right)

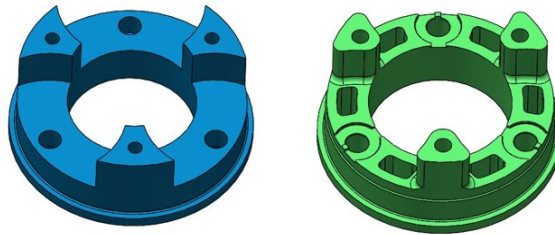


Figure 8.10. Planetary carrier before (left) and after optimization (right)

The weight of the optimized parts resulted to be:

- Hub (aluminum): 0.612 kg
- Planetary carrier (aluminum): 0.141 kg

### 8.4.3 Final FEM model

#### Model set-up

In this model also the wheel bearings inner rings are meshed along with the planetary carrier and the hub in order to better represent the constrain of the hub-carrier assembly.

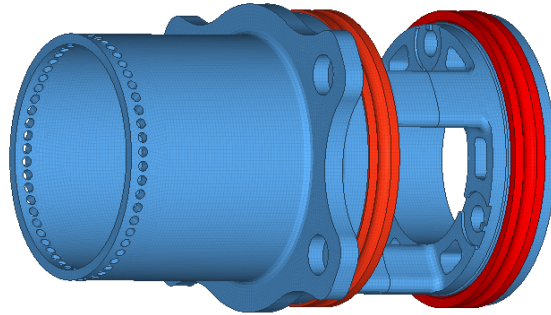


Figure 8.11. Components meshed in the model

All the components are meshed separately, before the surface is meshed and then the 3D mesh is generated starting from the surface mesh. This permits to tune and refine the surface mesh before generating the 3D mesh and consequently to be able to control the quality of the solid mesh. In order to optimize the computational times, the mesh is automatically refined in proximity of the geometrical irregularities (fillets, holes, etc...) and it becomes progressively coarser where the geometry is more regular. The elements size spans from 0.5 mm in the finest areas to 2 mm in the coarser ones. Finally the solid mesh is also finer near the surface and coarser

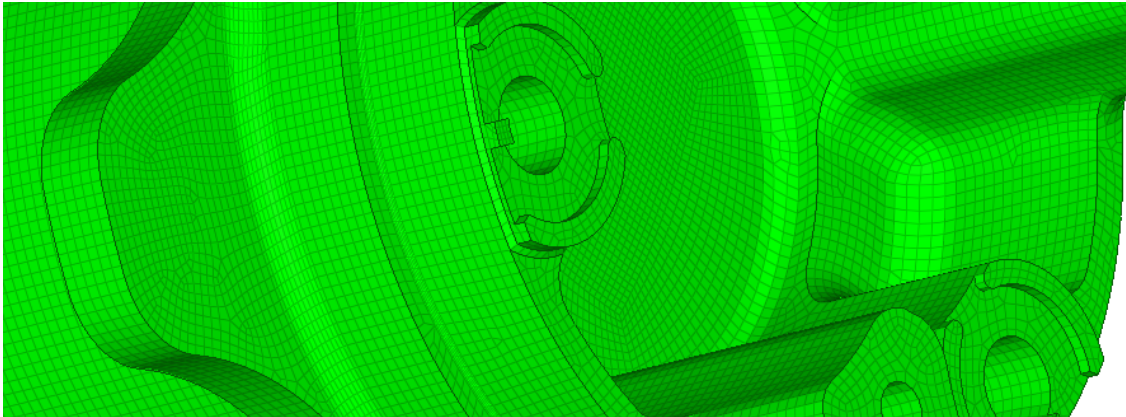


Figure 8.12. Particular showing the mesh size variation in the hub

The various elements are connected between each other according to the following interfaces (or contact surfaces):

- Hub-carrier
- Hub-bearing inner ring 1
- Carrier-bearing inner ring 2

All those contact surfaces are of the "stick" type, i.e. the slip is prevented for all the mating surfaces with respect to each other. This implies the following hypothesis: the threaded coupling between the hub and the carrier works in design condition and all the loads are transmitted by friction, there is no slip of the inner ring of the bearing with respect to the supported elements.

- Case
- Planet gears

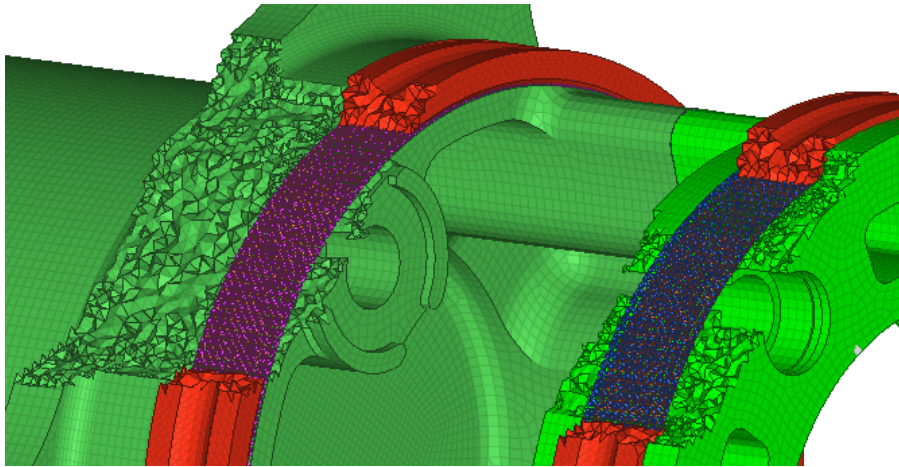


Figure 8.13. View of the contact interfaces between the hub-carrier and the bearings inner rings

The reaction of the planet gears avoids the hub to rotate around its axis. For this reason, the surfaces where the hub and the planetary carrier are coupled with the pin shafts are constrained via RBE2 rigid elements to a master node whose translations are locked.

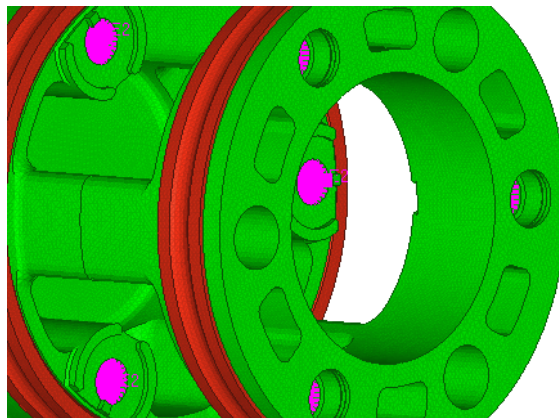


Figure 8.14. Pin shaft constraints

The case (upright) supports the hub-carrier assembly through the two wheel bearings. For this reason, the bearing inner races are constrained via RBE2 elements to two master nodes whose translational degrees of freedom

are constrained. Those master nodes are positioned in each bearing's centre.

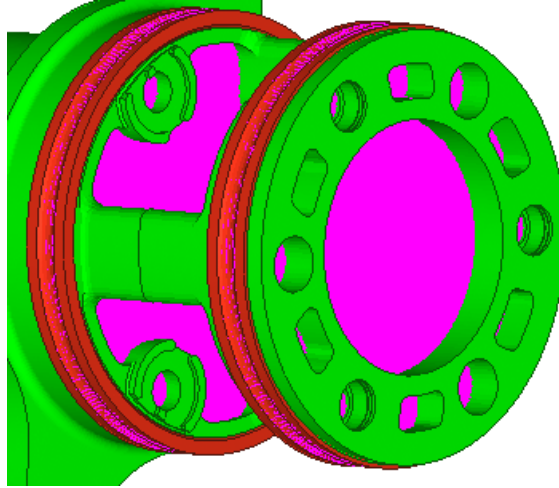


Figure 8.15. Wheel bearings constraints

The loads applied at the tire contact patch are brought to the hub by mean of RBE3 elements. This is a conservative model because all the loads are supposed to be sustained by the hub.

The axial force resulting from the locknut tightening is applied via RBE3 elements:

- As a tractive force on the hub threaded section on an area corresponding to the locknut one;
- As a compressive force on the hub flange.

Again, this representation is conservative because all the force is supposed to be sustained by the hub and not by the other parts between the hub and the locknut (rim, wheel spacer and brake carrier).

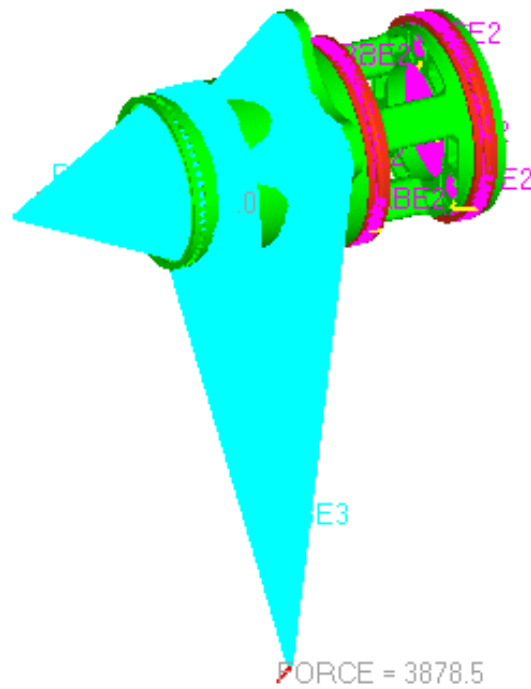


Figure 8.16. Loads application

The load step chosen is the acceleration turn because it resulted to be the most critical. The analysis performed is linear static.

## Results

Below is shown the contour plot of the mean stresses (the ones due to the locknut tightening) on the hub are shown, both in the Von Mises and in the Signed Von Mises form, the latter being useful to identify where the stress in a compressive or a tensile one.

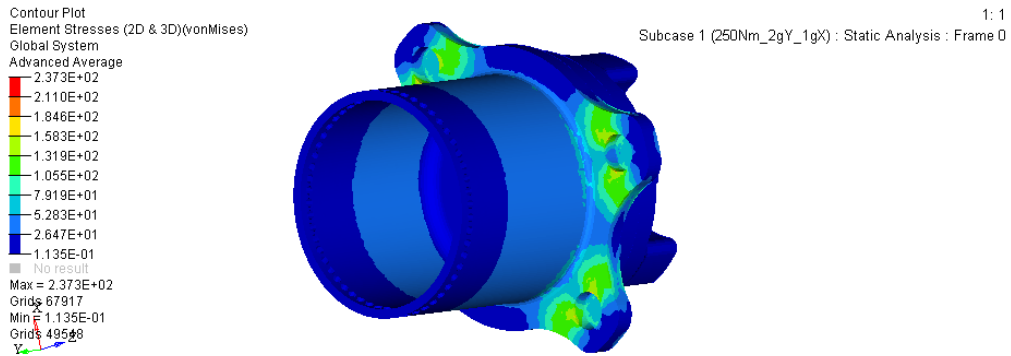


Figure 8.17. Von Mises average stress contour plot - Hub

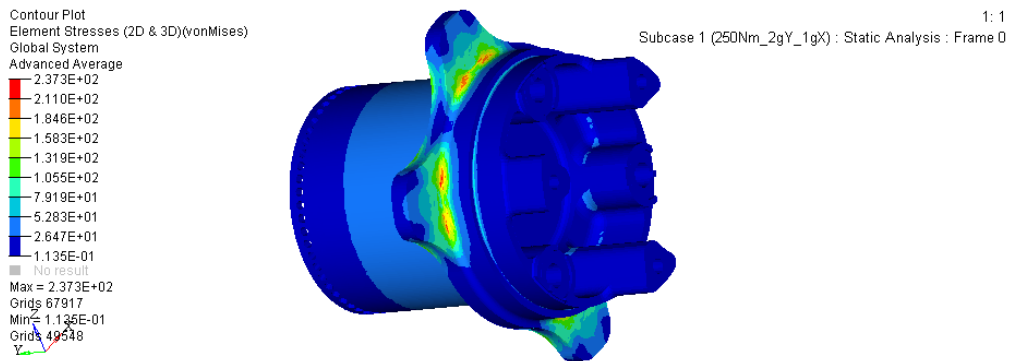


Figure 8.18. Von Mises average stress contour plot - Hub

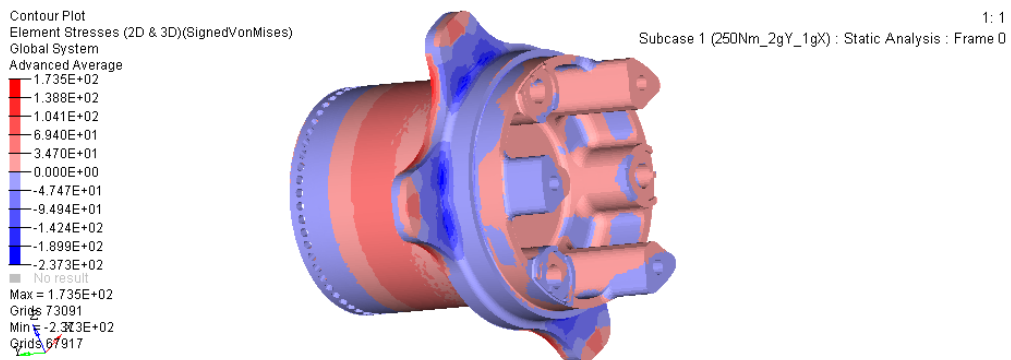


Figure 8.19. Signed Von Mises average stress contour plot - Hub

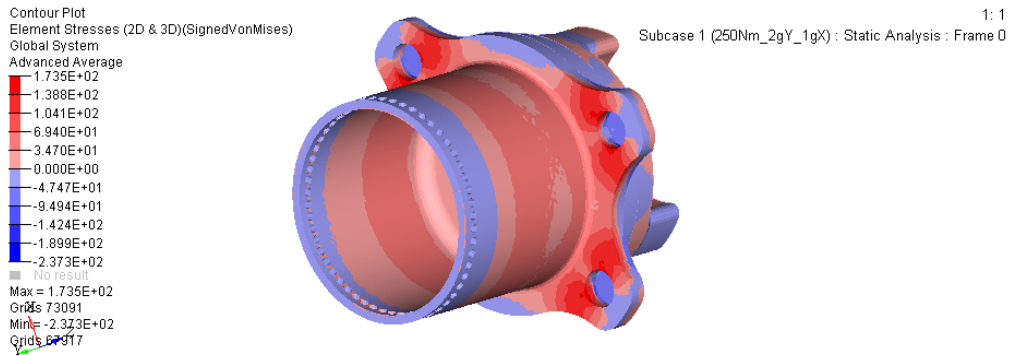


Figure 8.20. Signed Von Mises average stress contour plot - Hub

It can be noticed that the peak tensile stress due to the axial force produced by the locknut tightening is located on the hub flange facing the rim, this area is defined as the most critical one for the hub resistance. Clearly on the other side of the flange an high compressive stress is found. A slight stress concentration is present at the bearing interface with the hub.

Below is shown the contour plot of the mean stresses (the ones due to the loads at the tire contact patch) on the hub are shown, both in the Von Mises and in the Signed Von Mises form, focusing of the most critical are of the hub.

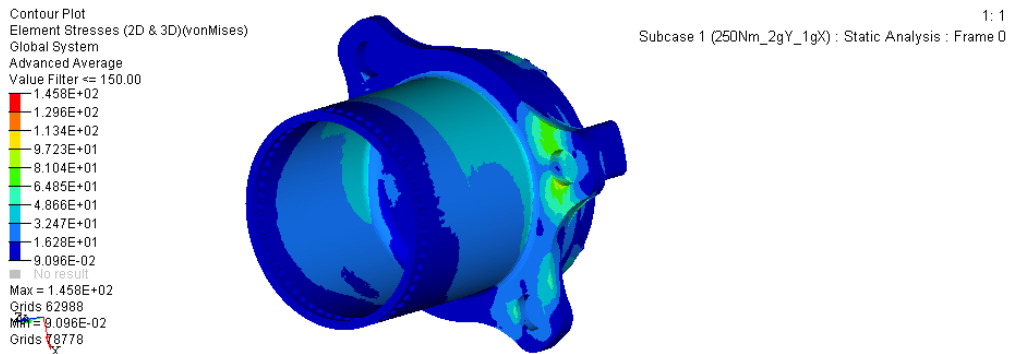


Figure 8.21. Von Mises alternate stress contour plot - Hub

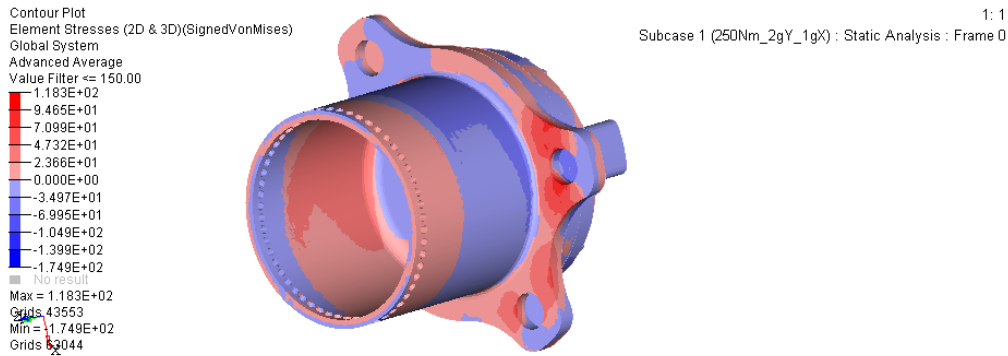


Figure 8.22. Signed Von Mises alternate stress contour plot - Hub

The Haigh diagram for the most stressed section of the hub is used to determine the its safety factor over infinite life, thus at  $10^7$  cycles according to the material datasheet.

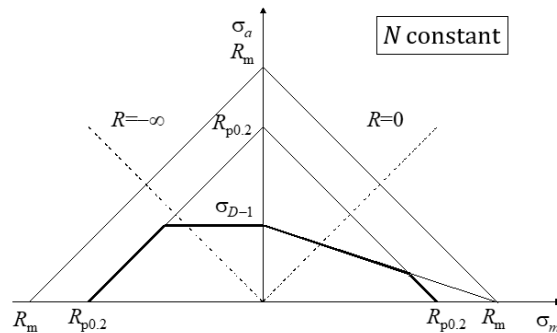


Figure 8.23. Haigh diagram example

The fatigue limit of the titanium alloy is taken as for a notched specimen in order to stay on the safe side. Also this analysis is carried only on the peak load sustained by the hub and not on a load spectrum so it is surely conservative.

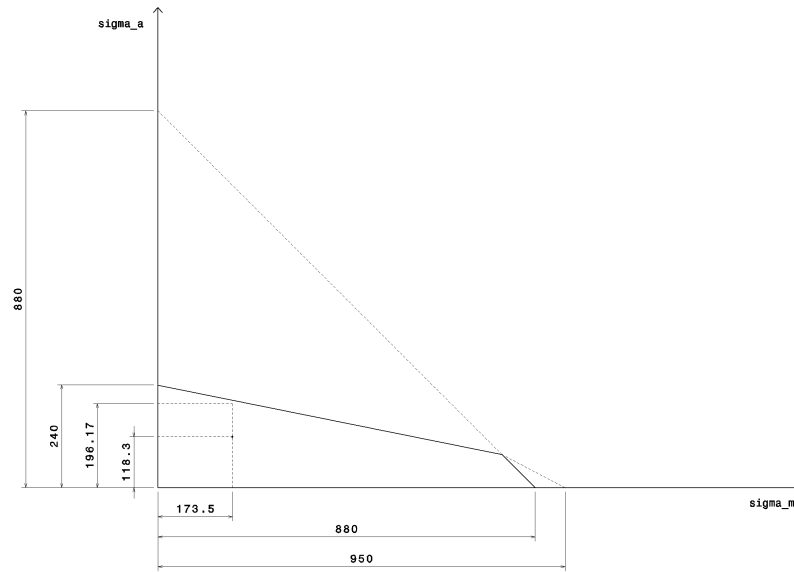


Figure 8.24. Haigh diagram of the most stressed section of the wheel hub

Given the fact that the average stress is constant, the safety factor for infinite life is given by the following equation:

$$SF = \frac{\sigma_D^{lim}}{\sigma_a^P} = \frac{196.2}{118.3} = 1.65 \quad (8.1)$$

The safety factor computed above is totally acceptable for this purpose.

Due to the fact that it is far less stressed, for the planetary carrier only a static verification is performed. Below the overall Von Mises contour plots are shown.

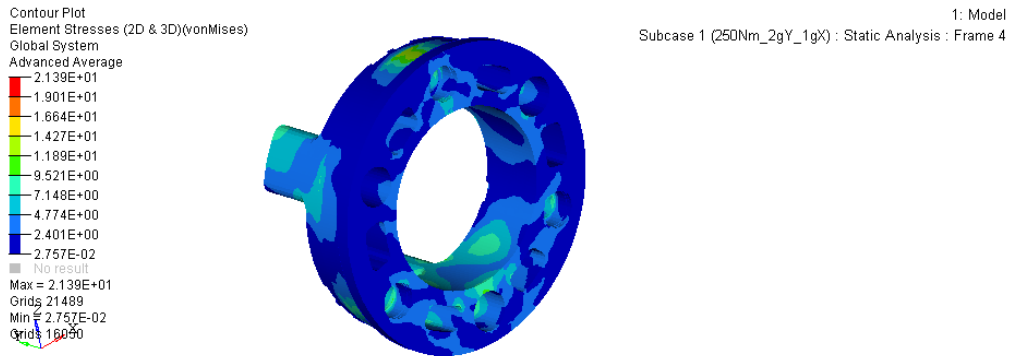


Figure 8.25. Von Mises stress contour plot - Planetary carrier

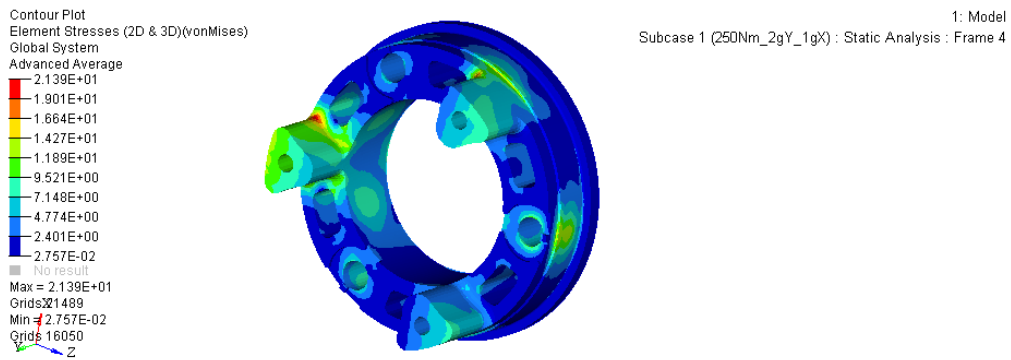


Figure 8.26. Von Mises stress contour plot - Planetary carrier

$$SF = \frac{R_p}{\sigma_{max}} = \frac{503MPa}{214MPa} = 2.35 \quad (8.2)$$

Finally, the displacement are shown.

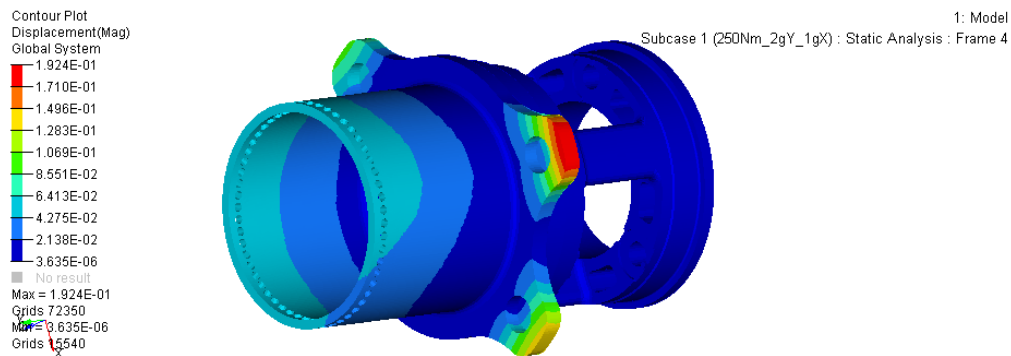


Figure 8.27. Displacement contour plot

Being all the displacements, apart from the hub flange, lower than 0.09 mm, they are acceptable for this purpose.

## 8.5 Manufacturing and tolerances

Both the planetary carrier and the hub are thought to be produced through turning and milling. Turning process is used for the first machining process on the raw bar, the diameters with tolerances and the threads, while milling process is used to machine the weight reduction pockets, all those profiles that cannot be turned and, in general, to finish the parts.

Tight tolerances must be kept on both planetary carrier and hub because those parts give the position to the planet pin shafts and also the wheel bearings must be fitted onto them.

The process starts with the machining of the hub and the planetary carrier separately. Particular care must be taken when machining the bores where the three calibrated screws couple with the hub and the planetary carrier. Also, both the components are not finished at this stage: the bores for the

pin shafts are not machined and the coupling surfaces with the wheel bearings are left with some oversize.

After that preliminary phase, the planetary carrier and the hub are bolted together with the three calibrated screws, then the machining of the bearings coupling surfaces and the machining of the bores that house the pin shafts is performed. The machining with hub and carrier mating is useful to guarantee the best coaxiality between the pin shaft bore in the hub and the one in the planetary carrier, also it allows the best coaxiality between the bearing mating diameters.

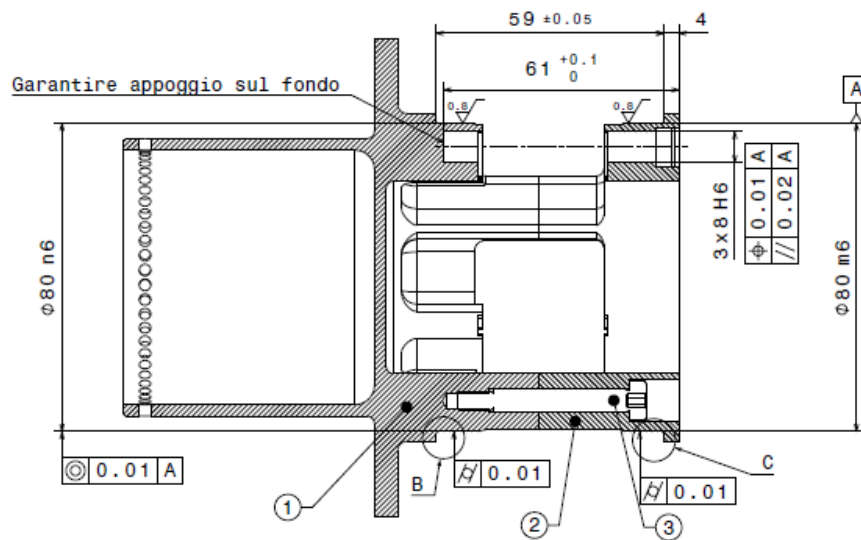


Figure 8.28. View of the technical drawing about the machining process with mating hub and planetary carrier

# Chapter 9

## Lubrication

### 9.1 Lubricant choice

The gearbox oil in this application carries the following duties:

- Gears lubrication;
- Bearings lubrication;
- Protect metal parts from corrosion;
- Dirt removal.

Due to the numerous tasks that the lubricant can perform, its choice is indeed really important, in particular because it needs to lubricate both the gears and the bearings. At the same time is difficult to find a method of choice that is not empirical.

The lubricant film thickness between the teeth is adequate when it is larger than the average surface roughness of the flank, a high viscosity of the oil helps to have an adequate film thickness even at low rotational speeds. The gear resistance to scuffing and pitting improves with the increase of viscosity

of the oil. A too high viscosity has however also negative aspects, as the increase of the friction losses of the gearbox and so its efficiency.

For all the reasons mentioned above the lubricant choice is often a compromise. In the following table an empirical suggestion is made as a function of the ambient temperature and of the peripheral velocity.

Peripheral velocity [m/s]	10-20 °C	10-50 °C
Up to 10	150	320
10-20	68	150
20-35	32	68

Table 9.1. ISO grade per ambient temperature, mineral oil [4]

The peripheral velocities are:

- Sun gear = 38.0 m/s;
- Planet gear first stage = 35.6 m/s;
- Planet gear second stage = 14.5 m/s.

Considering an ambient temperature of around 60 °C, the suggestion from the above table regarding a mineral oil is ISO 68 so with an average kinematic viscosity of 68  $mm^2/s$ . Due to the fact that for this application a synthetic oil is used, even if the peripheral velocity of the sun gear is slightly higher than 35 m/s, it is not a critical condition.

A viscosity value between 40 and 100  $mm^2/s$  at 40 °C is also suitable for bearings lubrication, ISO 68 is included in this interval.

Motul Gear 300 75w90 is chosen, a fully synthetic lubricant whose viscosity at the 40 °C reference temperature is 72.6  $mm^2/s$  [27]. This oil is very

common amongst gearboxes and it was already successfully employed in the SCdiciassette's transmission.

## 9.2 Seals

The transmission case (i.e. the upright) must be sealed in order to prevent the oil to exit the case itself. A section view of the transmission inside the upright is shown in Figure 9.1.

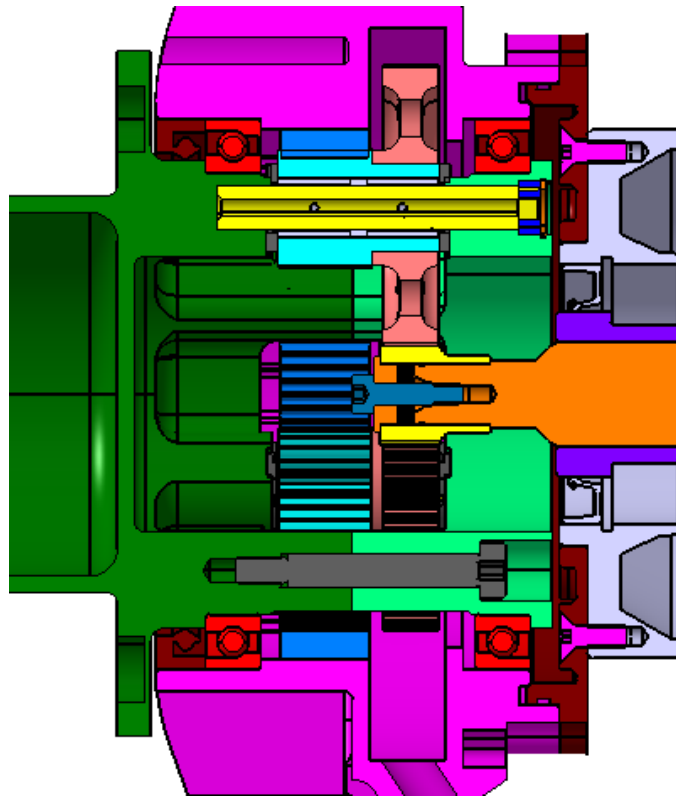


Figure 9.1. Section view of the transmission inside the upright

On the wheel side the sealing is provided by a radial shaft seal, while on the motor side the sealing is provided by an O-Ring.

### 9.2.1 Radial shaft seal

Due to the fact that the seal on the motor side must provide sealing between a rotating part (the hub) and a static one (the upright), a radial shaft seal is mandatory. Moreover, the element to be retained is oil so a spring loaded radial shaft seal is mandatory.

In the SCdiciassette gearbox, the shaft seal was supplied by SKF and it was of the type CRW1, with reference to Figure 9.2.



Figure 9.2. CRW1 type seal (left and HMS5 type seal (right) [13]

With the abovementioned type of seal some issues related to reliability emerged, the steel outer layer is poorly tolerant to the surface finish of the upright, making the manufacturing more complex and impairing the serviceability of the component: particular care must be taken during assembly and when disassembling because even minimal scratches of the surface prevent

the seal to be effective.

For the present project it was decided to switch to a seal of the type HMS5 (Figure 9.2). The rubber coating of the outer layer make the seal by far more tolerant to the surface finish.

According to the installation dimensions available, the final choice was on HMS5 85x100x9 RG, the suffix RG indicating that the nitrile rubber works as a sealant. Due to the fact that the rotating part to be sealed is the wheel hub, the following working conditions hold for the radial shaft seal:

- Circumferential speed: 6.0 m/s;
- Rotational speed: 1350 rpm;
- Shaft diameter: 85 mm.

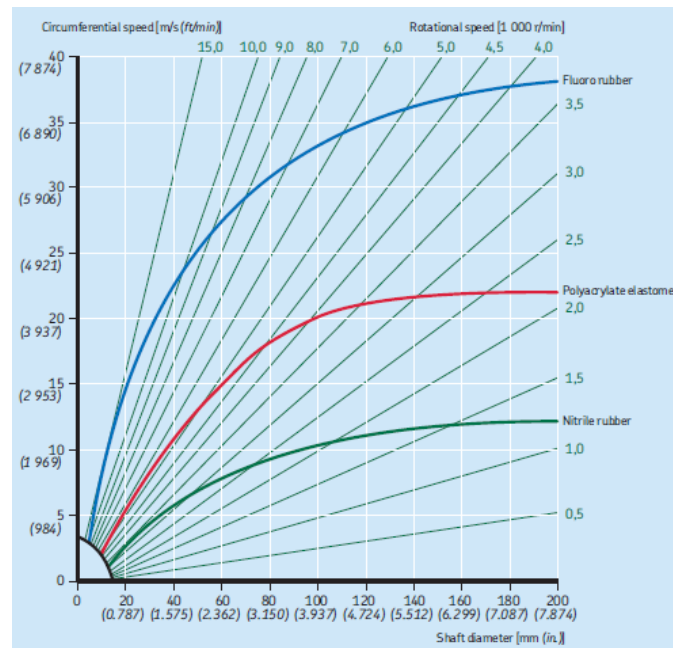


Figure 9.3. Permissible speeds for spring-loaded sealing lips when no pressure differential exists across the seal in operation [13]

Given the working conditions of the radial shaft seal and the graph shown in Figure 9.3 it is easy to verify that the nitrile rubber can be used for this application. Also the allowable temperature ranges from  $-40\text{ }^{\circ}\text{C}$  to  $100\text{ }^{\circ}\text{C}$ , expecting a  $60\text{ }^{\circ}\text{C}$  temperature of the oil in the case, the proper working conditions are assured.

Finally the following tolerances must be guaranteed for the shaft:  $h11$  for the diameter and  $1.2\text{ }\mu\text{m}$  as surface roughness, for the bore:  $+0.10/+0.25$  mm for the diameter [13].

### 9.2.2 O-Ring

On the motor side, the two parts to be sealed are both static (the upright and the motor flange), making appropriate the usage of an O-Ring.

Apart from the assembly operation, the O-Ring always work in static axial and radial condition.

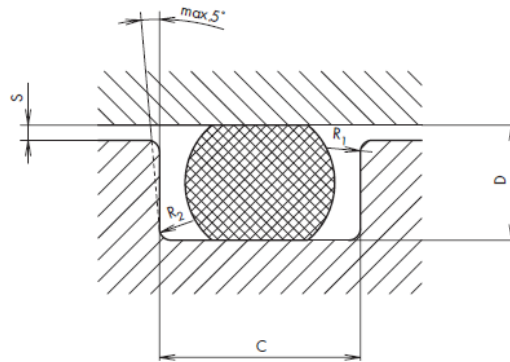


Figure 9.4. O-Ring groove [15]

According to the working condition of the O-Ring, choosing a ring with a diameter of  $1.78\text{ mm}$ , the groove must have the following dimensions [15], with reference to Figure 9.4:

- $D = 1.3$  mm;
- $C = 2.5 \pm 0.1$  mm;
- $R_1 = 0.1$  mm;
- $R_2 = 0.25$  mm.

### 9.3 Lubricant level

An excessive lubricant quantity can cause higher temperature inside the gearbox and also impair its performance, increasing the work done by the gears against the oil during splashing, at the expense of the efficiency.

A rule of thumb commonly used for planetary gearboxes with splashing lubrication is to have the oil level slightly above the planet pin shaft when the latter is in the lowermost position. With this oil level, a large number of spheres of the bearing is also cyclically in the oil bath.

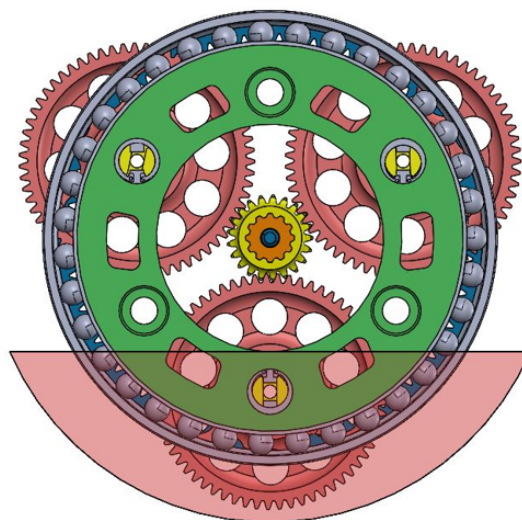


Figure 9.5. CAD determined oil level

The correctness of the assumption previously described has been verified empirically: a polycarbonate sheet seals the gearbox on the motor side and makes the oil level visible, the gearbox is then operated manually by rotating the hub and it is checked whether the oil level poured is sufficient or not to lubricate all the meshing gears during the operation.

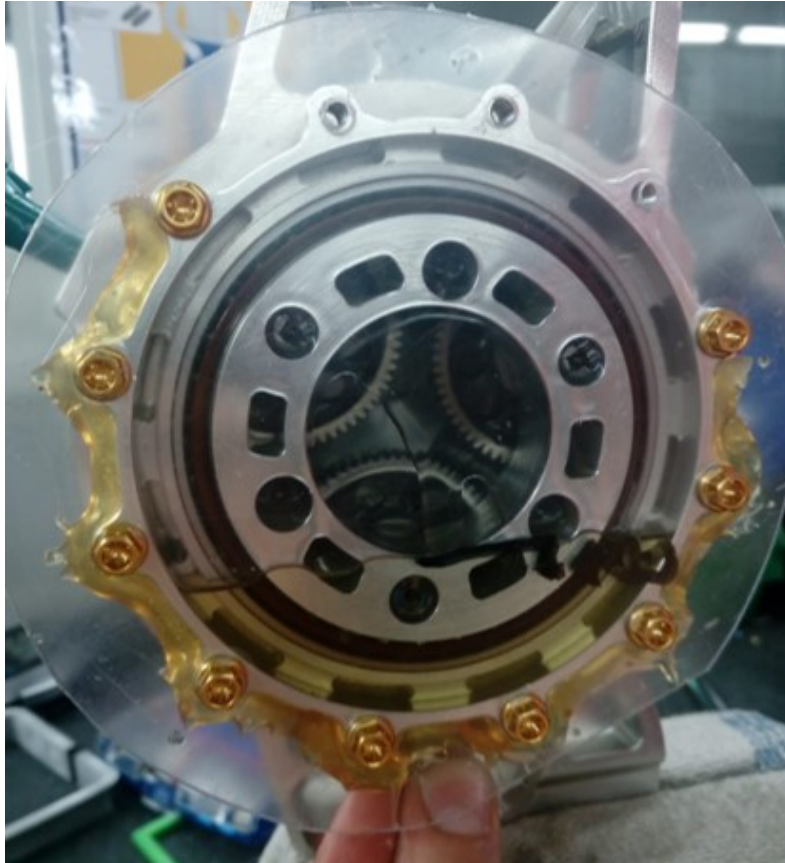


Figure 9.6. Tested oil level

This process allows to determine the optimal lubricant volume, resulted to be 100 ml. It is a significant weight reduction with respect to the SCdici-assette gearbox, that due to its higher case volume, used to run with 200 ml of poured oil.

# Chapter 10

## Efficiency analysis

### 10.1 Power losses

The losses of a gearbox can be due to different factors. The main contributors to the total losses of a gearbox of the type discussed in this work are shown below [17].

- Gear losses: generated by friction between engaging teet flanks (torque and speed dependent) and by friction of wheels rotating in the air and in the oil (only speed dependent)
- Bearing losses: generated by the extension of the contact area of rolling bodies and by their deformation (partly dependent and partly independent on power) and by their rotation in the air and in the oil (only speed dependent);
- Sealing losses: generated by friction between seals and rotating shafts (only speed dependent).

In this type of gearbox some losses that are commonly present in common automotive transmissions, for example the losses due to synchronizers and the losses due to the lubrication pump are not present.

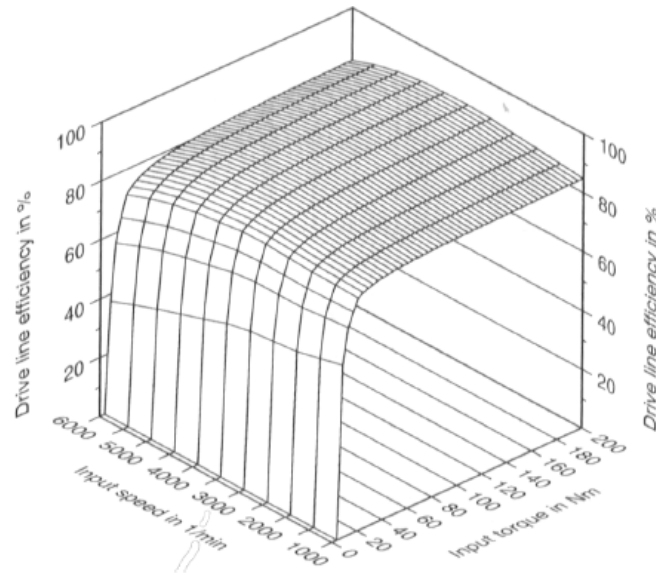


Figure 10.1. Gearbox efficiency example [17]

The best way to evaluate the efficiency of a gearbox is clearly to measure it. However the set-up of a proper test bench is very costly and time-demanding, for those reason there are no possibilities to perform it during the racing season.

Alternatively the efficiency can be calculated in an analytical way, this calculation can be carried in KISSsys where the gear meshing losses are calculated according to Niemann/Winter method, the bearing losses are calculated by mean of the formulas suggested by the catalogue, the gear churning losses (i.e. the losses caused by gear striking, pumping or otherwise moving the lubricant around in the gearbox) are calculated according to the method proposed by ISO TR 14179, finally also to seal losses are calculated according to ISO TR 14179 [18].

The losses of the gearbox can be expressed as:

$$P_V = P_{VZ0} + P_{VZ} + P_{VL0} + P_{VL} + P_{VD} \quad (10.1)$$

Where:

- $P_{VZ0}$  are the gear churning losses;
- $P_{VZ}$  are the gear meshing losses;
- $P_{VL0}$  and  $P_{VL}$  are the bearings losses;
- $P_{VD}$  are the seal losses.

## 10.2 Gearbox efficiency model

The efficiency model is developed starting from the gearbox model explained in Section 4, already used for the gears sizing and life calculation. A devoted template in KISSsys suite is used for this purpose.

The transmission case geometry is modeled in a simplified way because in this suite only rectangular and cylindrical cases can be modeled and the oil level is given as an input. Further settings may allow also to model an oil cooler, obviously not present in this case. The oil specification and its working temperature are taken from the gear calculation (ISO-VG 68, 60 °C working temperature).

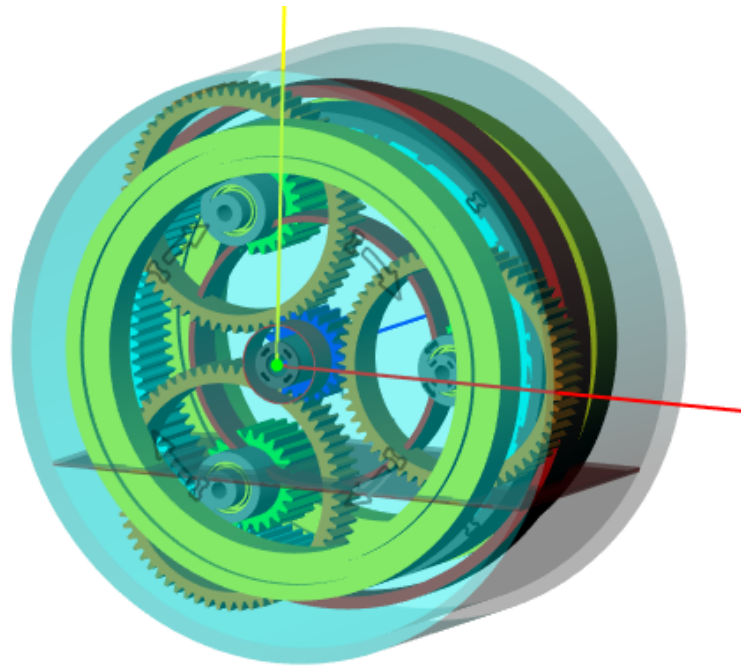


Figure 10.2. Transmission case model for efficiency analysis

The bearing model is taken from the software's library and reflects most of the characteristics that the bearing used for this application has (SKF Super Precision bearings are not present in the software library).

A radial shaft seal is automatically added by the software because the planetary carrier is not fully enclosed in the case volume modeled (Figure 10.3) with the characteristics of a "general oil seal" described by ISO TR 14179-2 (Eq. 31) [18].

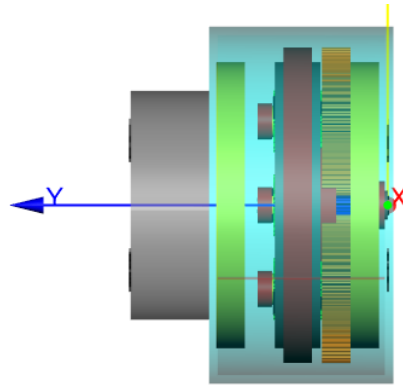


Figure 10.3. Side view of the transmission model in its case

## 10.3 Results

Below the efficiency contour plots both in traction conditions and in regenerative braking conditions are shown.

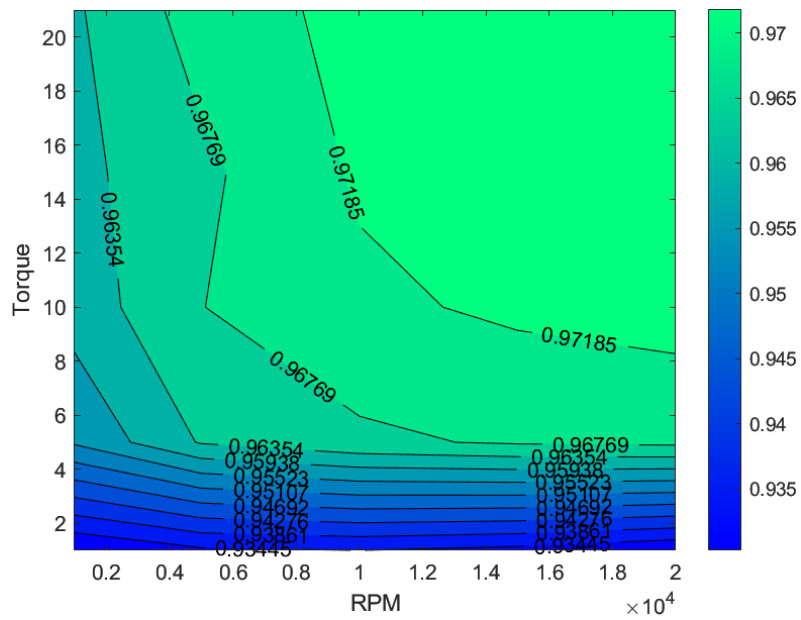


Figure 10.4. SC18integrale direct efficiency (traction conditions)

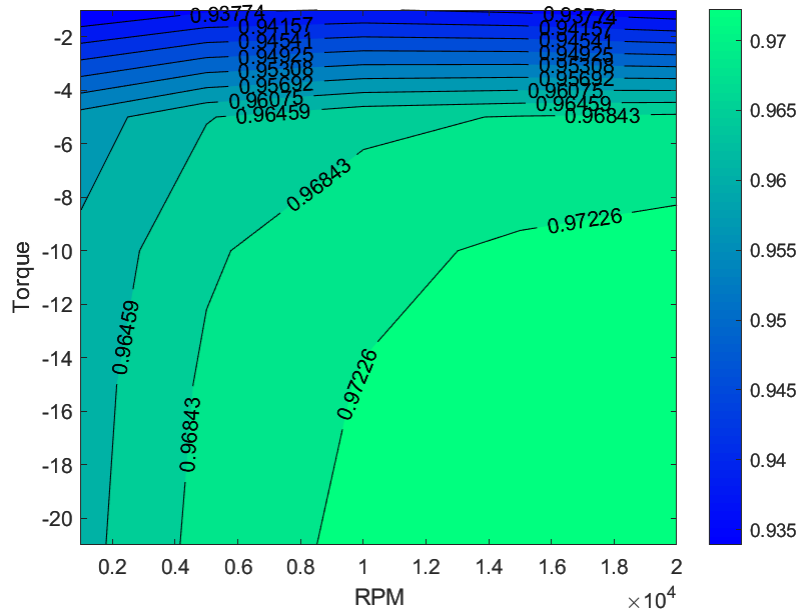


Figure 10.5. SC18integrale inverse efficiency (regenerative braking conditions)

As a comparison, below also the SCdiciassette efficiency contour plot are shown.

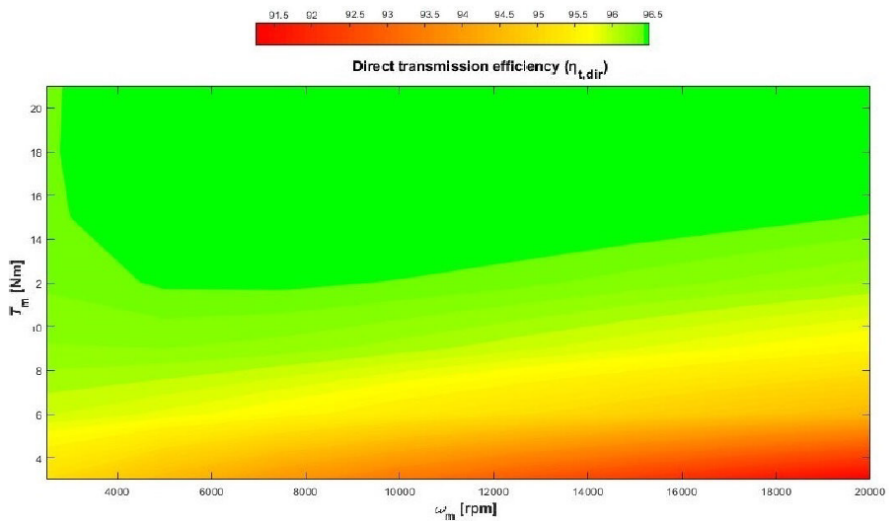


Figure 10.6. SCdiciassette direct efficiency (traction conditions) [22]

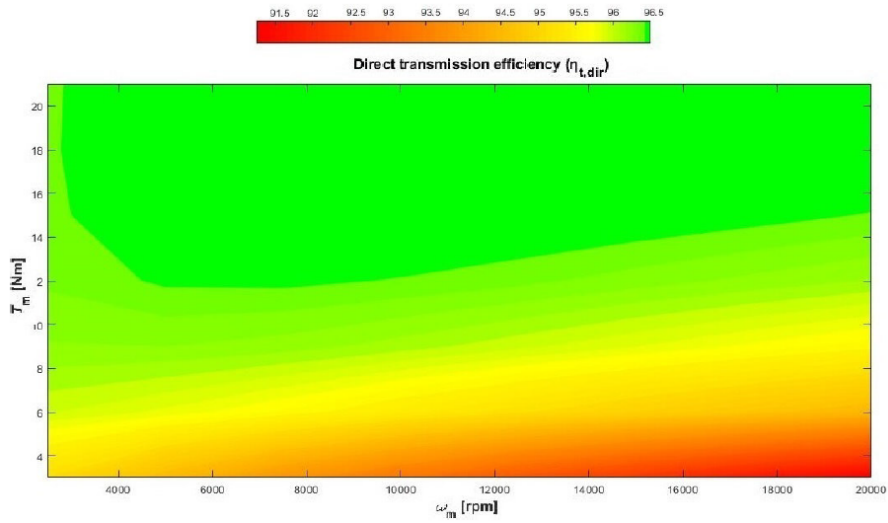


Figure 10.7. SCdiciassette inverse efficiency (regenerative braking conditions) [22]

An improvement of both the minimum and the maximum efficiency is observed, both in traction and in regenerative braking, with respect to the SCdiciassette gearbox. The efficiencies in traction and regenerative braking resulted to be almost equal.

	Minimum efficiency	Minimum efficiency
SCdiciassette	90	96.5
SC18integrale	93	97.6

Table 10.1. SC18integrale recorded running time and distances

It must be noted that not all the points present in the efficiency map are actually reachable because the motor power is limited to 20 kW.



# Chapter 11

## Assembly

In this chapter the designed assembly procedure is described in detail. Knowing the assembly procedure will allow to understand better all the solutions described in the previous sections.

### 11.1 Upright group assembly

With reference to the Figure [11.1](#).

1. Insert the radial shaft seal (22) into the hub (24).
2. Mount the wheel bearing (21) onto the hub (24) paying attention to orient the spheres into the proper way, respecting the “O” mount (Figure [11.2](#)). Press fit.
3. Insert the ring gear (20) into the proper groove into the upright (18) (Figure [11.3](#)).
4. Retain the ring gear (20) to the upright by mean of the special screws (19). Pay attention that the ring gear maintain some backlash even after the screws are positioned (Figure [11.3](#)).

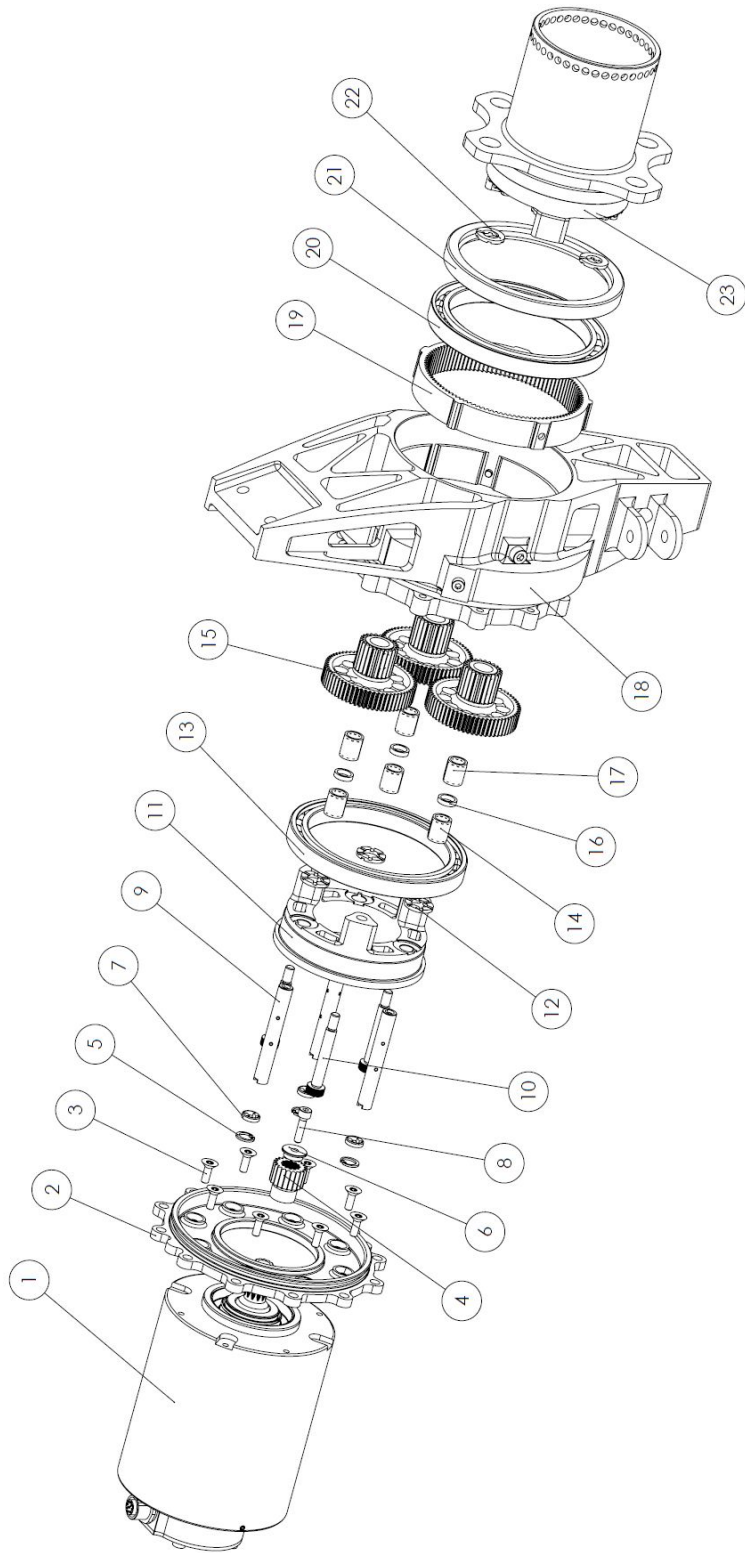


Figure 11.1. Transmission assembly  
164

5. Insert the hub + bearing + shaft seal assembled at point 2 into the upright (18). Care must be taken to fit properly the shaft seal into the upright bore (Figure 11.4).
6. Insert the shims (23) into the proper locations of the hub (24).
7. Insert the three planet gears (15) into the upright (18) and align the bores in the planet gears with those in the hub (24). Care must be taken to the phase of the teeth of the planet gears (11.5).
8. In the planet gears (15) bores insert: a needle bearing (17), a spacer ring (16) and a second needle bearing (17). Lubricate all parts with 75W90 oil (Figure 11.6).
9. Insert the planet pin shaft (9) into the planet gears, making sure that the component fits the needle bearings (17) and the spacer ring (16) and that touches the bottom of the bore in the hub location (24) (Figure 11.7).
10. Insert the H-shaped bushings (7) in the proper locations in the planetary carrier (11). If necessary warm up the planetary carrier (11) in order to ease the procedure.
11. Mount the elastic rings (4) in the proper locations inside the planetary carrier.
12. Fit the ball bearing (13) in the proper location on the planetay carrier (11) (80mm diameter), making sure the orientation of the spheres is correct.
13. Mount the spacers (12) in the proper locations on the planetary carrier. If necessary, glue the spacers to the planetary carrier.
14. Insert the preload spacer (25) of the ball bearing (13) into the upright.

15. Insert the planetary carrier + bearing group into the upright (18). In order to allow the mounting process, phase the pin shafts (9) so that the groove is aligned with the notches of the bushings.

Observe the orientation of the planetary carrier with respect to the hub (marks are present).

16. Insert calibrated screws (10) in the proper locations and tightening them with a 10 Nm torque.

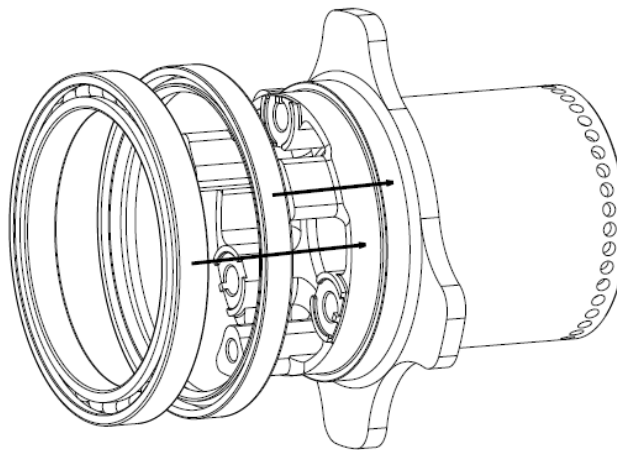


Figure 11.2. Fit of the bearing and of the seal onto the hub

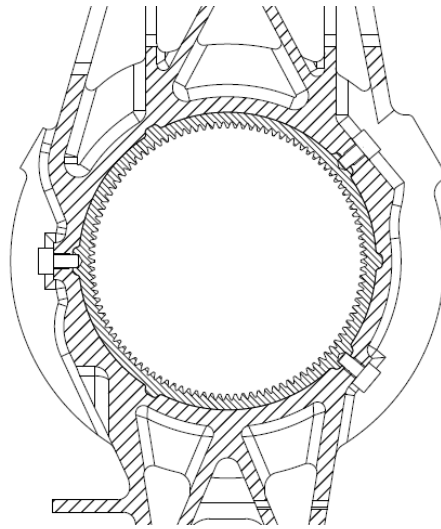


Figure 11.3. Ring gear installation

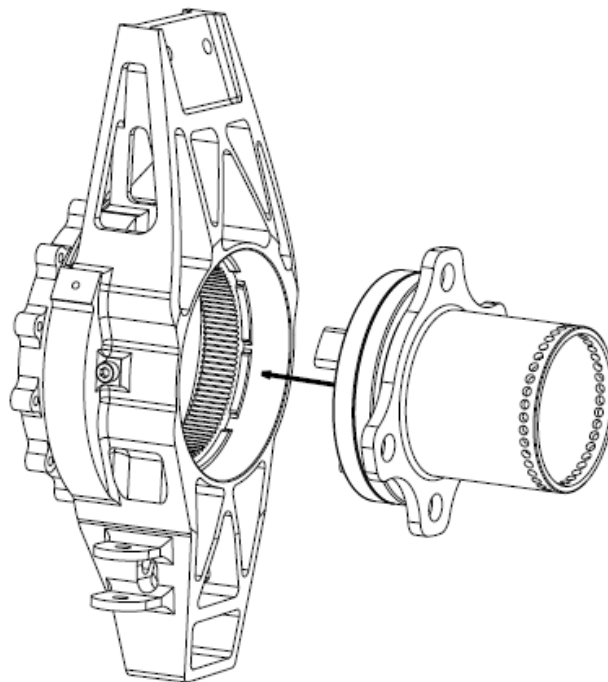


Figure 11.4. Fit of the hub into the upright

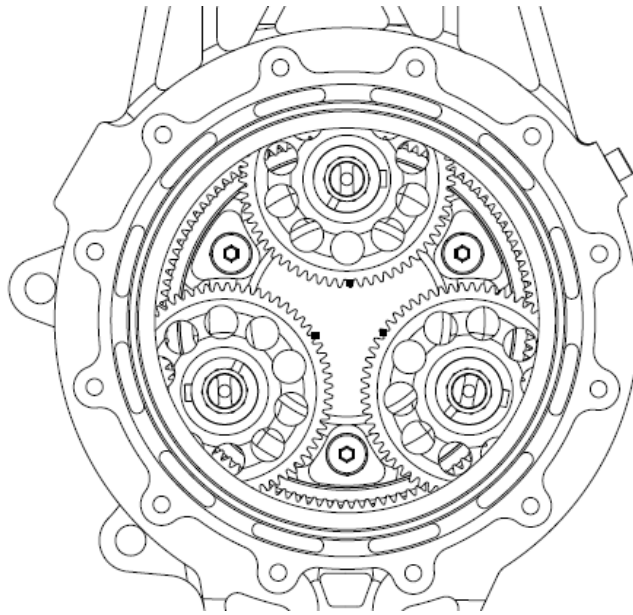


Figure 11.5. Satellites phase

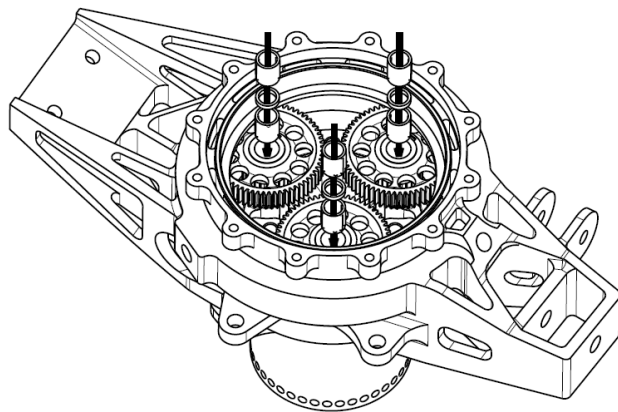


Figure 11.6. Needle roller bearings assembly

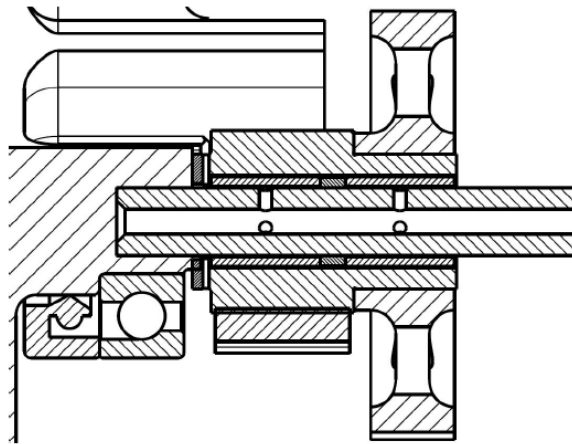


Figure 11.7. Planet pin shaft correct position

## 11.2 Motor group assembly

1. Mount the flange (1) on the motor, sealing the interface with sealant paste (3), tightening them with a 4 Nm torque.
2. Fit the sun gear (4) on the splined section of the motor output shaft (1).
3. Insert the bushing (6) into the sun gear (4) bore.
4. Insert the screw (8) in the bushing bore (4) and tighten it onto the motor output shaft with a 4 Nm torque. During this step constrain the motor shaft by means of the proper splined tool.



# Chapter 12

## Final transmission assembly

### 12.1 Transmission assembly

Below an isometric view of the final release of the gears is shown.

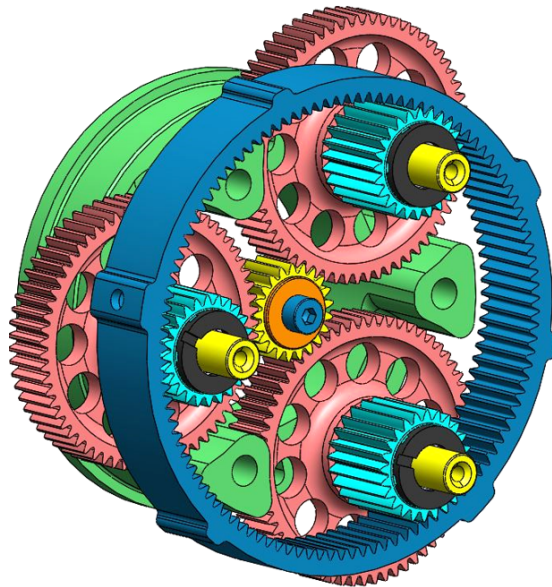


Figure 12.1. Final gears assembly

Also, below the full final transmission assembly is shown. also the wheel bearings and the hub are shown.

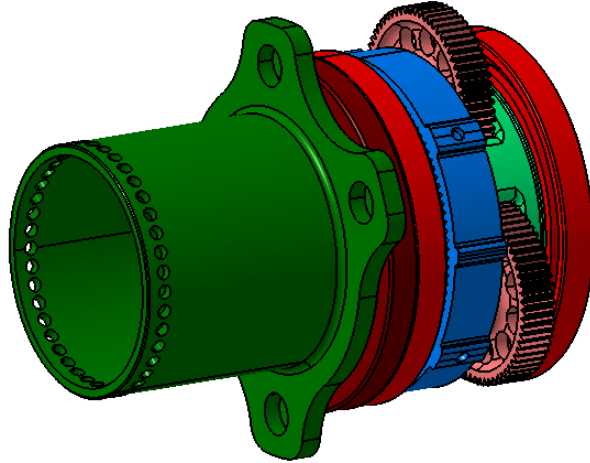


Figure 12.2. Final gearbox assembly

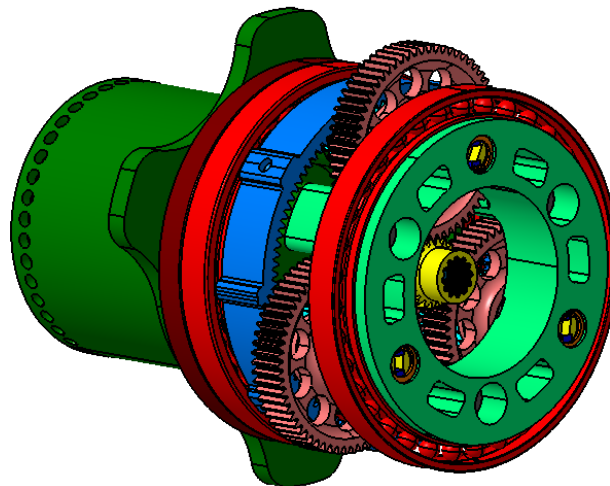


Figure 12.3. Final gearbox assembly

## 12.2 Transmission integration

Below a view of the transmission and the motor assembled is shown. Also the motor mounting flange can be seen.

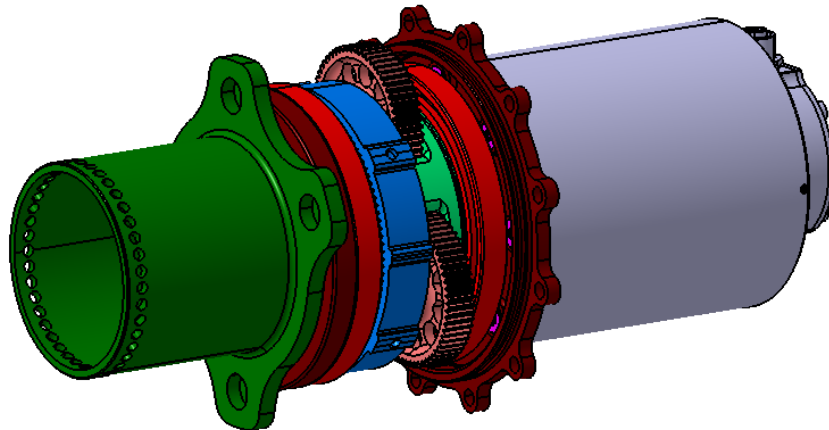


Figure 12.4. Final gearbox assembly

Finally the integration of the gearbox into the wheel assembly is shown. It is then clear that the package in this area is critical and how reducing the volume of the transmission is beneficial for the freedom in suspension design.



Figure 12.5. SC18integrale transmission assembled



## Part II

# Second part



# Chapter 13

## Results obtained

### 13.1 Weight reduction

Below a table with the weight reduction per each components with respect to SCdiciassette upright is shown.

Component	N	Weight 2017 [kg]	Weight 2018 [kg]
Sun gear assembly	1	0.141	0.024
Planet gears assembly	3	0.192	0.138
Ring gear assembly	1	0.412	0.157
Planetary carrier	1	0.278	0.141
Hub	1	0.771	0.612
Wheel bearings	2	0.28	0.15
Wheel bearings locknut	1	0.053	-
Screws	3	0.02	0.011
Oil	1	0.18	0.09
Total	-	2.871	1.693

Table 13.1. Weight comparison

Total weight reduction: - 1.178 kg, - 41 %, overtaking the 30 % target at the beginning of the project. It must be noticed that the reduction in volume and in weight of the transmission impacts largely also on the weight of the

upright and of the motor flange, thus increasing even more the advantages coming from its volume reduction.

Note:

- The planet gears assembly includes the needle roller bearings and the pin shaft (if any)
- The SCdiciassette sun gear assembly includes its bearings and the bearings preload locknut
- The ring gear assembly includes its retention system



Figure 13.1. Comparison between the SCdiciassette ring gear (left) and the SC18integrale one (right)



Figure 13.2. Comparison between the SCdiciassette planet gears assembly (left) and the SC18integrale one (right)

## 13.2 Volume reduction

Below a comparison between the SCdiciassette and SC18integrale transmission main dimensions is shown.

Dimension	Size 2017 [mm]	Size 2018 [mm]
Overall length	89.5	72
Bearings outer diameter	125	100
Planet gears maximum diameter	133	120

Table 13.2. Main dimensions comparison

The "Planet gear maximum diameter" is in absolute terms the maximum diameter of the gearbox. It impacts into the upright because the higher this diameter is with respect to the bearings diameter, the deeper the groove into the upright to allow the planetary gear movement should be. Its impact on the overall volume is however limited due to the fact that the groove axial length is just slightly higher than the second stage planetary gear facewidth.

The main contributors to the overall size of the transmission are indeed the bearings outer diameter and the overall length. For this reasons those two parameters are used to compare the volume reduction: both the diameter and the overall length have been reduced by 20 %, overtaking the 15 % target.

### 13.3 Assembly process



Figure 13.3. Transmission parts before assembly

Due to tight tolerances imposed and good material properties required, all the components have been checked before assembly. The teeth have been verified according to their Wildhaber dimension specified in the technical drawing and the phase between the teeth in the planetary gear have been measured with a coordinate measurement machine. The surface hardness of all the components has been also checked, in particular the one of the ring gear that was the most critical components in terms of safety factors

according to the calculations.



Figure 13.4. Hardness check on the ring gear

The grooves machined into the upright to house the ring gear revealed to be difficult to be realized during manufacturing due to low fillet radius and large tool overhang. This forced the manufacturer to test the ring gear fit while machining a progressively removing material from the upright until the required fit was guaranteed, resulting in having to fit each ring gear in the proper upright (both those two components were punched with the same letter in order to avoid assembly errors).



Figure 13.5. Ring gear mounted into the upright

With a coordinate measurement machine the measures needed to determine the thickness of the wheel bearings preload ring (as shown in Section 6.3) are taken.

The whole transmission assembly process takes 2 hours per each group for the first it is performed, for this reason it was possible to speed up the assembly of the car. Performing a gear maintenance without removing the bearings is really quick, it lasts less than an hour, this assembly times are really a progress with respect to the previous year's one, SCdiciassette transmission assembly for the first time took around four/five hours.

The transmission assembled is shown below.

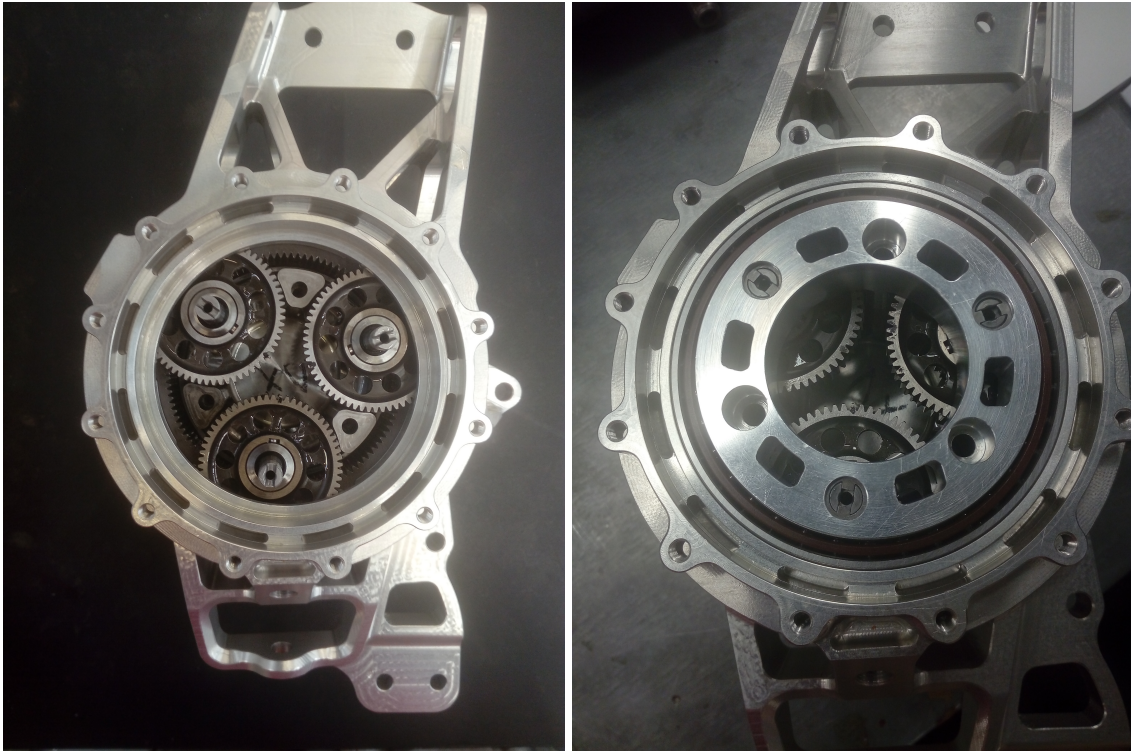


Figure 13.6. SC18itegrale transmission assembled

## 13.4 Formula Student Spain failure

During the practice session of Formula Student Spain a failure is reported because the retaining screw of one of the sun gears got loose and caused the sun gear to move from its design position.

This failure was repaired quickly due to the easiness of assembly of the gearbox and the car was ready to be back on track in less than an hour. Anyway, this failure raise concern regarding the necessity of a preveiling mechanism for the retaining screw of the sun gear.

Below some pictures of the failure are shown.

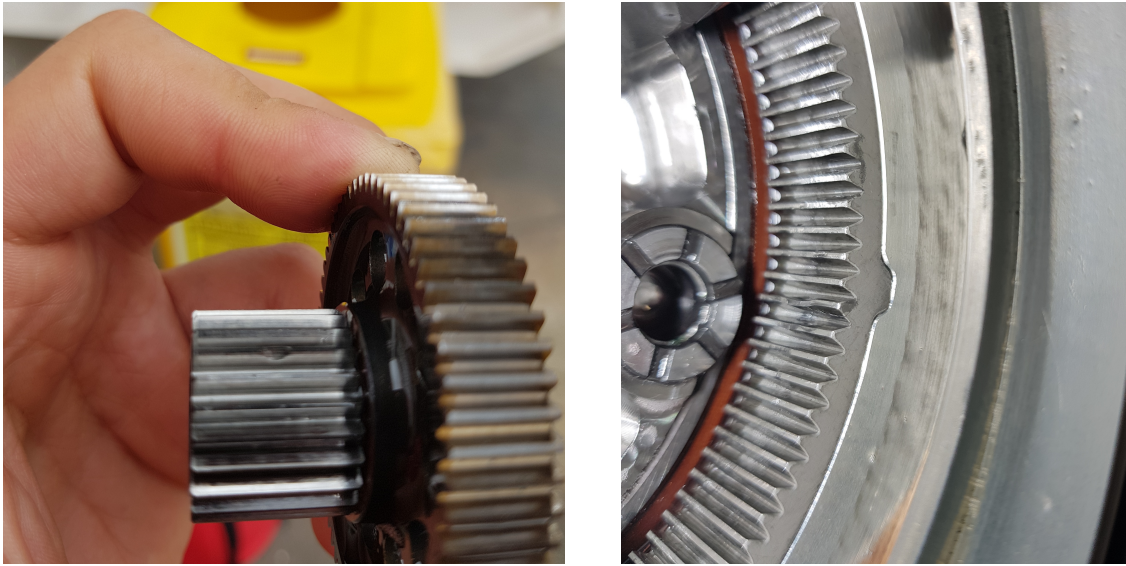


Figure 13.7. Formula Student Spain Failure

## 13.5 Gearbox life

Through log files post-processing the overall vehicle and so the gearbox life could be exactly determined.

Event	Working time [h]	Distance [km]
June 2018 pre-season testing	1.9	62
July 2018 mid-season testing	3.1	121
August 2018 mid-season testing	3.8	150
October 2018 post-season testing	0.4	21
November 2018 post-season testing	1.4	63
April 2019 post-season testing	1.7	73
May 2019 post-season testing	5.4	212
June 2019 post-season testing	6.0	257
FSAE Italy	0.9	29
Formula Student Spain	1.1	36
Total	25.7	1024

Table 13.3. SC18integrale recorded running time and distances

The life of the vehicle and so of the transmission resulted to be lower with respect to what was predicted at the beginning of the project. This is due to the fact that the predicted life was an estimation and most of all that important delays is the production conditioned the pre-season tests, forcing them to be far less with respect to what was predicted.

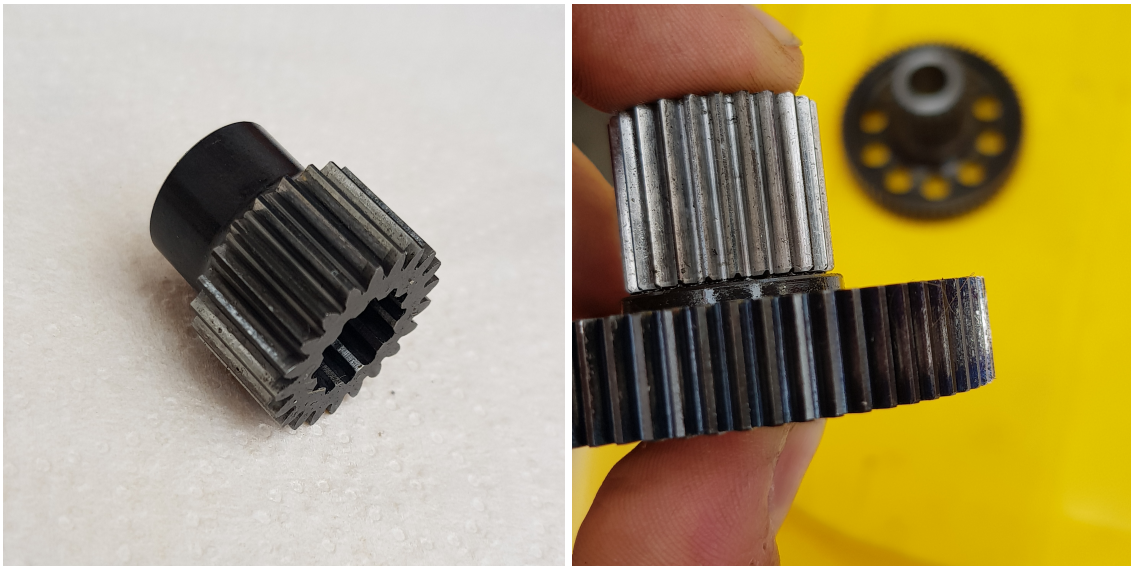


Figure 13.8. SC18itegrale gears inspection after 25 h

## 13.6 Motor working points

In this section the motor working points logged during a track test are superimposed to the efficiency map, both for a rear and a front motor and both in traction and in regenerative braking.



reachable due to the power limit of the motor (20 kW). The power limit curve is clearly visible in Figure 13.9.

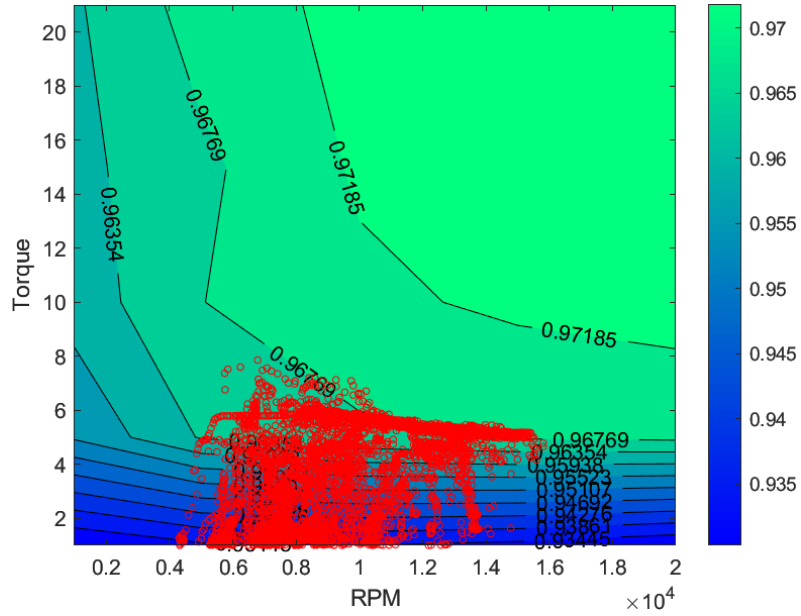


Figure 13.11. Front motor working points in traction

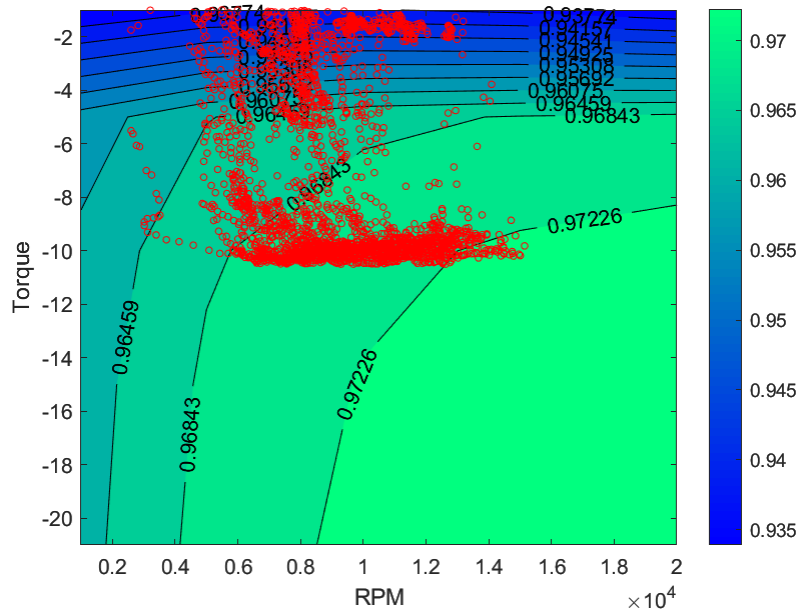


Figure 13.12. Front motor working points in regenerative braking

It can be also noticed that the regenerative braking is the regenerative braking torque is demanded mostly to the front motors rather than the rear ones.

Finally it can be noticed that during acceleration the front wheels are traction-limited rather than power-limited.

# Chapter 14

## Conclusions and future perspectives

### 14.1 Conclusions

Both the weight reduction and the volume reduction targets were overtaken, bringing to a really satisfactory result.

As seen, also the assembly time was considerably reduced, permitting to recover part of the delay coming from manufacturing and saving fundamental time for testing. The easiness of assembly and rebuild was also seen during the accident in Formula Student Spain, where in less than an hour the car was ready to be back on the race track.

Unfortunately due to production delays the life of the car resulted to be significantly lower than expected so correctness of the gear life calculation was not tested properly. However, apart from the little accident during Formula Student Spain, the gearbox operated in a satisfactory way for the whole season and also post-season testing, without the need of further maintenance.

In general, all the vehicle's project was really successful both from a design and performances point of view. Important improvements in terms of overall vehicle mass, battery pack performance and reliability and controls systems have been implemented during the season.

Unfortunately the lack of time in pre-season tests prevented SC18integrale to express its full potential during races. An important third place during Formula SAE Italy was achieved by the Team.

## 14.2 Future perspectives

The present work showed that even reducing significantly the normal module and the size of the gears, large safety factors can be achieved and a good reliability is obtained. Ideally the size of those gears can be reduced even more, clearly the manufacturing aspect must be kept in mind when choosing an extremely small normal module.

Also, further investigation on the fatigue behaviour is worthy to be carried in order to design properly an aluminum hub and reducing even more the weight of the component.

In conclusion, it will be really interesting to be able to effectively test bench the transmission, in order to validate properly both the expected life and the efficiency of the gear train.

# Appendix A

## AMK motor datasheet

Bezeichnung/name **DD5-14-10-POW - 18600-B5** Formula Student Datum/date: 25.03.2015

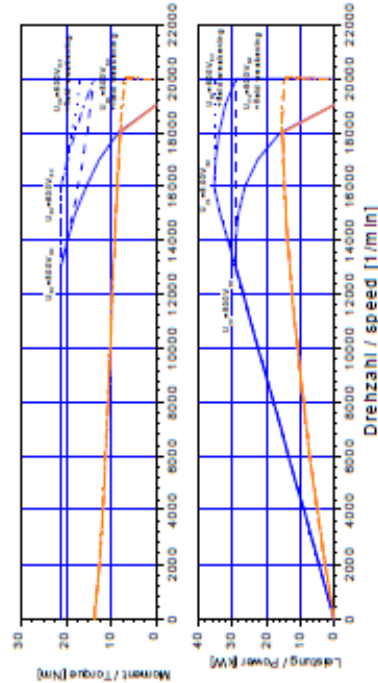
Teile-Nr./part number **A2370DD** Zeichn.-Nr./drawing no.:12703-01260

### Motorbeschreibung motor description:

Motorprinzip/motor principle: synchron  
 Kühlung/cooling type: IMB5  
 Bauform/mounting type: IP 54  
 Schutzart/degree of protection: F  
 Isolierklasse/insulation class: F

**Leistungsdaten performance data:**  
 Betriebsart/duty type: S1  $\sigma T=80K$   
 Dauerstillstandsmoment/continuous Stall Torque "Mo": 13,8 Nm  
 Maximales Moment/maximum torque "Mmax": 21 Nm  
 Bemessungsmoment/rated torque "Mn" (ID32771): 9,8 Nm  
 Bemessungsleistung/rated power "Pn": 12,3 kW  
 Bemessungsdrehzahl/rated speed "n" (ID32772): 12000 rpm  
 Theo. Leerlaufdrehzahl/theor. no-load-speed "No": 18617 rpm

### Motorcharakteristiken performance - characteristics:



Kennlinie kann die maximal zulässige Drehzahl übersteigen / Characteristic may exceed mechanical speed limit of motor

### Elektrische Daten electrical data:

Nennspannung/rated voltage "Un" (ID32768): 350 V  
 Nennstrom/rated current "In" (ID111): 41 Arms  
 Dauerstillstandstrom/cont. stall current "Io" (ID34086): 53,1 Arms  
 Maximalstrom/maximum current "Imax" (ID109): 100 Arms  
 Maximale Dauer für/duration for "Imax" (ID34168): 1,24 s  
 Drehmomentkonstante/torque constant "kt": 0,26 Nmi/Arms  
 Spannungskonstante/voltage constant "ke" (ID 34234): 18,8 V/ku/min  
 Schaltung/connection type: D  
 Polzahl/number of poles "2p" (ID32775): 10 Pole  
 Klemmenwiderstand/terminal resistance "Rtt" (ID34164): 0,13 Ohm  
 Klemmeninduktivität/terminal inductance "Ltt" (ID34167): 0,3 mH  
 Querscheninduktivität/quadrature axis inductance "Lq" (ID34048): 0,54 mH  
 Hauptachseninduktivität/direct axis inductance "Ld" (ID34045): 0,44 mH  
 Magn.-Strom/magn. current "Im" (ID32769): 70 Arms  
 Magn.-Strom/magn. current "Im1" (ID32770): 3,5 Arms  
 Rotorzeitkonstante/rotor time constant "Tr" (ID32774): 0,01 s

### Reglereinstellungen controller settings:

**Stromregler current controller:**  
 Verstärkung q-Achse/gain q-axis "kpq" (ID34151): 1,62 V/A  
 Verstärkung d-Achse/gain d-axis "kpd" (ID34152): 1,72 V/A  
 Nachstellzeitkonstante/time constant "Tnq" (ID34050): 1,2 ms  
 Nachstellzeitkonstante/time constant "Tnd" (ID34052): 1,2 ms  
 Adaption Verstärkung/adaption gain "kppq2" (ID 34179): 20 %  
 Adaption Nachstellzeit/adaption time constant "Tnq2" (ID 34180): 400 %  
 Untere Anpaßschwelle/lower adaption limit "lua" (ID34177): 32 %  
 Obere Anpaßschwelle/upper adaption limit "lua" (ID34178): 78 %  
 Drehzahlregler speed controller (default for plain motor):  
 Verstärkung/gain "kp\_n" (ID100): 40  
 Nachstellzeitkonstante/time constant "Tn\_n" (ID101): 10 ms

**Spannungsregler voltage controller:**  
 Spannungsregler/voltage controller "kp" (ID34148): 0,08 AV  
 Spannungsregler/voltage controller "Tn" (ID34149): 6 ms  
 Spannungserhöhung "du" (ID34235): 116 %  
 Systemwiderstand "Rs" (ID34233): 0 Ohm

Figure A.1. AMK motor datasheet [20]

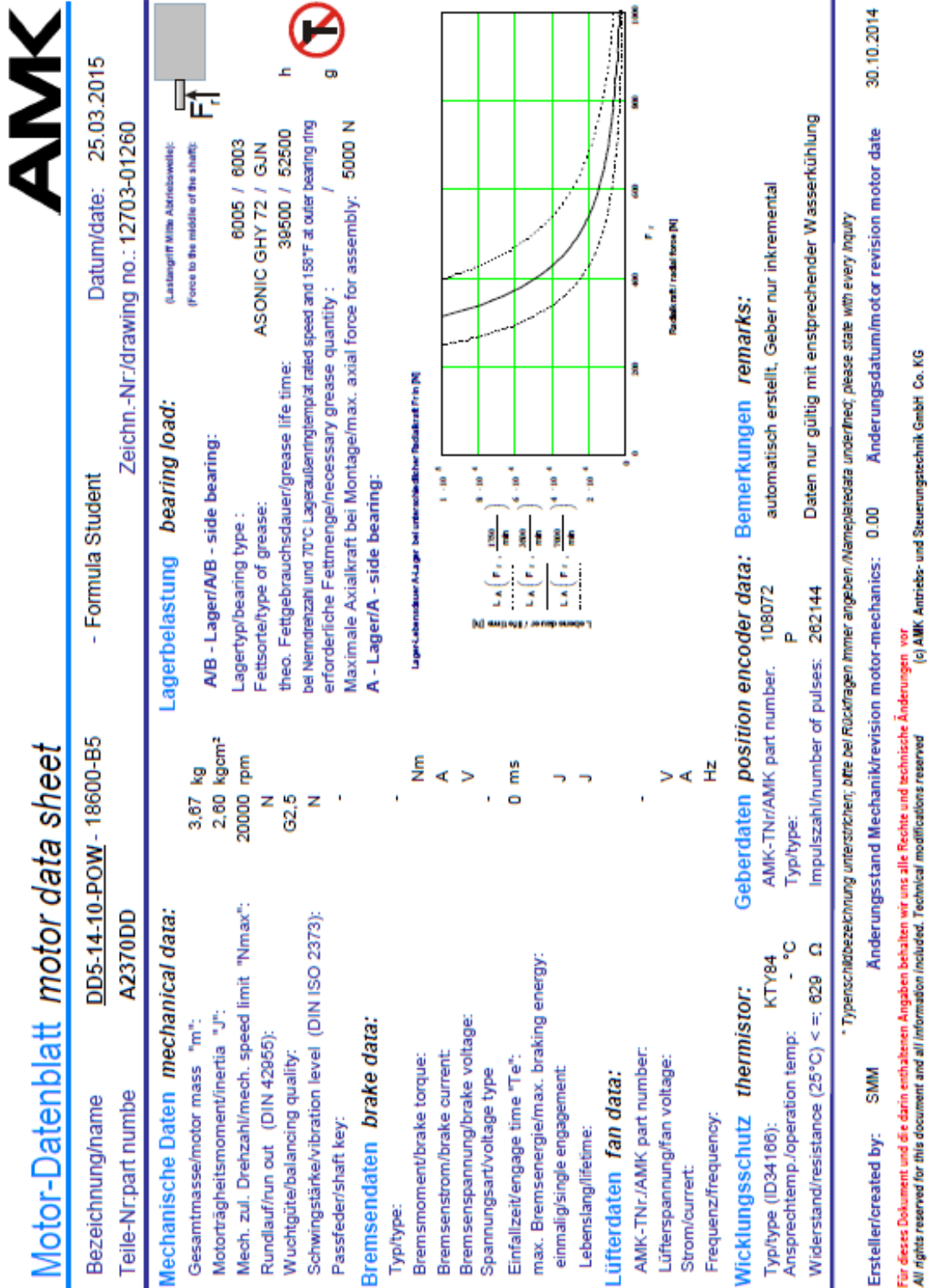


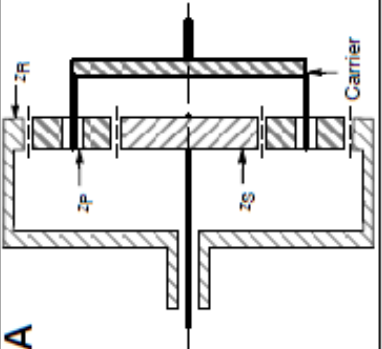
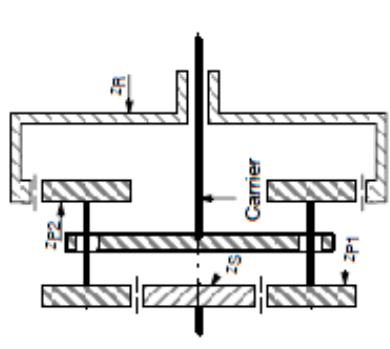
Figure A.2. AMK motor datasheet [20]



## Appendix B

# Double stage epicycloidal gearboxes layouts

Table 3 - Speed ratios

Gear arrangement	Input	Fixed	Output	Direction of rotation	Speed ratio <sup>1)</sup>	Fundamental mesh frequency (Hz)	
						High speed	Low speed
 <p><b>A</b></p>	Sun	Carrier	Ring	Opposite	$\frac{z_R}{z_P - z_S}$	$\frac{n_R z_R}{60}$	
	Sun	Ring	Carrier	Same	$\frac{z_S + z_R}{z_S}$	$\frac{n_C z_R}{60}$	
	Ring	Carrier	Sun	Opposite	$\frac{z_S}{z_R}$	$\frac{n_R z_R}{60}$	
	Ring	Sun	Carrier	Same	$\frac{z_S + z_R}{z_R}$	$\frac{n_C z_S}{60}$	
	Carrier	Ring	Sun	Same	$\frac{z_S}{z_S + z_R}$	$\frac{n_C z_R}{60}$	
	Carrier	Sun	Ring	Same	$\frac{z_R}{z_S + z_R}$	$\frac{n_C z_S}{60}$	
	Sun	Ring	Carrier	Same	$\frac{z_P z_S + z_P z_R}{z_P z_S}$	$\frac{(n_S - n_C) z_S}{60}$	$\frac{n_C z_R}{60}$
	Sun	Carrier	Ring	Opposite	$-\frac{z_P z_R}{z_P z_S}$	$\frac{n_S z_S}{60}$	$\frac{n_R z_R}{60}$
 <p><b>B</b></p>	Carrier	Ring	Sun	Same	$\frac{z_P z_S}{z_P z_S + z_P z_R}$	$\frac{(n_S - n_C) z_S}{60}$	$\frac{n_C z_R}{60}$
	Carrier	Sun	Ring	Same	$\frac{z_P z_R}{z_P z_S + z_P z_R}$	$\frac{n_C z_S}{60}$	$\frac{(n_R - n_C) z_R}{60}$
	Ring	Carrier	Sun	Opposite	$-\frac{z_P z_S}{z_P z_R}$	$\frac{n_S z_S}{60}$	$\frac{n_R z_R}{60}$
	Ring	Sun	Carrier	Same	$\frac{z_P z_S + z_P z_R}{z_P z_R}$	$\frac{n_C z_S}{60}$	$\frac{(n_R - n_C) z_R}{60}$

(continued)

Figure B.1. ANSI/AGMA 6123-B06 [1]

## Appendix C

# Wheel locknut tightening torque computation

As discussed in Section 8.2 it is decided to size the wheel locknut tightening torque in order to be able to transmit entirely by friction the tangential loads during traction. The maximum torque available at the wheel during traction ( $T_{max}$ ) is given by:

$$T_{max} = T_m * \tau = 21 * 14.8 = 311Nm \quad (C.1)$$

Where:

- $T_m$  is the maximum torque supplied by the motor
- $\tau$  is the transmission ratio

The axial force ( $F_a$ ) required to transmit all the loads by friction is equal to:

$$F_a = \frac{T_{max}}{f * R_f} \quad (C.2)$$

Where:

- $R_f$  is the friction radius
- SF is the required safety factor
- $f$  is the friction coefficient

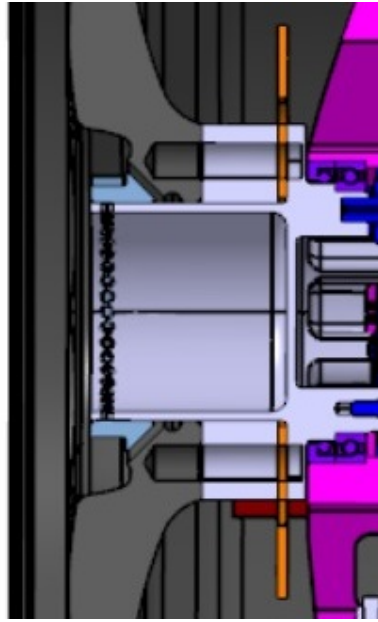


Figure C.1. Section view of the clamped parts between the hub and the wheel locknut

As shown in Figure C.1 various components are clamped between the locknut and the hub flange (rim, wheel spacer and brake disc carrier). In this computation the effect on the load distribution between the clamped parts have been neglected. Also, it was not possible to find the magnesium-aluminum and aluminum-titanium friction coefficients in literature. For the mentioned reason friction coefficient  $f$  is set to 0.4, arbitrarily low in order to stay on the safe side for this analysis.

The required safety factor is set to 1.5 due to the fact that the locknut is tightened every time with a certified torque wrench.

The friction radius  $R_f$  is the average radius of the surface involved in the shear forces transmission by friction, assuming the axial force evenly distributed on the surface, i.e. constant pressure exerted by the axial force due to tightening. Defining as  $R_i$  the inner radius of the surface  $A_t$  involved in the threaded coupling (the one where the shear forces are transmitted by friction) and as  $R_o$  the outer radius that the surface  $A_t$  would have if it was ring-shaped, the following expression can be written:

$$A_t = \pi(R_o^2 - R_i^2) = 3436\text{mm}^2 \quad (\text{C.3})$$

The outer radius  $R_o$  can be then computed.

$$R_f = \sqrt{\left(\frac{A_t}{\pi} + R_i^2\right)} = 49.6\text{mm} \quad (\text{C.4})$$

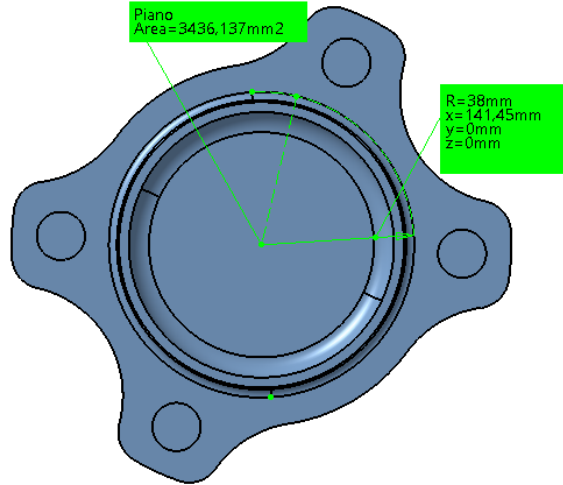


Figure C.2. Measures on the wheel hub

$A_t$  and  $R_i$  are measured from the hub CAD model, as shown in Figure ??  
 At this stage the average friction radius  $R_f$  can be computed as:

$$R_f = \frac{R_i + R_o}{2} = 43.3mm \quad (C.5)$$

The axial load need to ensure that all the shear loads are transmitted by friction can be now calculated, resulting to be:

$$F_a = 26909N \quad (C.6)$$

The thread is of the metric type, M72x1.5, below its characteristic dimensions are reported.

- $d = 72mm$  (nominal diameter)
- $d_m = 71.026mm$  (mean diameter)
- $p = 1.5mm$  (pitch)
- $\beta = 30\check{r}$  (thread angle)

Knowing the characteristics of the thread, the tightening torque needed to guarantee the axial force  $F_a$  previously determined can be finally computed [16].

$$M_T = \frac{F_a}{2} \left( \frac{p}{\pi} + d_m * \frac{\tan\phi}{\cos\beta} + d_t * \tan\phi_s \right) = 242.7Nm \simeq 250Nm \quad (C.7)$$

Where:

- $\tan\phi = \tan\phi_s = 0.4$
- $d_t = 1.3 * d$  (average locknut diameter)

# Appendix D

## Gear train technical drawings

D – Gear train technical drawings

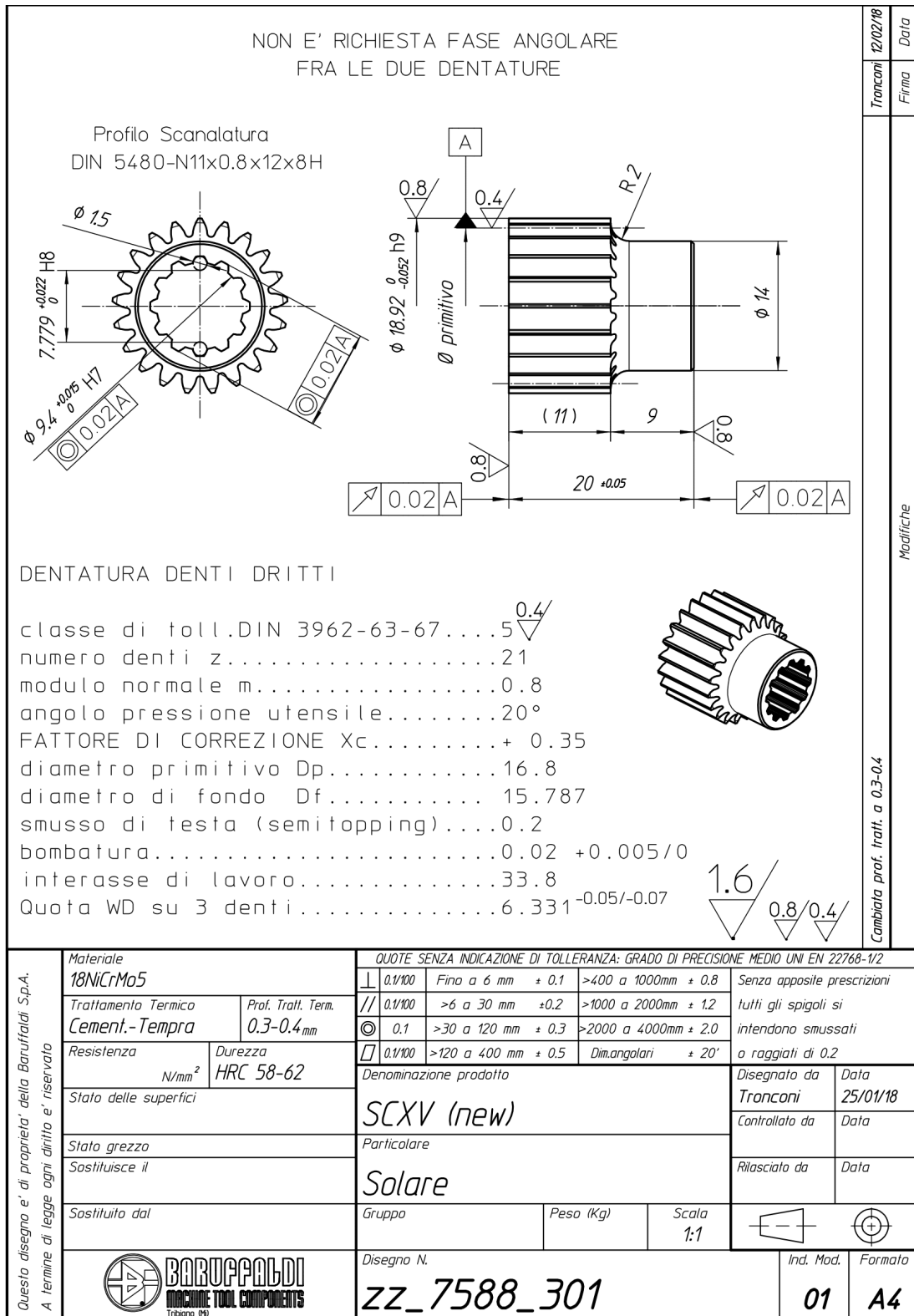


Figure D.1. Sun gear drawing [28]

D – Gear train technical drawings

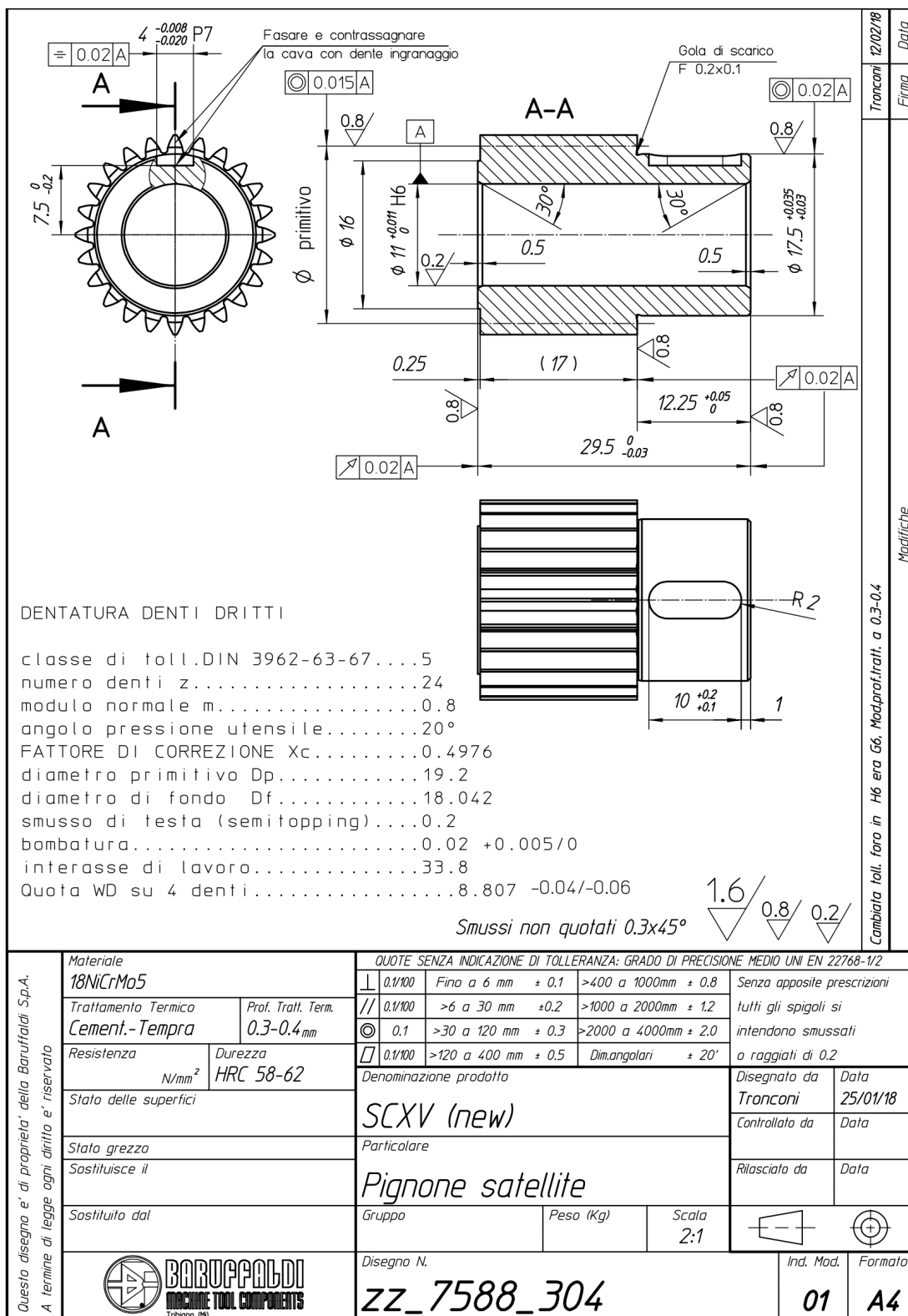


Figure D.2. First stage planet gear drawing [28]





D – Gear train technical drawings

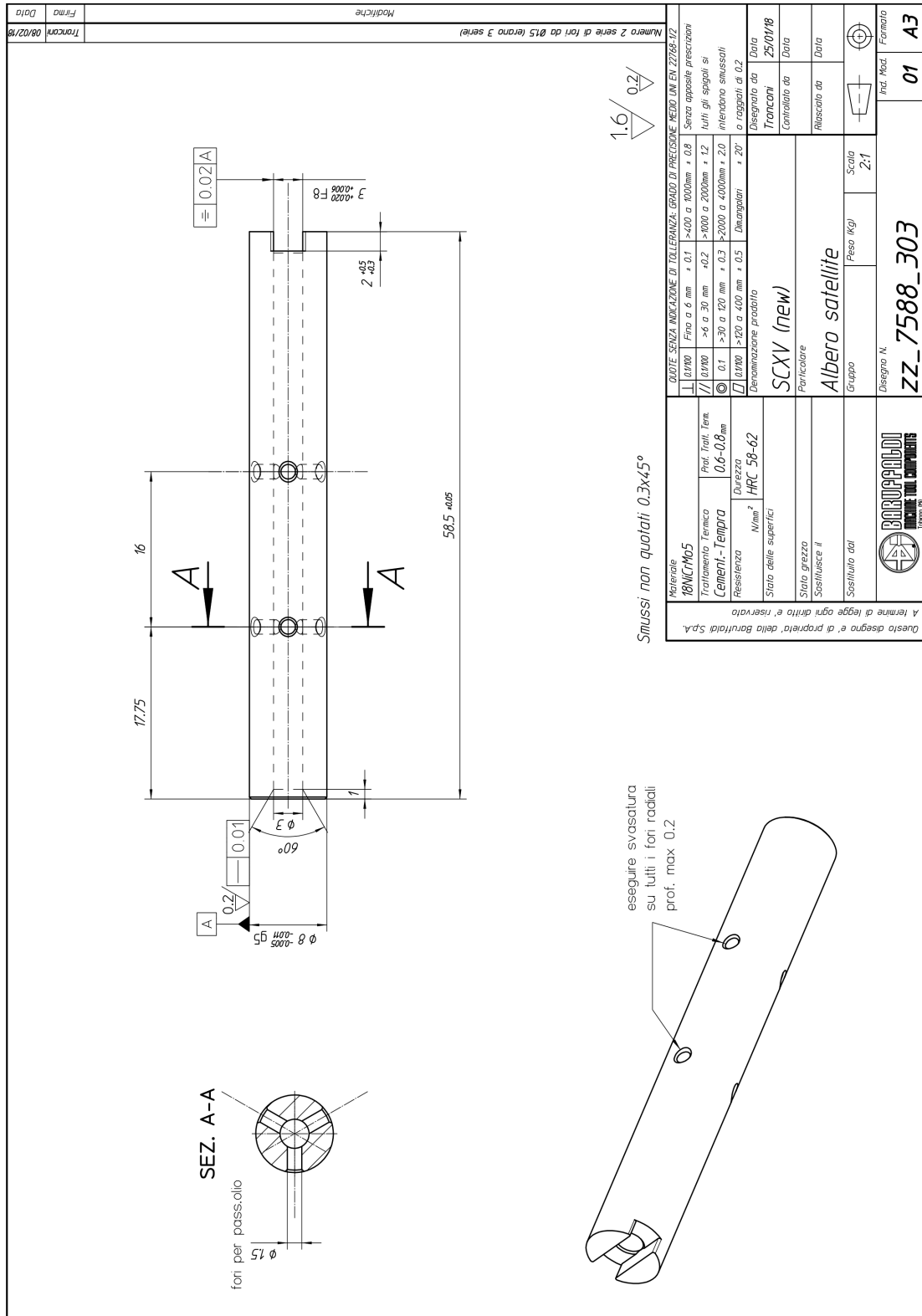
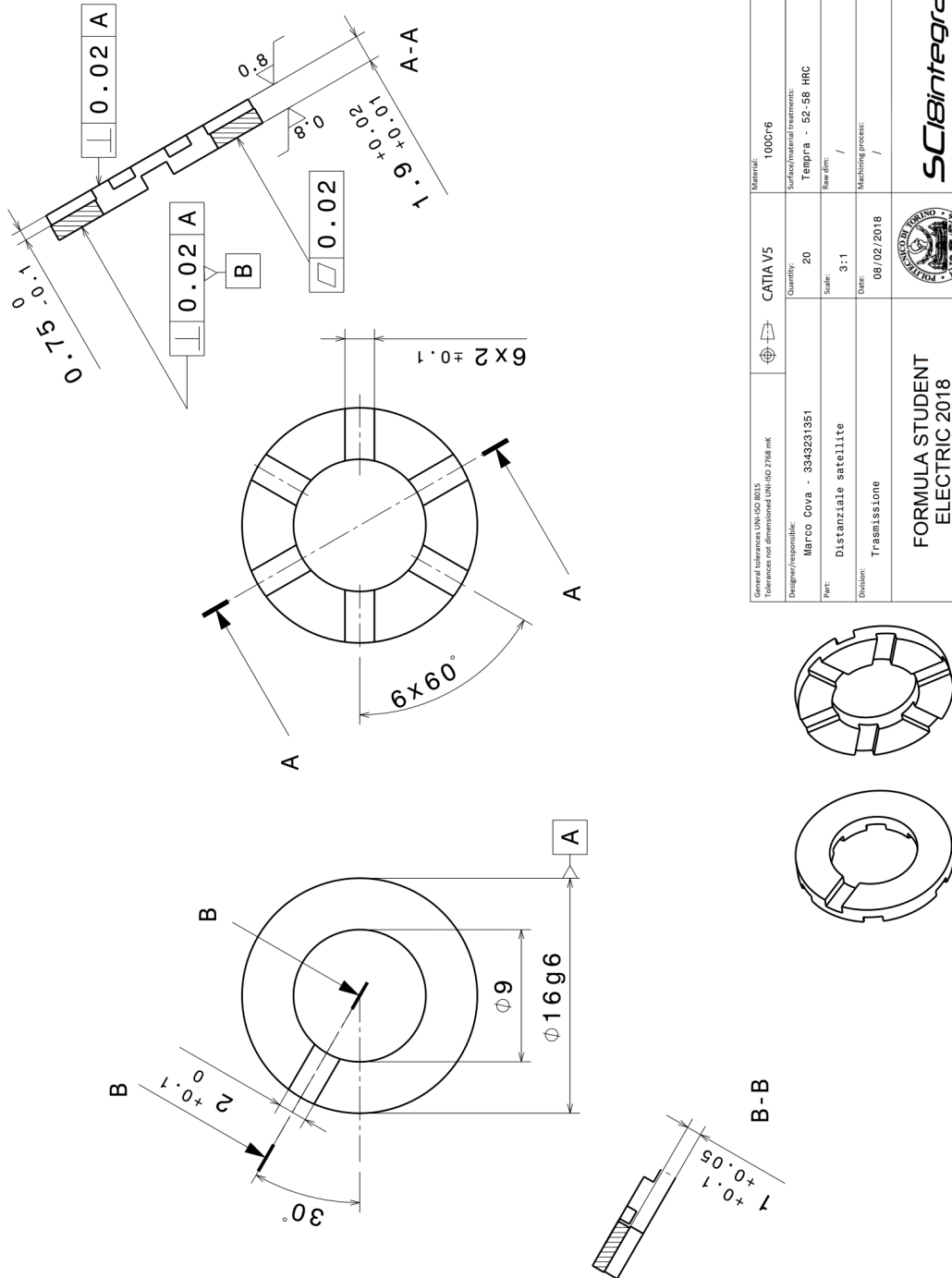


Figure D.5. Planet pin shaft drawing [28]



General tolerances UNI-ISO 8013 Tolerances not dimensioned UNI-ISO 2768 mK	Material: 100Cr6	RESERVED RIGHTS, NOT TO BE COPIED OR USED WITHOUT PERMISSION
Designer/responsible: Marco Cova - 3349231951	Surface/textural treatment: Tempira - 52-58 HRC	 <b>SCBintegrale</b> <b>A4</b>
Part: Distanziale satellite	Quantity: 20	
Division: Trasmissione	Scale: 3:1	
	Date: 08/02/2018	
<b>FORMULA STUDENT</b> <b>ELECTRIC 2018</b>		

Figure D.6. Planet gears spacer drawing

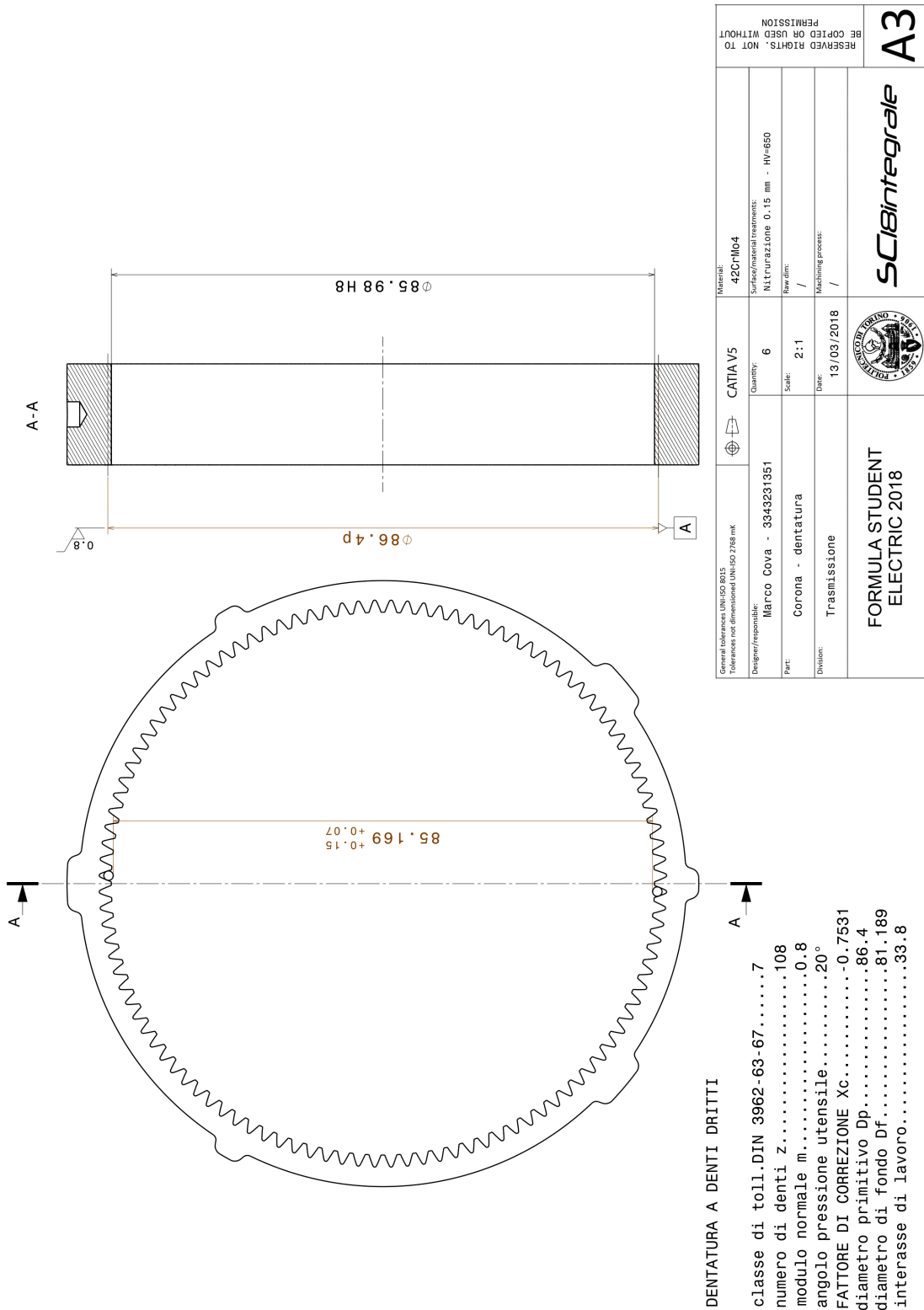
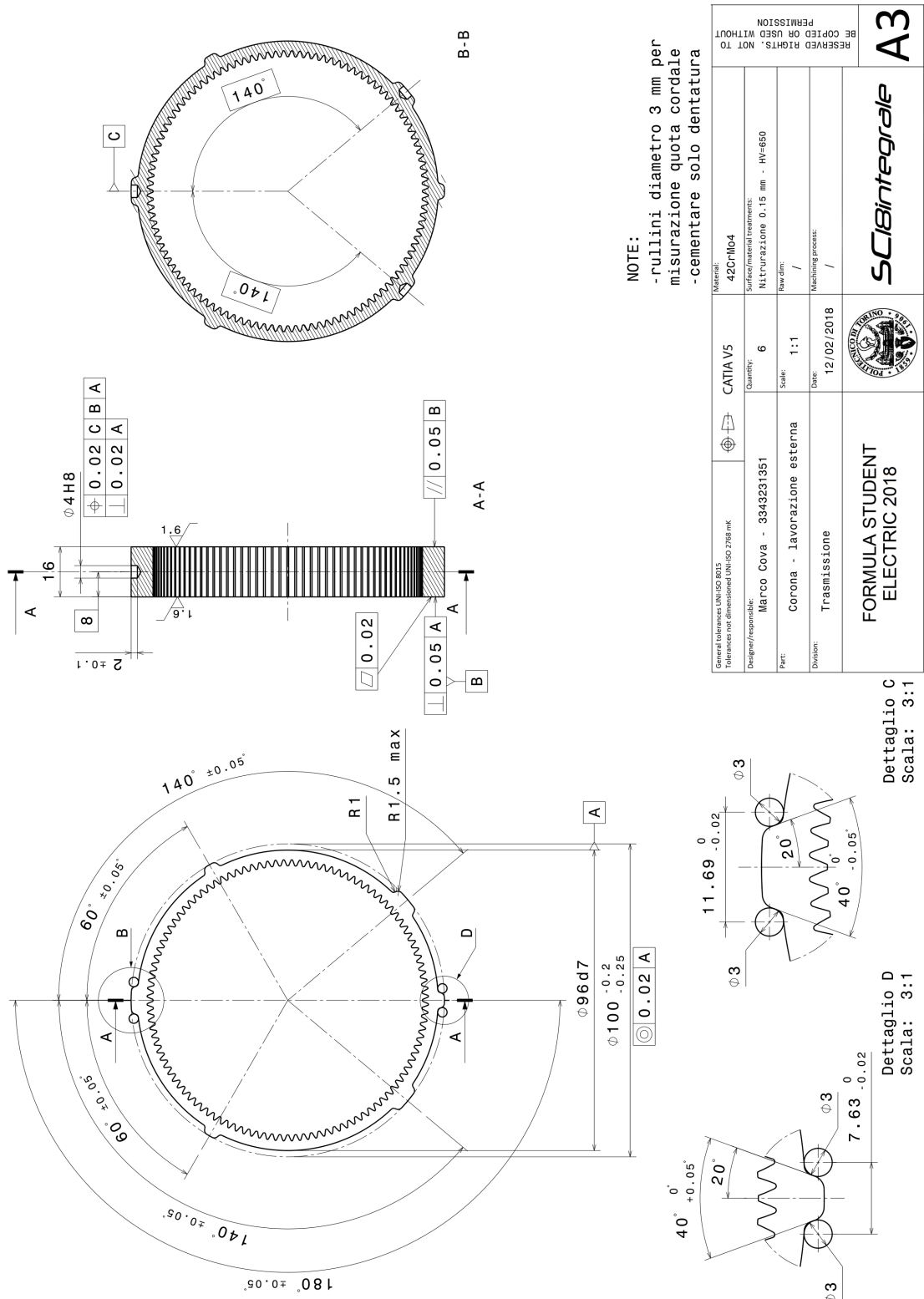


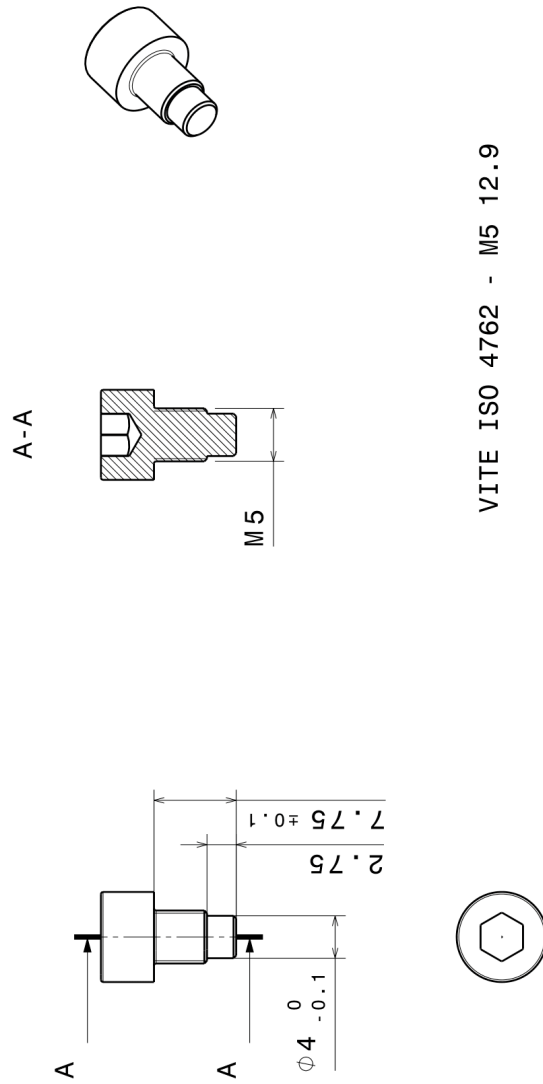
Figure D.7. Ring gear drawing  
208

D – Gear train technical drawings



General tolerances UNI-ISO 8015 Tolerances not dimensioned UNI-ISO 2768 mk	CATIA V5	Material: 42CrMo4	RESERVED RIGHTS. NOT TO BE COPIED OR USED WITHOUT PERMISSION
Designer/responsible: Marco Cova - 3343231351	Quantity: 6	Surface/material treatments: Nitrucciatura 0.15 mm - HV=650	
Part: Corona - lavorazione esterna	Scale: 1:1	Raw dim: /	
Division: Trasmissione	Date: 12/02/2018	Machining process: /	
FORMULA STUDENT ELECTRIC 2018			
			
			

Figure D.8. Ring gear drawing  
209



VITE ISO 4762 - M5 12.9

General tolerances UNI-ISO 8015 Tolerances not dimensioned UNI-ISO 2768 mK		Material: /
Designer/responsible: Edoardo Zo' - 349 916 0096	Quantity: 20	Surface/material treatment: /
Part: Viti fissaggio corona	Scale: 2:1	Raw dim: VITE ISO 4762 - M5 12.9
Division: Power train	Date: 01/03/2018	Machining process: /
FORMULA STUDENT ELECTRIC 2018		
		RESERVED RIGHTS, NOT TO BE COPIED OR USED WITHOUT PERMISSION
		<b>A4</b>

Figure D.9. Ring gear screws drawing  
210

## Appendix E

# Planetary carrier assembly technical drawings

E – Planetary carrier assembly technical drawings

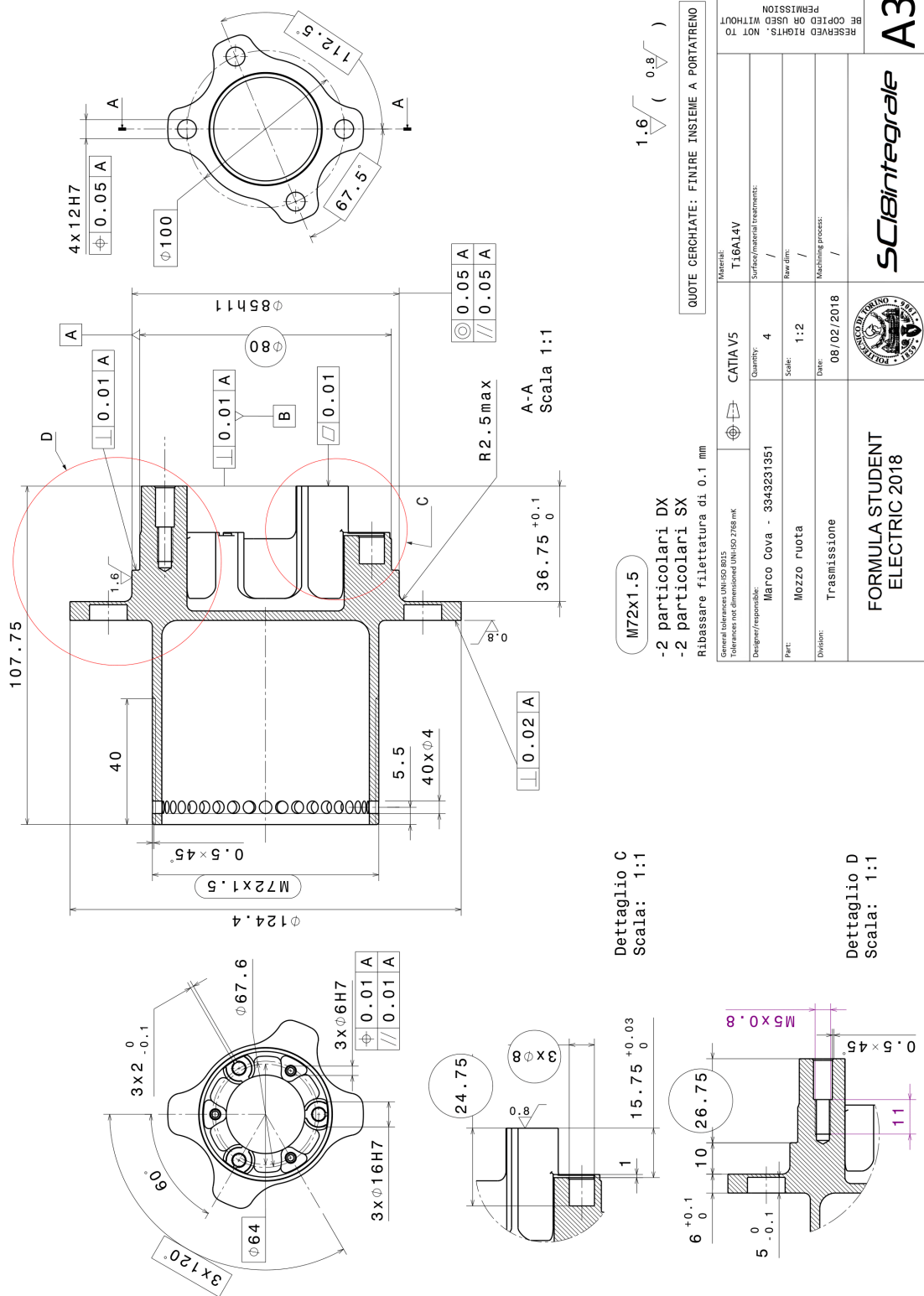


Figure E.1. Hub drawing

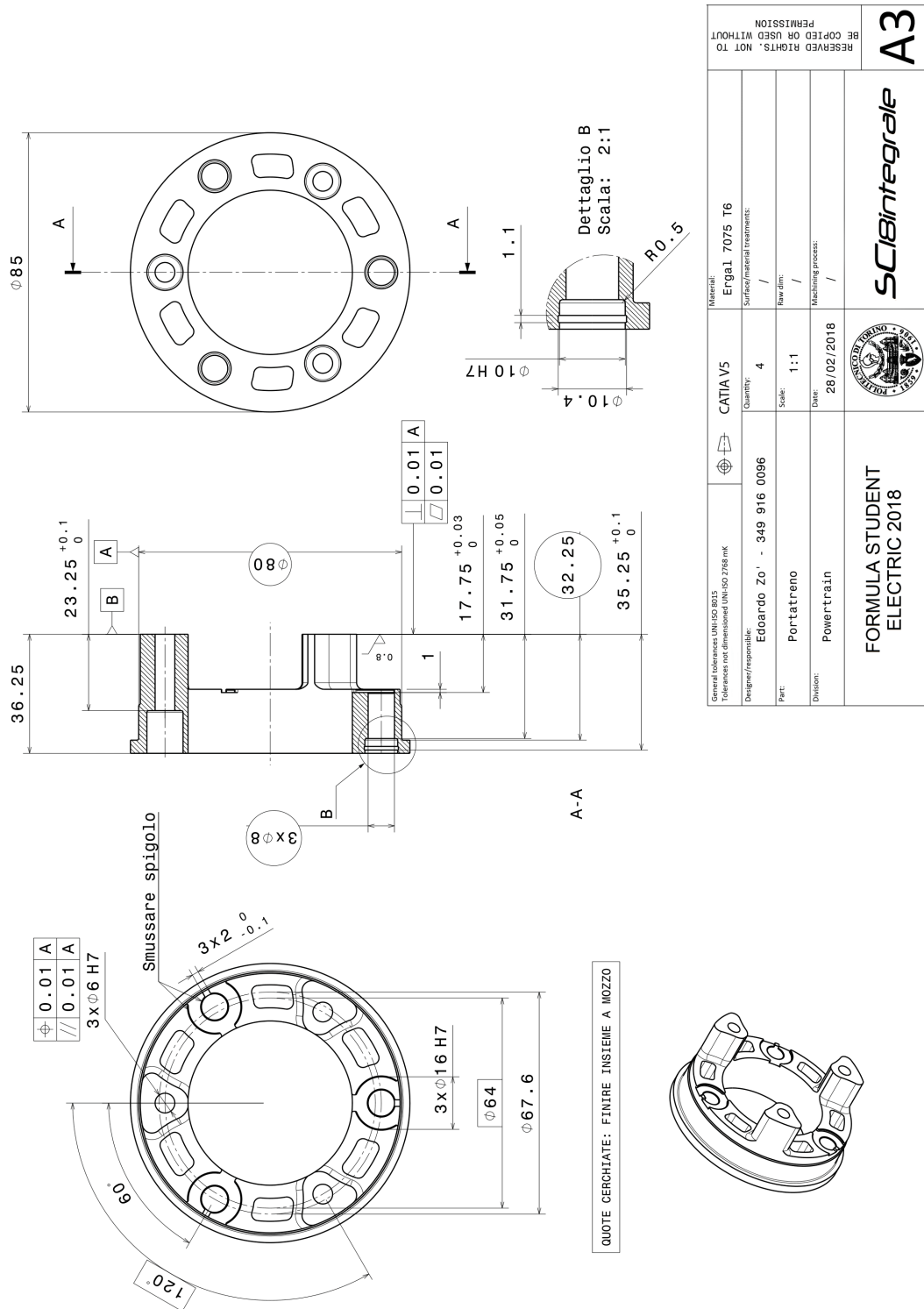


Figure E.2. Planetary carrier drawing



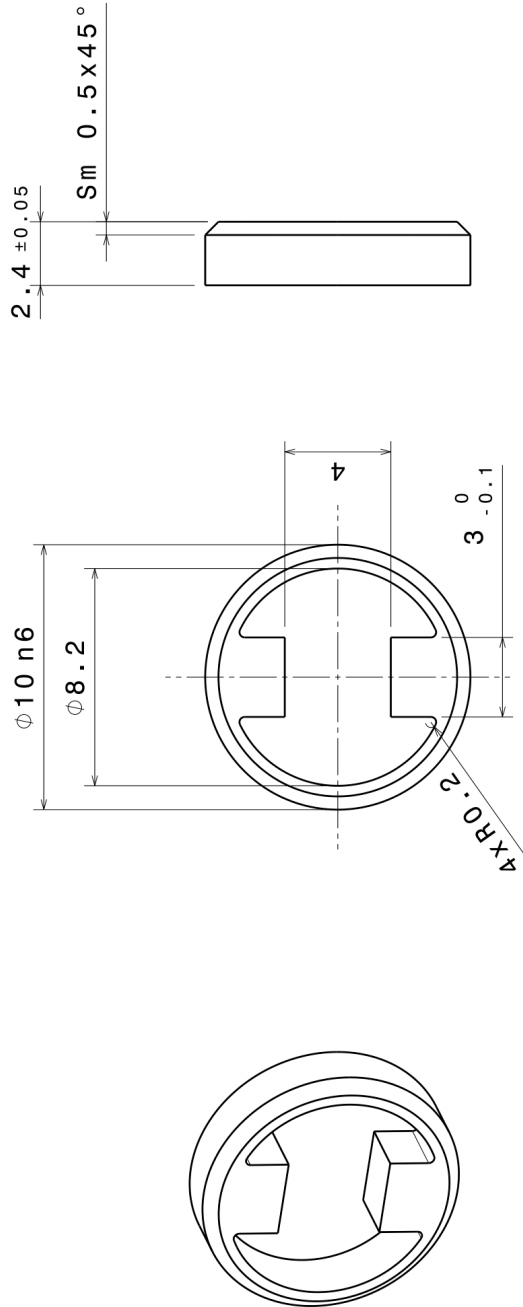


Figure E.4. H-shaped bushing drawing

General tolerances UNI-ISO 8015 Tolerances not dimensioned UNI-ISO 2768 mK		Material: Acciaio C40	RESERVED RIGHTS, NOT TO BE COPIED OR USED WITHOUT PERMISSION
Designer/responsible: Edoardo Zo' - 349 916 0096	Quantity: 20	Surface/material treatment: /	
Part: Boccola antirotazione	Scale: 1:1	Raw dim: /	
Division: Powertrain	Date: 12/02/2018	Machining process: Elettroerosione a filo	
FORMULA STUDENT ELECTRIC 2018			<b>A4</b>

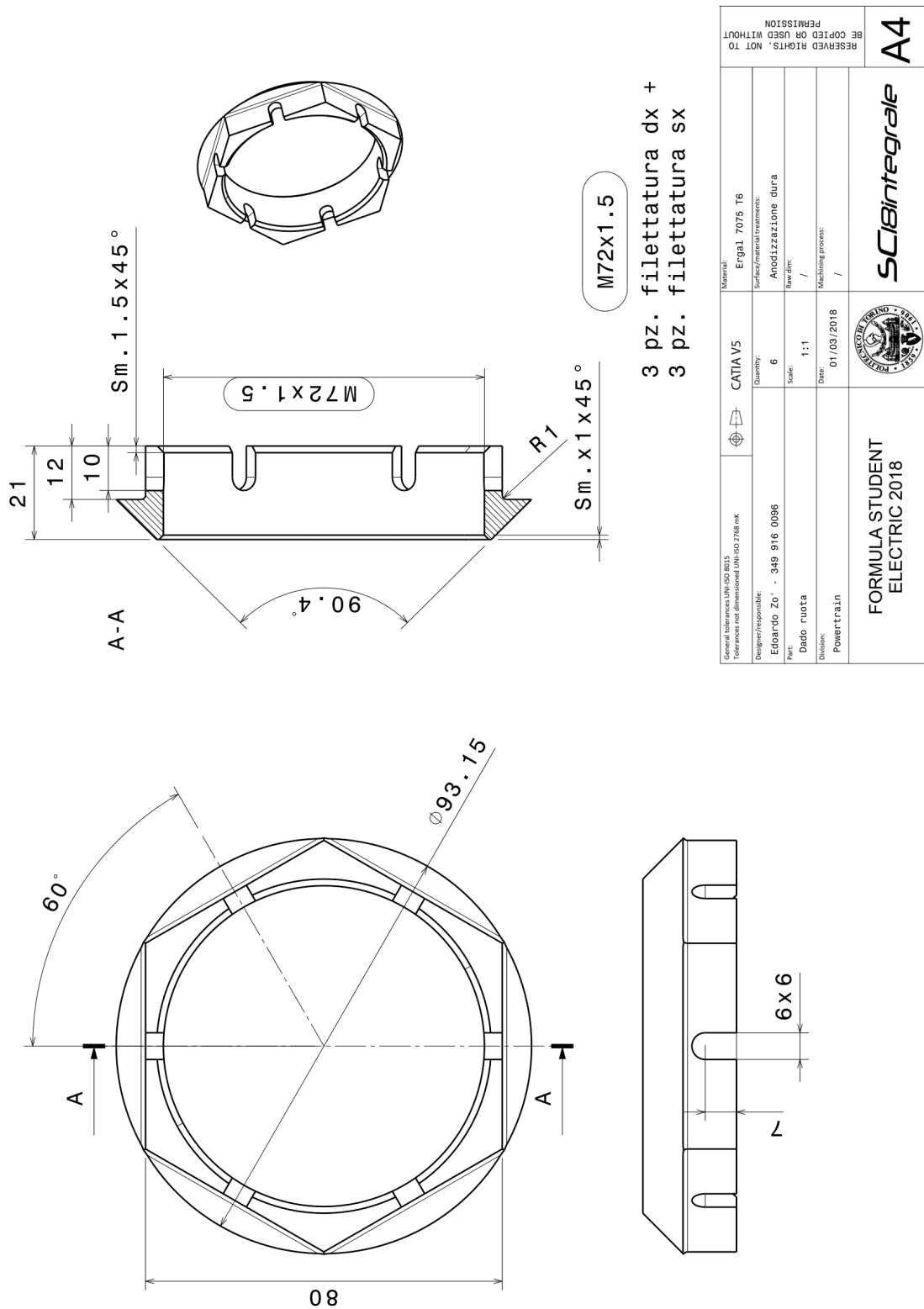


Figure E.5. Wheel locknut drawing

# Appendix F

## Lubricant datasheet



# GEAR 300 75W-90

**Racing gearbox and differential lubricant**

**100% Synthetic – Ester based**

## TYPE OF USE

Specially designed for racing vehicle gearboxes : speed way, rally, raid...

All mechanical transmission, synchronized or not synchronized gearboxes, gearbox/differential, transfer gearboxes and hypoid differentials without limited slip system operating under shocks, heavy loads and low revolution speed or moderate loads and high revolution speed.

## PERFORMANCES

STANDARDS API GL4 and GL5 / MIL-L-2105D

100% synthetic extreme pressure lubricant for an efficient anti-wear protection, a better resistance at high temperature and a longer life time.

0% shear loss : Unshearable oil film in extreme conditions.

Stays in 90 grade after KRL 20 hours shear test as requested by SAE J306 standard, July 1998 update.

Very high lubricating power which decreases friction and wear.

90 grade at hot temperature to provide outstanding oil film resistance at hot temperature and/or to reduce transmission noise.

Fluid at low temperature to allow easier gear shifting when the gearbox is cold.

Less effort required on the gear lever to shift the gears.

Suitable for any type of seal and yellow material used in gearboxes design.

Anti-corrosion, Anti-foam.

## RECOMMENDATIONS

Oil change: According to manufacturers' requirements and adjust according to your own use.

## PROPERTIES

Viscosity grade	SAE J306	<b>75W-90</b>
Density at 20°C (68°F)	ASTM D1298	0.897
Viscosity at 40°C (104°F)	ASTM D445	72.6 mm <sup>2</sup> /s
Viscosity at 100°C (212°F)	ASTM D445	15.2 mm <sup>2</sup> /s
Viscosity index	ASTM D2270	222
Flash point	ASTM D92	200°C / 392°F
Pour point	ASTM D97	-60°C / -76°F

We retain the right to modify the general characteristics of our products in order to offer to our customers the latest technical development.

Product specifications are not definitive from the order which is subject to our general conditions of sale and warranty.

MOTUL - 119 Bd Félix Faure - 93303 AUBERVILLIERS CEDEX - BP 94 - Tel : 33 1 48 11 70 00 - Fax : 33 1 48 33 28 79 - Web Site : www.motul.fr

09/10

Figure F.1. Motul Gear 300 75w90 dataheet [27]

# Bibliography

- [1] ANSI/AGMA 6123-B06, *Design Manual for Enclosed Epicyclic Gear Drives*, American Gear Manufacturers Association, 2006.
  
- [2] ISO 6336:2006, *Calculation of load capacity of spur and helical gears*, International Organization for Standardization, 2006.
  
- [3] Stephen P. Radzevich, *Dudley's Handbook of Practical Gear Design and Manufacture*, CRC Press, 2016.
  
- [4] D.W. Dudley, J. Sprengers, D. Schröder, H. Yamashina *Manuale del Motoriduttore - Bonfiglioli*, Springer, 1997.
  
- [5] A. Dobler, M. Hergessel, T. Tobie, K. Stahl, *Increased Tooth Bending Strength and Pitting Load Capacity of Fine Module Gears*, *Geartechnology* (September/October 2016), 48-53, 2016.
  
- [6] B. Jeong, M. Kato, K. Inoue, N. Takatsu, *The Bending Strength of Carburized Fine Module Gear Teeth*, *JSME International Journal* (Vol. 35, No. 1, 1992), 136-141, 1992.
  
- [7] Heinz Linke, *Cylindrical Gears: Calculation, Materials, Manufacturing*,

Carl Hanser Verlag, 2010.

[8] Massimiliano Turci, *Errore di trasmissione e modifiche di ingranaggi*, 2019.

[9] KISSsoft AG, *Help manual*.

[10] KISSsoft AG, *KISSsys 03/2014 – Tutorial 2: One Stage Planetary Gearbox*, 2014.

[11] SKF, *Super-precision bearings catalogue*, 2015.

[12] SKF, *Needle roller bearings catalogue*, 2015.

[13] SKF, *Industrial shaft seals catalogue*, 2013.

[14] Fabrizio Mandrile, *Squadra Corse calculations report*, 2018.

[15] Angst+Pfister, *Basic catalogue*, 2007.

[16] Giovanni Belingardi, *Slides from the "Machine Design" course*, Politecnico di Torino, 2016.

[17] Carlo Emilio Baret, Enrico Galvagno, *Slides from the "Powertrain Components Design: Transmission" course*, Politecnico di Torino, 2018.

[18] ISO Technical Report 1417, *Gears - Thermal capacity*, International Organization for Standardization, 2001.

- [19] Squadra Corse PoliTO, *Gear train design presentation*, 2015.
- [20] AMK, *DD5-14-10 POW Motor-Datenblatt*, 2015.
- [21] Edoardo Zo', *Design of a Planetary Gear Train for a FSAE Full Electric Vehicle*, 2019.
- [22] Mattia Viteritti, *Drivetrain optimization of a Formula SAE racing prototype*, 2017.
- [23] Luis Daniel Medina Querecuto, *Design and Validation of the Unsprung Masses of a Formula SAE vehicle*, 2020.
- [24] R. Boyer, G. Welsch, E. W. Collings, *Materials Properties Handbook: Titanium Alloys*, ASM International, Materials Park, OH, 1994.
- [25] Kaiser Aluminum, *Aluminum alloy 7068 brochure*.
- [26] Kaiser Aluminum, *Aluminum alloy 7075 technical data*.
- [27] Motul, *Gear 300 75W90 technical datasheet*.
- [28] Thomas Tronconi, *Tavole riduttore per Squadra Corse PoliTo*, Baruffaldi S.p.A., 2018